SETTING AND NANOSTRUCTURAL EVOLUTION OF METAKAOLIN GEOPOLYMER

BY

XU CHEN

DISSERTATION

Submitted in partial fulfillment of the requirements
for the degree of Doctor of Philosophy in Civil Engineering
in the Graduate College of the
University of Illinois at Urbana-Champaign, 2017

Urbana, Illinois

Doctoral Committee:

Professor Leslie J. Struble, Chair and Director of Research
Adjunct Professor Paramita Mondal
Professor John S. Popovics
Professor Waltraud M. Kriven
Professor R. James Kirkpatrick, Michigan State University

Abstract

Geopolymers are being promoted as a sustainable alternative to the ordinary cements mainly because their production is associated with much less CO_2 emissions. They also show advantages including compressive strength comparable to portland cements, high temperature resistance, and stability under acid attack. However, before geopolymers can be widely used in practice, certain other behaviors must be understood and controlled, among which is setting, the transition from fluid to solid. Geopolymer setting is repeatedly seen to be substantially accelerated by addition of calcium. The objective of this study is to understand the setting at the nanostructural level for calcium and non-calcium geopolymers using a relatively pure aluminosilicate metakaolin precursor.

Prior to probing nanostructural evolution, a combination of water treatment to extract soluble species and solvent treatment to extract water was developed for use to stop the geopolymer formation for early-age geopolymers with and without calcium, allowing enough time for nuclear magnetic resonance (NMR) tests. Additionally, a protocol to quantify structures of early-age geopolymers was developed using NMR deconvolution and validated by intensity analysis of NMR spectra and by quantitative chemical extractions.

The nanostructural evolution during formation of geopolymer was investigated and correlated with setting. In the non-calcium mix, aluminum was released rapidly right after mixing and immediately condensed with silicates to form aluminosilicate units with growing sizes on metakaolin surface. Set occurred as the remaining aqueous silicates began attaching to these units to form a gel with an interconnected network structure. The structural connectivity during this evolution, for the first

time, was monitored experimentally. Additionally, accelerated setting by calcium was investigated. With calcium, enhanced rate and extent of metakaolin dissolution were observed and were found to decrease Si/Al ratio available for geopolymer formation and thus to further enhance geopolymer gel formation. These observed effects caused the faster setting. The Al-substituted calcium silicate hydrate (C-A-S-H) was identified in the calcium mix, but no evidence showed that it is directly involved in setting.

Considering faster dissolution by calcium noted above, the reaction extent after set was examined. A higher amount of calcium resulted in a higher reaction extent. A higher reaction extent resulted in a higher compressive strength, a relationship also observed in the non-calcium mixes when reaction extent was controlled independently of the Si/Al ratios of geopolymer gel.

Acknowledgements

I would like to express my greatest gratitude to my advisor Professor Leslie J. Struble for giving me the opportunity to undertake a PhD. She is knowledgeable and helped me substantially improve my understanding in cement chemistry and its characterization. Her critical and constructive comments guided me to solve difficult problems one after another during the course of the PhD studies. She provided me support whenever I needed it. She allowed me to chase different and sometimes crazy ideas and prepared me to be an individual researcher. Her patience to help revise my manuscripts not only provided me opportunities to improve my logical thinking and critical writing but also exposed me to the beauty of pursuing perfection. Her enthusiasm for conducting scientific research has inspired me and will definitely motivate me to go far in my future career.

I would like to thank other professors from the construction materials group at University of Illinois. Professor Paramita Mondal, my unofficial second advisor, made my time at Illinois even more valuable. Discussion with her allowed me to understand geopolymerization mechanism in a greater depth and to further improve my critical-thinking skills. In her group meetings, I developed my vision for construction materials beyond the perspective only from geopolymers. I am forever grateful for this learning opportunity provided by her. Professor John S. Popovics provided substantial support to troubleshoot the issues during setting measurement and to interpret data. Both of his graduate-level courses are challenging but I have learned much more than I could ever imagine. By working with him to teach an undergraduate course and revise the teaching documents, I was impressed by his smartness and carefulness, which have influenced my working and life greatly. Professor David A. Lange is not in this PhD committee but his lectures improved my understanding in construction materials and his career stories that he shared inspired me so much.

I would like to thank my doctoral committee members from outside of the department of civil engineering. They provided equally important help and support. Professor Waltraud M. Kriven helped me understand the differences between the geopolymers and alkali-activated materials in a critical way. Her insight into the composition and mechanical properties of geopolymers inspired me and allowed me to study geopolymer structures at a deeper level. After taking the course with her, I was able to discuss ceramic processing issues with confidence in conferences. It was so nice of her to give me the access to her lab for sample preparation, a huge help that made this research possible. Professor R. James Kirkpatrick has communicated with me on interpretation of nuclear magnetic resonance (NMR) spectra, the most important analysis in this research. His critical questions and constructive suggestions helped me improve the NMR quantitative analysis in this research, especially in the spectrum deconvolution part, to a much greater extent.

I would like to acknowledge the financial support from National Science Foundation (DMR 10-08109) and University of Illinois. This support made the experiments in this research possible and provided me research assistantship. Additionally, I would like to thank the financial support of teaching assistantship by working with Professor Leslie J. Struble, John S. Popovics and Paramita Mondal in the department of civil engineering, and of graduate assistantship by working with Dr. David Farrow in the mechanical testing instructional laboratory (MTIL) at University of Illinois.

I was fortunate to have the great support from staff across the campus of University of Illinois. The staffs from the NMR laboratory in the school of chemical sciences, Dr. Jennifer Rapp, Dr. Andre Sutrisno, Dr. Lingyang Zhu, Dr. Dean Olson and Miss Tracie Hubert helped me with the NMR experiments in all aspects. Dr. Olson trained me liquid-state NMR spectroscopy. Dr. Rapp helped me understand basics of NMR spectroscopy and taught me to collect and interpret solid-

state NMR spectra. Dr. Sutrisno helped me further understand NMR spectroscopy, taught me simulation of NMR spectra. Dr. Lingyang Zhu helped me conduct liquid-state NMR tests. Both Dr. Sutrisno and Dr. Zhu provided critical suggestions for my conference presentations. I would also like to acknowledge the great help from Dr. Mauro Sardela and Dr. Matthew D. Bresin in materials research laboratory at University of Illinois. Dr. Sardela is knowledge and provided substantial help with data collection and analysis for X-ray diffraction tests. Dr. David Farrow at MTIL encouraged me to overcome difficulties by sharing his experience of undertaking a PhD. Thanks the help from Joan Etta Christian, Rachel Renee Rayburn, Marvis Ann Orzek, Donna Marie, Timothy J Prunkard, Darold Marrow and many other staff members in the civil engineering department.

Undergraduate helpers contributed substantially to this project. Jenna M. Diestelmeier and Chloe Shi helped with setting measurements. Cesar Rojas helped with compressive strength measurements. Their hard working is greatly appreciated.

I was also fortunate to have the substantial support from many people outside of University of Illinois. I am grateful for the exciting discussions with Professor Amr S. Meawad at Helwan University in Egypt and for his company day and night in the lab during his visit at Illinois finalizing the protocol to stop geopolymer reaction for later quantitative characterization. I want to thank Professor Xueying Li at Harbin Institute of Technology and Professor Xiaolu Guo at Tongji University for the discussions on geopolymers and cement chemistry and for the great help in daily life and thank Professor Givanildo Azeredo and Aline Figueirêdo Nóbrega de Azerêdo from Universidade Federal da Paraíba for their help when we were at Illinois. I would like to thank Professor En-Hua Yang for the invitation to discuss geopolymers and characterization techniques

at Nanyang Technological University in summer 2015. I appreciate so much the Skype discussion with Professor John L. Provis at University of Sheffield regarding NMR analysis of geopolymers, and the face-to-face discussions regarding various geopolymers issues in conferences. I was also fortunate to discuss the future of geopolymers as construction materials with Professor Zongjin Li at Hong Kong University of Science and Technology. I was inspired by ideas in studying kinetics of cementitious materials from Professor Xiaosheng Wei at Huazhong University of Science and Technology in China. Discussions with Professor Jinping Ou at Harbin Institute of Technology, Professor Jianzhuang Xiao at Tongji University and Professor Changdong Zhou at Beijing Jiaotong University helped me think about locating my nanoscale-geopolymer research in a broad map of civil engineering.

I would not be at the stage of finishing up this thesis study without the support and company of my dear colleagues and classmates at University of Illinois. They made me love here even more. Eric Kim and Sravanthi Pulligilla helped me start this geopolymer research. Numerous discussions with them and with William A. Hunnicutt provided me suggestions to solve many difficult problems in this research. Eric Kim collected the NMR and compressive strength data presented in Chapter 8. William A. Hunnicutt provided synthesized C-S-H and C-A-S-H specimens, which I used to validate chemical extractions as shown in the Appendix. Substantial support for setting measurement from Hajin Choi and Chul-Woo Chung made this part of my research much possible, and I am so grateful for their time and effort. Discussions with Weiping Zhu and feedback on my presentations from him during his visit at University of Illinois are greatly appreciated. Help from Piyush Chaunsali is greatly appreciated especially when I taught the lab for the course concrete materials. Discussions with Ranjani Mosale about research and about teaching CEE300 were so

helpful. Discussions on geopolymers with Dipobrato Sarbapalli were interesting and helpful. I acknowledge the help and company from Sujing Zhao, Daniel I. Castaneda, Bin Zhang, Chang Sun, Zhifang Zhao, Homin Song, Robbie Damiani, Palash Badjatya, Peter Stynoski, Di Wu, Seungmin Lim, Ardavan Ardeshirilajimi, Yu Song, Ruofei Zou, Ang Li, Jamie V Clark, Alexander Brand, James Bittner, Jacob Henschen, Kavya Vallurupalli, Abhishek Master, Agustin Spalvier Blanco, Kathleen Adelle Hawkins, Bartik Pandel.

My best friends at University of Illinois James Yifei Yang, Ruilong Zhang, Xu Wu, Tong Wu Sihang Wei, Yu Qian, Sujing Zhao, Zhanquan Zhang, Qiwen Chen, Siang Zhou, Jiaxin Chen, Yuxiang Wang, Feifei Wu, Xiaoyue Zhang, Danni Wang, Lili Su, Jiaming Xu made my life at Illinois so beautiful. My best friends outside of Illinois Pengcheng Hu, Ning Wei, Xiong Zhao, Yanfei Bai, Hongyang Song, Jingwei Lu, Yegang Wu and Qin Xiao have always supported me no matter how far apart we are. I would like to thank Yuanyuan Zhang for her unyielding support. Professor Guang Zhang at Northwestern Polytechnical University in China has been a good friend of mine and supported me since we first met in Hong Kong.

The unconditional support and love from my parents, grandparents and sister are beyond measure. My parents and grandparents are the most typical farmers in a small county in the central part of China. Their hard work, determination, perseverance and patience influenced me since I was a little kid. They made me who I am.

Table of contents

Chapter 1. Introduction

1.1 Geopolymers

The term ‘geopolymer’ was coined by the French scientist, Professor Joseph Davidovits, to refer to alkali-activated aluminosilicates (Davidovits 1982, Joseph 2011). Geopolymers are produced by reaction of an amorphous aluminosilicate precursor powder with a highly concentrated aqueous alkali hydroxide or silicate activating solution (Duxson et al. 2007a). The products have three-dimensional framework structures composed of silica and alumina tetrahedra. Water is generally entrapped in rather than chemically bonded with the framework structures.

There are many advantages of geopolymers. They are environmentally friendly as compared to the ordinary portland cements, as waste materials such as fly ash and slag can be utilized as the precursors (Palomo et al. 1999, Duxson et al. 2007a), and CO_2 emissions are substantially reduced by eliminating the high-temperature sintering and the limestone decomposition process in cement manufacturing (McLellan et al. 2011). They have shown high performance including high strength, low shrinkage, wide range of setting times, good high-temperature stability, and acid resistance, and potential to immobilize toxic metals (Van Jaarsveld et al. 1997, Palomo et al. 1999, Bakharev 2005, Duxson et al. 2007a, Duxson et al. 2007c, Suraneni et al. 2014, Provis et al. 2015).

The precursors can be metakaolin, fly ash or other reactive aluminosilicates (Duxson et al. 2007a). Metakaolin is suggested to be a model precursor, probably because it is amorphous and can be fully reacted. However, metakaolin geopolymers were suggested to be microstructurally different, as compared to fly ash ones (White et al. 2011b), probably because of the difference in the morphology of the precursors.

Long before geopolymers were promoted as sustainable construction materials, synthesis of alkali-activated slags was demonstrated in 1940s (Purdon 1940) and then discussed in review papers and/or books (Talling and Brandstetr 1989, Wang et al. 1995, Roy 1999, Shi et al. 2006). Products from these reactions are mainly calcium silicate hydrates (C-S-H), in which each calcium oxide layer is sandwiched by chains of silica tetrahedra, or C-A-S-H in which some silica tetrahedra are substituted by alumina. These chain-based structures are different from the three dimensional structures of geopolymers. While both these material systems are alkali activated materials, the geopolymer gel is mostly aluminosilicates with low calcium content and has highly coordinated zeolitic structure (Provis and van Deventer 2013).

Geopolymers have attracted great research interest since 1990s. Alkali-activated fly ash concrete with high strength and high acid-resistance was reported in 1994 (Wastiels et al.). Later, geopolymers made from precursors including metakaolin, low-, high-calcium fly ashes have attracted great research interest. Provis and van Deventer (2009) summarized initial patents (mainly from 1980s) and early technical papers (mainly in 1990s), as well as more comprehensive and deeper studies until 2008 on various geopolymers. In review papers by Shi et al. (2011) and by Provis and Bernal (2014), the chemistry of geopolymerization and phase assemblages that influence both early-age properties and long-term durability were discussed. Most recently, advances in characterization, durability, processing and environmental assessment of geopolymer gel and related alkali-activated materials were reviewed (Provis et al. 2015).

1.2 Setting of geopolymers

To promote applications of geopolymers in infrastructures, it is important to control their setting behaviors. Setting is the process by which a material changes from a fluid to a solid. In structural concrete, setting controls the time during which the material can be mixed, transported, and shaped. In ordinary portland cement, setting occurs approximately at the end of the induction period and the beginning of the acceleration period (Mindess et al. 2003). From the microstructural perspective, setting is associated with coagulation of cement particles and rigidification of the coagulated structure as hydration product forms (Bentz and Garboczi 1991, Jiang et al. 1995).

For geopolymers, setting has not been defined with respective to structural evolution. During geopolymer formation, Si and Al ions are released from dissolution of the aluminosilicate precursor, and they condense with each other to form a rigid three-dimensional network structure, as depicted in an often cited conceptual model (Duxson et al. 2007a). Experimental evidence from various techniques supports this model (Rees et al. 2007b, Silva et al. 2007, Favier et al. 2015, Rouyer and Poulesquen 2015). However, there remains a lack of information on detailed structural evolution during dissolution and condensation and its direct correlation with setting. One of the technical barriers is the difficulty to quantify structural evolution at early ages as the geopolymerization proceeds.

When calcium is added to geopolymers, setting is substantially accelerated. Several hypotheses have been proposed, such as the enhanced dissolution of the precursor, formation of C-A-S-H and nucleation effects (Lee and Van Deventer 2002, Yip et al. 2008, Lloyd et al. 2009, Temuujin et al. 2009, Puligilla and Mondal 2013, Puligilla and Mondal 2015). However, there remains lack of

direct experimental evidence, as it is not straightforward to quantify all the phases in the multiple-phase material system (the unreacted precursor, dissolved Si and Al, geopolymer gel and C-A-S-H) with evolving structures.

1.3 Objectives and organization of thesis

The overall objective of this study was to understand the setting behavior of geopolymers with and without calcium by probing structures down to nanostructural level. Metakaolin, a relatively pure aluminosilicate, was selected as the precursor. Setting behavior was measured. The solid-state ^{29}Si NMR tests are quantitative and commonly used for mature geopolymers. But they take too long to study the nanostructures of early-age geopolymers. The first task was therefore to develop a protocol to stop the geopolymerization reaction and also to quantify the early age structures. Another task was to probe the structural evolution during the dissolution and condensation process and examine its correlation with setting for non-calcium mixes. An additional task was to provide direct structural evidence to explain the accelerated setting with calcium.

In this thesis, Chapter 2 presents a detailed literature review. Methods for setting measurement, current understanding in structures and structural evolution of geopolymers, and commonly adopted characterization techniques are reviewed. Chapter 3 summarizes experimental methods, including both setting measurement and structural characterization. For quantification of early-age geopolymers, Chapter 4 aims to develop and validate a protocol to stop geopolymer formation. Chapter 5 presents another protocol to quantify structures using NMR tests. Chapter 6 explores correlation between nanostructural evolution and setting for geopolymers without calcium, by monitoring the structural connectivity of reactive Al and Si species during dissolution and

condensation. Chapter 7 examines setting and structural studies on calcium geopolymers, by monitoring the structural connectivity of the reactive species and quantifying the amounts of phases at different early ages. In Chapters 6 and 7, the metakaolin dissolution rate and extent were seen to substantially affect reaction kinetics and setting. Chapter 8 examines the effects of calcium on the reaction and on compressive strength at a later age. Chapter 9 presents conclusions.

Chapter 2. Literature review

2.1 Setting of geopolymers

Setting of geopolymers and cements is defined in a similar way, that is when the mix can no longer be properly handled and placed. To measure setting, penetration resistance methods are commonly used. The Vicat (ASTM C191) and Proctor (ASTM C403, Chung et al. 2010) tests are designed for cement pastes and mortar, respectively. The Vicat test uses one needle to measure penetration depth, and the Proctor test uses multiple-sized needles to monitor penetration strength. Both the methods are inexpensive but only allow discrete measurements. The Vicat test (Cheng and Chiu 2003, Silva et al. 2007) and the Proctor test (Puligilla and Mondal 2013, Suraneni et al. 2014) has been used in metakaolin and fly-ash geopolymers.

For continuous measurements, an ultrasonic wave reflection (UWR) method (Chung 2010, Chung et al. 2012) has been developed. The intensity of shear wave (S-wave) reflected at the interface between the buffer and the sample is monitored as a function of time. Ideally, this wave can be totally reflected when the sample is in fluid state but partially or none reflected when the sample is solid state. Reflection coefficient reduces during conversion from a fluid to a solid. The UWR method has been used to study metakaolin and fly ash geopolymers (Puligilla and Mondal 2013, Suraneni et al. 2014).

Setting times of geopolymer vary substantially depending on factors including (but not limited to) Si/Al ratio, calcium presence and water content. Lower Si/Al ratio accelerates setting in metakaolin geopolymers (Silva et al. 2007), for example, from 435 to 205 minutes when Si/Al decreased from 1.6 to 1.5 (Suraneni et al. 2014). Similar acceleration has been seen in fly ash geopolymers

(Suraneni et al. 2014). Acceleration of setting by calcium is commonly observed (Yip et al. 2005, Temuujin et al. 2009), for example, from 205 minutes to 30 minutes by replacing 30 wt% metakaolin with calcium hydroxide (Suraneni et al. 2014). A number of calcium salts (including $CaCl_2$, $Ca(OH)_2$, CaO and $CaSO_3$) at a low dosage were found to shorten the final setting times (measured by the Vicat tests) (Lee and Van Deventer 2002). Additionally, higher water content appears to delay setting, probably because critical Si and Al concentrations are needed for gel formation (Suraneni et al. 2014). The structural evolution is believed to control the setting behaviors. The structures, characterization methods, and setting versus structural evolution for geopolymers are reviewed in the following subsections. Structures of both zeolites (with similar structures as geopolymers) and C-A-S-H (present in calcium-containing geopolymers) are reviewed.

2.2 Structures

2.2.1 Zeolites

Geopolymers are believed to show similar short-range structures as zeolites (Provis et al. 2005). The name ‘zeolite’ originates from the Greek word ‘zeo’ and ‘lithos’, which mean ‘to boil’ and ‘stone’, respectively (Engelhardt and Michel 1987). This name describes the property that water is lost upon rapid heating.

The structure of heulandite, a typical zeolite, is shown in Figure 2.1 (Bish and Ming 2001). The tetrahedra (red, both silica and alumina) are interconnected to form a three-dimensional framework with interconnected cavities and channels. Loosely bound cations, such as sodium (green sphere) and potassium (light-blue sphere), balance the negative charge that arises due to Al incorporation

in the framework and can be exchanged by other cations in solutions or by H^+ ions. Water (large dark-blue sphere), usually present in the cavity, is not part of the framework structure and can be lost upon heating, consistent with the origin of the name. Loewenstein's rule (Loewenstein 1954) excludes the possibility of Al-O-Al bonding, a phenomenon that is generally true in aluminosilicate structures (Davidovits 1991, Akporiaye et al. 1996, Rowles and O'Connor 2003) and thus the Si/Al ratio ranges from unity at the minimum up to infinity in Al-free frameworks.

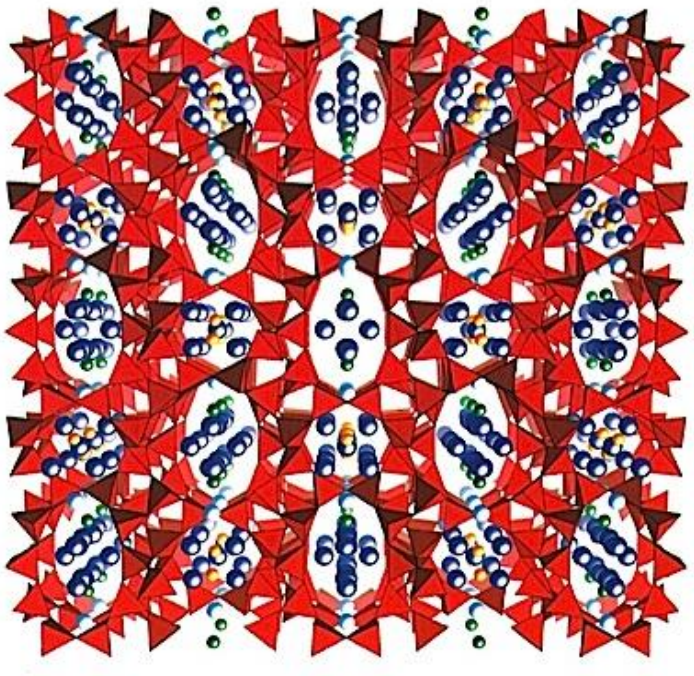

Figure 2.1. Schematic of structure for heulandite, a typical zeolite (Bish and Ming 2001).

Theoretical basis for strict application of Loewenstein's rule to the aluminosilicates is lacking. Many quantum chemical studies (Hass et al. 1981, Navrotsky et al. 1985, Pelmenschikov et al. 1992) indicate much higher energy (>400 kJ/mole of Al-O-Al bonding) is required to form Al-O-Al and Si-O-Si bond rather than Si-O-Al bond. In a later study (Tossell 1993), this value was

estimated to be much lower by considering appropriate charge balance and a different Si-O or Al-O bond distance, suggesting the presence of Al-O-Al is possible. More recently, Lee and Stebbins (2000) calculated distribution of Q^4(nAl) species in melt-quenched glasses and suggested the presence of Al-O-Al.

2.2.2 Geopolymers

Geopolymer structures at the short range are similar to zeolites, though not crystalline (Barbosa et al. 2000). A schematic is shown in Figure 2.2. The structures consist of a three dimensional network of Si and Al tetrahedra. Water and loosely bound cations (i.e., Na in Figure 2.2) are in the cavities. The chemical environment of each framework Si tetrahedron in geopolymer structures can be assigned as Q^4(nAl). Each tetrahedron is composed of one Si atom in the middle and four oxygen atoms at each point. The Q number denotes the number of oxygens in tetrahedron that are linked to other tetrahedra as depicted in Figure 2.3. For Q^4(nAl), the number of Al tetrahedra is "n" out of the total 4.

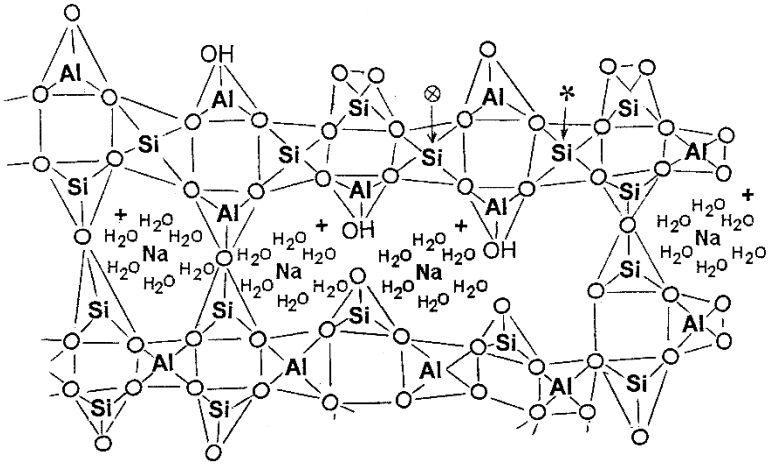

Figure 2.2. Proposed schematic structure of Na-geopolymers (Barbosa et al. 2000).

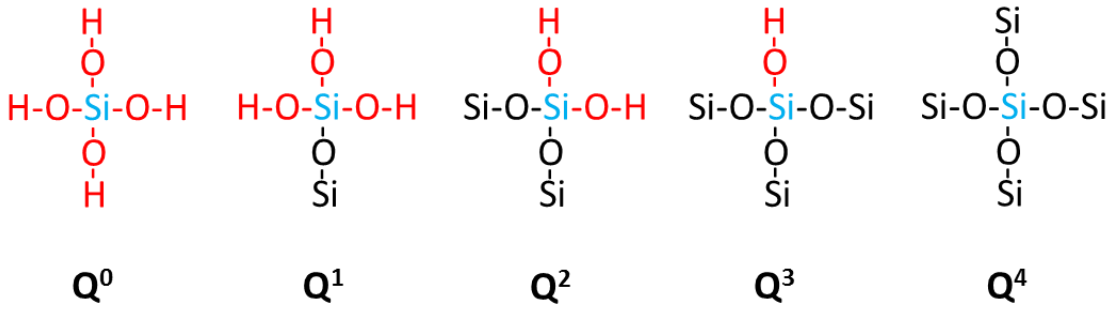

Figure 2.3. Schematics of Si environment with different Q numbers.

2.2.3 C-A-S-H

When calcium is present in the precursor, C-A-S-H (i.e., calcium aluminum silicate hydrate) forms in addition to the geopolymer gel. The structure of C-A-S-H is similar to C-S-H (i.e., calcium silicate hydrate), which is the main strength contributor in hydrated cements and concrete. Shown in Figure 2.4 (a), the C-S-H structure consists of calcium oxide layers sandwiched with chains composed of Si tetrahedra with either pairing (pointing toward the calcium oxide sheet) or bridging (pointing toward the other direction and linking the pairing ones) positions. The Si environment is Q^2 and Q^1, and mainly Q^2 when the chain is long. When Si tetrahedra are partially substituted by Al tetrahedra, usually in bridging tetrahedra, the C-S-H becomes C-A-S-H as shown in Figure 2.4 (b). With Al substitution, the structure usually becomes more polymerized than the original C-S-H, and Q^3 Si, probably with Al substitution, could be present (Hunnicutt 2013). Interlayer cations balance the charge. When the Ca/Si ratio decreases and/or Al/Si increases, more cations including H^+ are required to balance the charge. In either C-S-H or C-A-S-H, water is part of the structure, either associated with hydroxylated Si or present in the interlayer position (Taylor 1997).

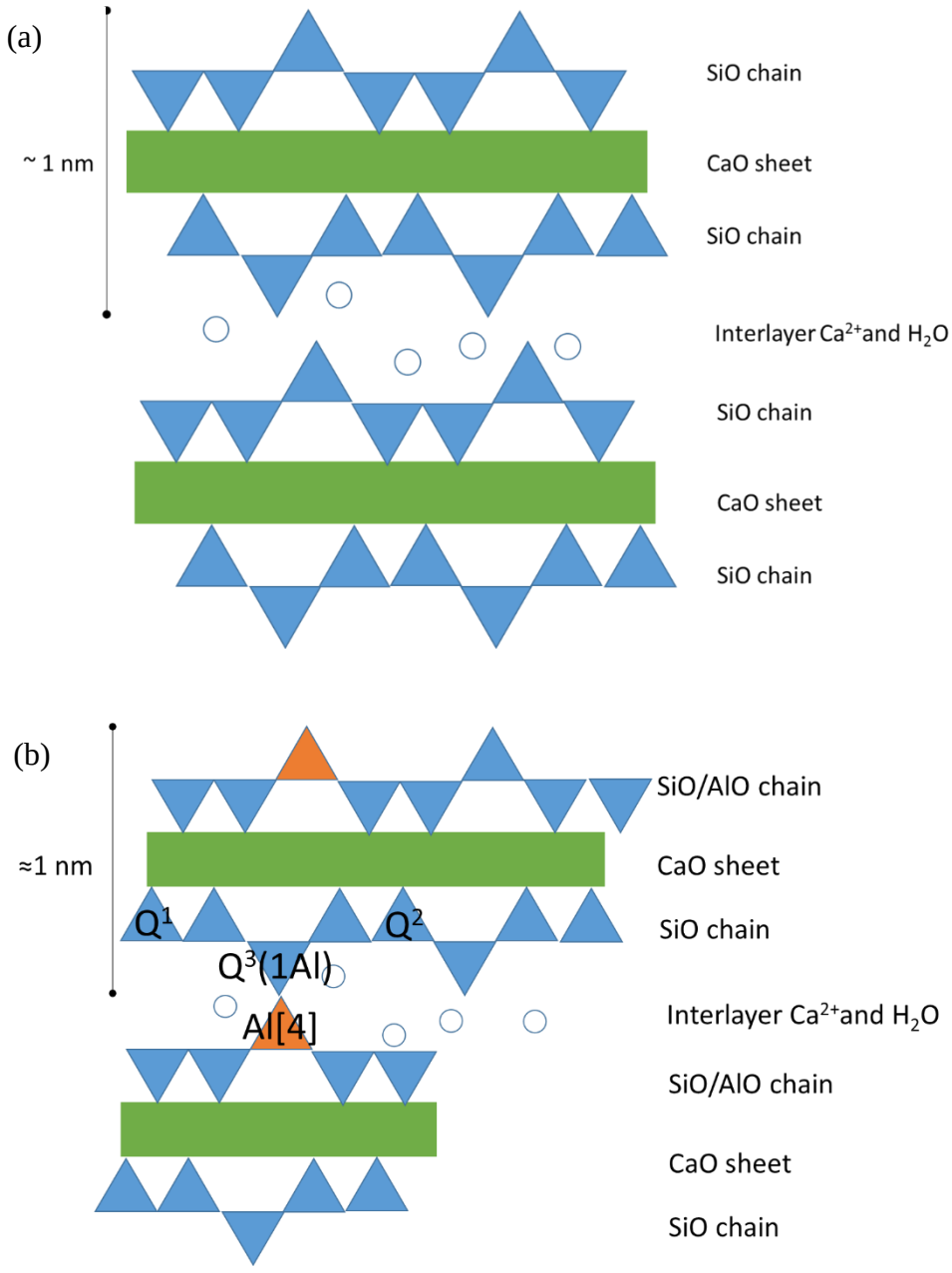

Figure 2.4 Schematics of nanostructures for (a) C-S-H and (b) C-A-S-H (Hunnicutt 2016).

There are a few differences in nanostructures between C-A-S-H and geopolymer gel. The Si environment in geopolymers is mainly Q^4 in the three-dimensional network structure, but in C-A-S-H is mainly Q^{1-2} and occasionally Q^3 in the two-dimensional structure. Water in geopolymers is

not an essential part of the framework, but in C-A-S-H is part of the nanostructure. The Na and K ions can balance the charge in both phases, but Ca is the main charge balancer in C-A-S-H.

2.2.4 Coexistence of geopolymers and C-A-S-H

In calcium-containing geopolymers, the geopolymer gel coexists with the C-A-S-H (Alonso and Palomo 2001b, Alonso and Palomo 2001a, Yip and van Deventer 2003, Yip et al. 2005, Yip et al. 2008, Temuujin et al. 2009, Garcia-Lodeiro et al. 2011, Puligilla and Mondal 2013, Puligilla and Mondal 2015). The coexistence of the two phases has been identified, for example, in alkali-activated metakaolin-slag mixes (Yip and van Deventer 2003, Yip et al. 2005) and in metakaolin-calcium hydroxide mixes (Alonso and Palomo 2001b). The geopolymer gel is the predominant phase at high pH, for example, at 7.5-M NaOH or higher in the metakaolin-slag mixes (Yip et al. 2005) and at 10-M NaOH or higher in the metakaolin-calcium hydroxide mixes (Alonso and Palomo 2001b).

The stability of the two phases mainly depends on alkalinity as depicted in Figure 2.5 (Garcia-Lodeiro et al. 2011). When pH is higher than 12, presence of Ca does destabilize geopolymer gel (N-A-S-H) to form C-A-S-H; when pH lower than 12, Ca would exchange with Na (for example) to form (Na, Ca)-A-S-H with a three-dimensional aluminosilicate framework. The Ca^{2+} is likely to form $[CaOH]^{+}$, due to its relatively high charge density and more negative enthalpy compared to Na^{+} and K^{+}, especially at high pH (> 12) when polarization of electron density enhances Ca-O bonding but weakens O-H bonds (Macphee and Garcia-Lodeiro 2011). The $[CaOH]^{+}$ species promote the formation of calcium hydroxide and C-A-S-H but degrade the geopolymer gel when pH is sufficient for this polarization.

A phase diagram for $CaO\text{-}SiO_2\text{-}Al_2O_3\text{-}H_2O$ was tentatively proposed as shown in Figure 2.6 (Garcia-Lodeiro et al. 2011). In the diagram, AFm represents hemicarboaluminate and monocarboaluminate phases, and C-A-S-H and N-A-S-H are included. Further work is needed on the Al-rich phases.

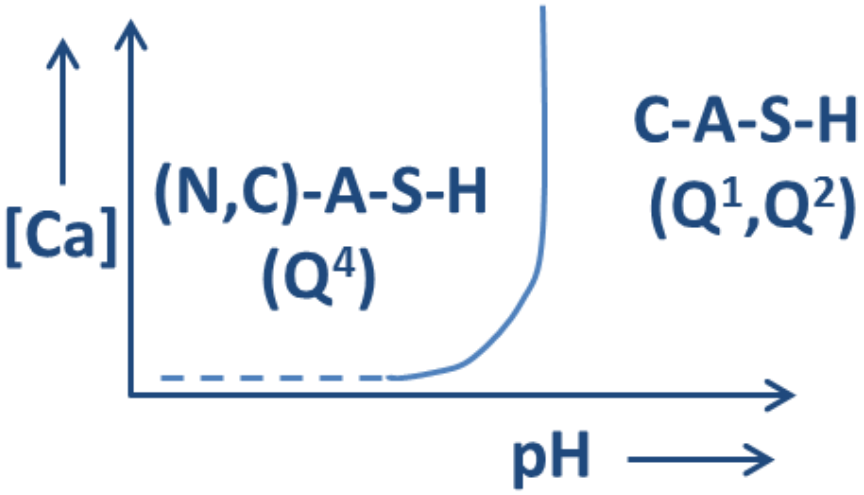

Figure 2.5. Proposed effects of pH and Ca concentration on the stability of N-A-S-H (geopolymer gel) adopted from Garcia-Lodeiro et al. (2011) and redrawn by Struble (2013).

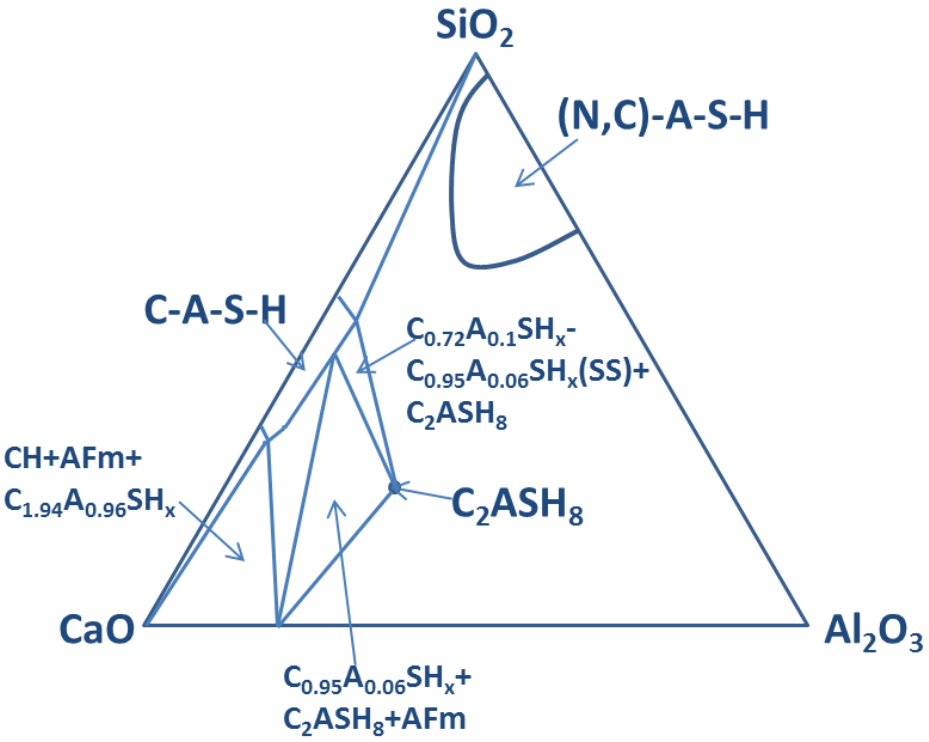

Figure 2.6. Proposed field boundaries in a CaO-Al_2O_3-SiO_2-H_2O phase diagram adopted from Garcia-Lodeiro et al. (2011) and redrawn by Struble (2013).

2.3 Characterization of geopolymer structures

The micro- and nanostructures of geopolymers have been examined by various techniques. Microscopy examination reveals the morphology. The X-ray diffraction (XRD) tests provide little information due to the amorphous feature of geopolymers. The infrared and magnetic-resonance-based spectroscopies yield substantial information on the chemical environment. All these characterization techniques are reviewed in this section. Some other techniques are covered in the review of nanostructural evolution (Section 2.4).

2.3.1 Microscopy

Geopolymers have been characterized by scanning electronic microscopy (SEM) and transmission electron microscopy (TEM), with typical micrographs shown in Figure 2.7 and Figure 2.8, respectively. In Figure 2.7, the polished surface of the geopolymer specimen shows certain porosity. The porosity was found to depend on the Si/Al ratio, less porous at Si/Al ≥ 1.65 but highly porous at Si/Al ≤ 1.40 (Duxson et al. 2005b). In Figure 2.8 at a smaller scale, the gel indicates amorphous nature but with a particle-like structure around 50 nm (Schmücker and MacKenzie 2005).

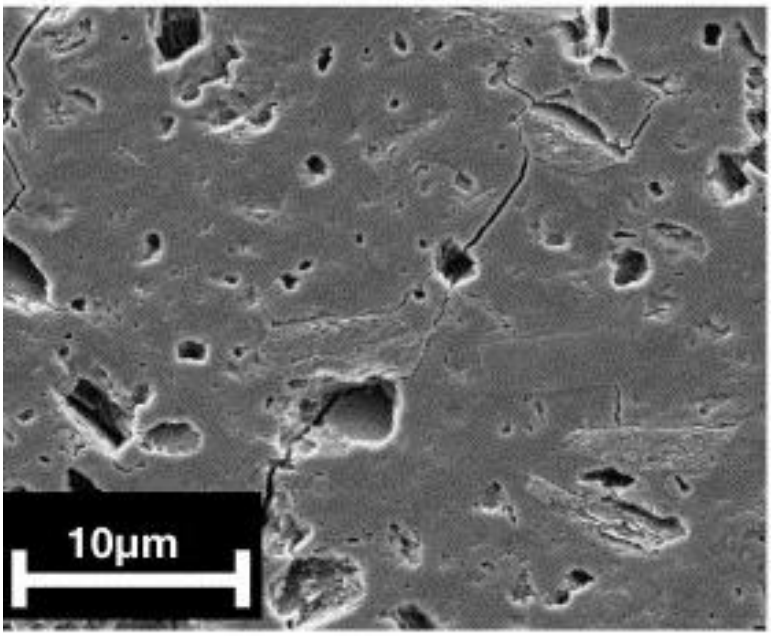

Figure 2.7. SEM micrograph of geopolymer with Si/Al ratio of 1.65 (Duxson et al. 2005b).

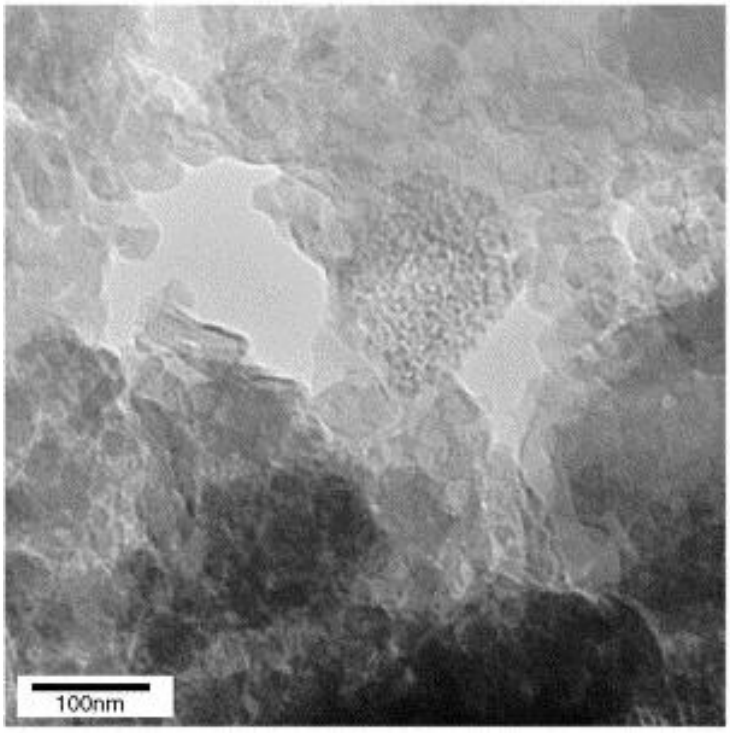

Figure 2.8. TEM micrograph of Na-geopolymer with Si/Al ratio of 1.65 (Schmücker and MacKenzie 2005).

2.3.2 XRD

XRD has been used to probe the long-range ordering structures of geopolymers. Typical patterns of the metakaolin (MK) and metakaolin geopolymers are shown in Figure 2.9 (Silva et al. 2007). The denotation "Si25", for example, represents the Si/Al ratio of 1.25 (i.e., $SiO_2/Al_2O_3 = 2.5$). In the MK pattern, there are sharp peaks assigned to quartz and TiO_2 and a hump centered around 22^o, a characteristic of metakaolin. After the geopolymerization reaction, the broad hump shifts to around 28^o, a characteristic of geopolymers. Because of the amorphous feature of geopolymers, XRD tests do not provide much information on the structures.

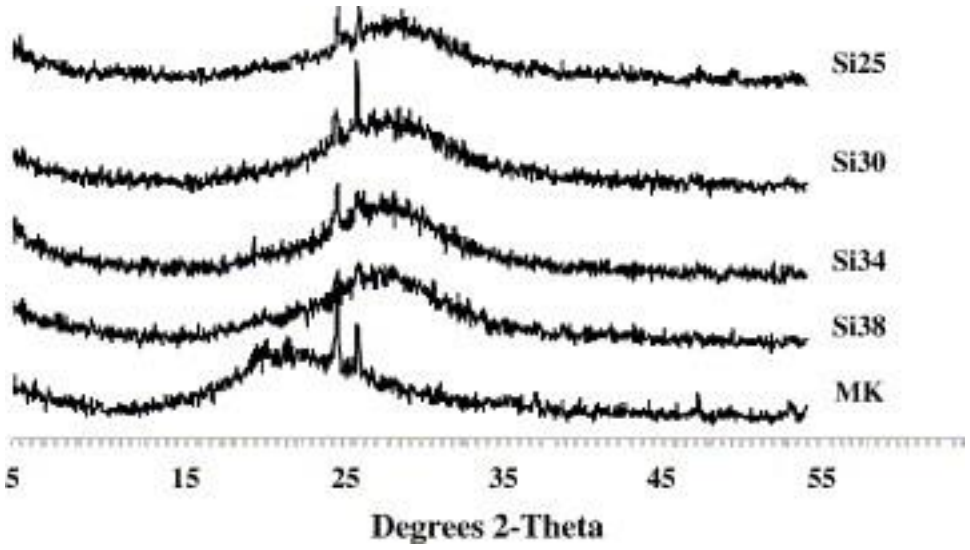

Figure 2.9. XRD patterns of metakaolin (MK) and metakaolin geopolymers with SiO_2/Al_2O_3 ratios from 2.5 to 3.8 (Silva et al. 2007).

2.3.3 Infrared spectroscopy

Compared to microscopy and XRD, infrared spectroscopy probes chemical environment at short range. Fourier transform infrared (FTIR) spectroscopy is commonly used. FTIR obtains an infrared spectrum of a material by collecting absorption/emission information and processing using a Fourier transform (Smith 2011). The instrument components include IR source, detector, beam splitter. For the mid-IR range (5000 – 400 cm^{-1}), the wavelength of the IR source is 2-25 μm. The detector is made of pyroelectric materials and responds to temperature changes upon the IR radiation. Beam splitter is used to divide a beam of IR radiation into multiple beams and is commonly made of KBr.

Two FTIR spectra of synthesized geopolymers are shown in Figure 2.10 (Garcia-Lodeiro et al. 2010). The main peaks at 1007 and 1020 cm^{-1} are attributed to asymmetric stretching vibrations

of Si-O-T bonds (T = Si or Al) for gels G1 (Si/Al = 1) and G2 (Si/Al = 2), respectively. Peaks at lower wavenumbers are assigned to the stretching vibrations of tetrahedral aluminum and bending vibrations of Si-O-Si or Si-O-Al as marked in the figure.

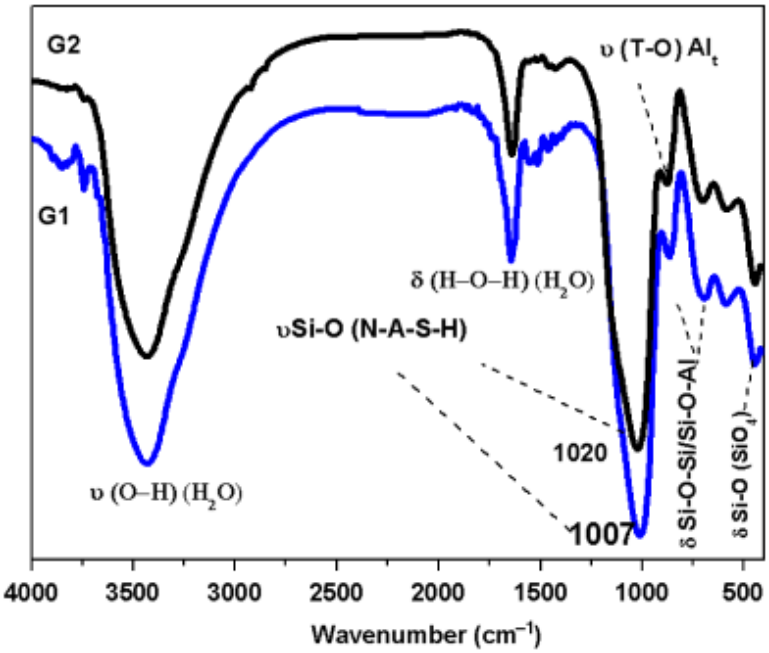

Figure 2.10. FTIR spectra of synthesized geopolymer gels with Si/Al ratio 1 (“G1”) and 2 (“G2”) (Garcia-Lodeiro et al. 2010).

FTIR shows some advantages over the other commonly used techniques to characterize geopolymer structures. It has been used to monitor the nanostructural evolution (Rees et al. 2007b, Puligilla and Mondal 2015) due to the rapid data collection. It has also been used to probe the nanostructural heterogeneity, which correlated with the reaction kinetics (Hajimohammadi et al. 2010). Both applications are discussed in the review of structural evolution later (Section 2.4). FTIR tests provide additional information, for example, presence of carbonate and hydroxide groups.

2.3.4 NMR spectroscopy

2.3.4.1 Introduction

NMR spectroscopy probes the short-range structures. It examines the absorption frequencies of electromagnetic radiation by certain nuclei in any chemical environment (Keeler 2011). Any changes in bond lengths, angles and molecular symmetry affect peak position and width in the NMR spectra.

The NMR spectrum originates from the interaction of an applied field with nuclear spins. The spin is a fundamental physical property. Atomic nuclei are made of neutrons and protons. The spin of a nucleus is NMR active (i.e., non-zero spin) when the number of protons or the number of neutrons are not both even. NMR signals can be contributed by Zeeman, chemical shielding, direct dipolar, indirect spin-spin (J-coupling) and quadrupolar interactions (Keeler 2011). The Zeeman interaction occurs between nuclear spins and the applied static magnetic field (B_0). The magnitude of this interaction is proportional to B_0 and is generally the highest among all the interactions. This interaction results in different energy level of spin states. Transitions between these energy states occur when an oscillating radio frequency (rf) pulses are applied, and thus an NMR signal is observed. The chemical shielding occurs when nuclear spins interact with a local secondary magnetic field. This field is due to overlaps of electron orbitals of atoms within a molecule. Therefore, chemical shielding is sensitive to the chemical environment within a molecule. Direct dipolar interactions occur between the magnetic moments of two spins through space, while indirect spin-spin interactions occur between the two spins by the electrons in the orbitals within a molecule. The indirect spin-spin coupling is usually too small to be observed in solid-state NMR tests. Quadrupolar interaction occurs between quadrupole moment and the local electric field

gradient. In quadrupolar nuclei (I > ½), the charge distribution is asymmetric, unlike the spherical distribution seen in spin-1/2 nuclei.

Magic-angle spinning (MAS) is a common technique used to reduce the line broadening in solid-state NMR spectroscopy. Unlike the sharp peaks of chemical shifts in liquid state due to rapid molecular tumbling, broad peaks are observed in solid due to anisotropic orientation of spins. With the MAS technique, the sample is rotated at an angle of 54.74^{o} with respect to the external magnetic field at frequency on the order of kHz. The anisotropic interactions are averaged to a certain extent so that the line width is substantially reduced.

2.3.4.2 Zeolites and other aluminosilicate minerals

Abundant literature of ^{29}Si and ^{27}Al NMR characterization can be found for zeolites and other aluminosilicate minerals, and is of great importance for the study of geopolymers due to the structural similarity. Zeolites can be used as catalysts and molecular sieves, and aluminosilicate minerals are the most abundant materials in the earth's crust.

In the zeolites, the Si and Al ordering is investigated based on the relative Q^4(nAl) (n = 0-4) populations from the ^{29}Si NMR spectra. When Loewenstein's rule is fulfilled (i.e., no Al-O-Al linkages), the Si/Al ratio of the three-dimensional framework in the zeolites can be estimated by Equation 2.1

$$\frac{Si}{Al} = \sum_{n=0}^{4} I_{Si(nAl)} / \sum_{n=0}^{4} \frac{n}{4} I_{Si(nAl)} \qquad (2.1)$$

where $I_{Si(nAl)}$ is the intensity of the Q^4(nAl) peaks (n = 0 - 4) in the ^{29}Si NMR spectra.

With this equation, the Si/Al ratios have been estimated for different types of zeolites, such as zeolite X and Y (Engelhardt and Michel 1987). These ratios are consistent with analytical chemical analysis over the whole range of compositions (Si/Al = 1.0~5.0). This consistency indicates Loewenstein's rule is obeyed. As an example in Figure 2.11 (Sartbaeva et al. 2013), the Si/Al ratio was calculated to be 2.06, in agreement with the 2.03 from the chemical analysis.

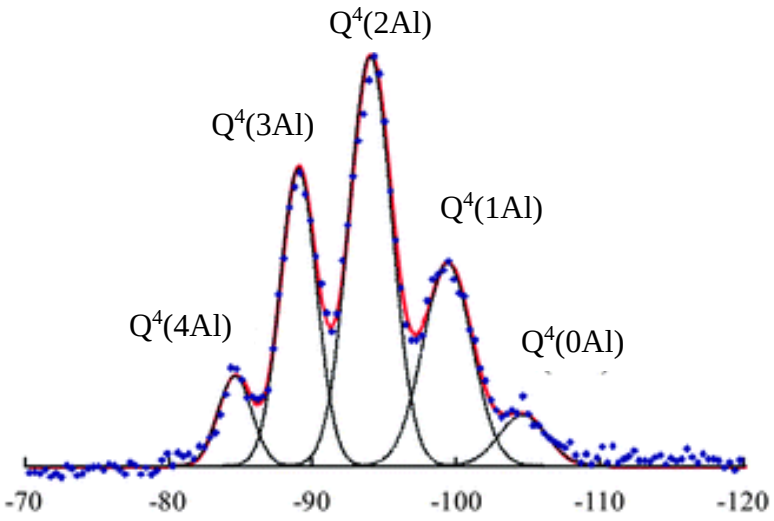

Figure 2.11. The ^{29}Si MAS NMR spectrum for a zeolite Y. Black peaks, red spectrum and blue symbols represent fitted peaks (all Q^4 Si sites), fitted spectrum and experimental spectrum, respectively (Sartbaeva et al. 2013).

The peak assignments of the Q^4(nAl) sites of the zeolites are not always straightforward. For zeolite A, inconsistency of the calculated Si/Al ratio (from the ^{29}Si NMR tests) with the actual composition (Si/Al = 1) initiated debates for a while (Engelhardt and Michel 1987). With this composition, only Q^4(4Al) should be present, i.e., Si and Al atoms occupy alternate positions.

However, the single peak was observed at -89.6 ppm, a position generally corresponding to the Q^4(3Al) peak in other zeolites, such as zeolite X and Y. Differences in peak assignment were seen in a number of investigations. Later, more evidence on the crystal structures suggested the Si and Al atoms occupy alternative positions, and thus the assignment of Q^4(4Al) is regarded reasonable.

The NMR studies of aluminosilicate minerals are also important to the study of geopolymer structures. The structural changes during the conversion from kaolin to metakaolin are of significant interest (MacKenzie et al. 1985, Rocha and Klinowski 1990), as metakaolin is a common precursor to synthesize geopolymers. The Q^4(nAl) sites of analcime, a typical aluminosilicate material, were quantified based on the ^{29}Si NMR spectra, and the Si/Al ratio was found to be consistent with the chemical composition (Kim and Kirkpatrick 1998). A same methodology applies to geopolymers. Additionally, results from the high-resolution ^{17}O triple quantum-MAS (3Q-MAS) NMR further confirmed analcimes adheres to Loewenstein's rule (Lee et al. 2003), providing insight into geopolymer structures.

The ^{27}Al NMR tests have also been conducted to examine the structures of the zeolites and aluminosilicate minerals but with limited success. With quadrupolar interactions of the ^{27}Al nuclei, the line widths become broad and the quantitative analysis is difficult. The chemical shifts for 4-, 5- and 6-coordinated Al are +50 to +80 ppm, +30 to +40 ppm and -10 to +20 ppm, respectively (Engelhardt and Michel 1987).

2.3.4.3 Geopolymers

In this section, characterization of geopolymers by the ^{29}Si NMR tests is reviewed. The ^{27}Al NMR characterization is covered during the review of the nanostructural evolution (Section 2.4). As an

initial NMR investigation, the ^{29}Si MAS spectrum of a metakaolin geopolymer is shown in Figure 2.12 (Davidovits 1991). This spectrum is believed to contain five Q^4(nAl) (n = 0-4) sites, with typical peak ranges shown under the spectrum.

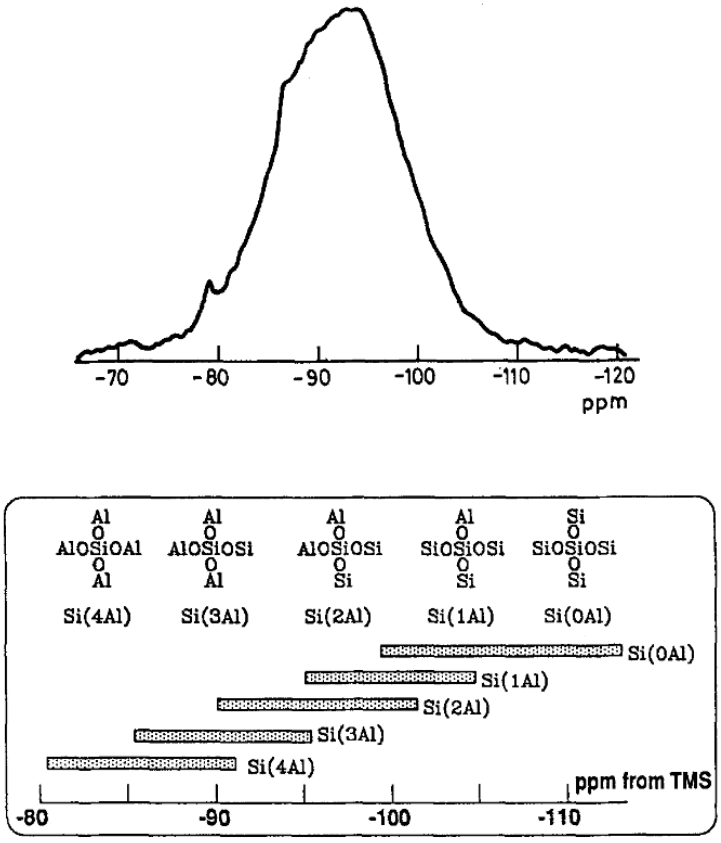

Figure 2.12. ^{29}Si MAS NMR spectrum of a metakaolin geopolymer (Davidovits 1991), with all Q^4 sites.

Duxson et al. (2005d) quantified the structural ordering by the ^{29}Si MAS NMR tests. A typical deconvolution of a metakaolin based Na-geopolymer (Si/Al 2.15) spectrum is shown in Figure 2.13. The five deconvoluted peaks from left to right are assigned to Q^4(4Al), Q^4(3Al), Q^4(2Al),

Q^4(1Al) and Q^4(0Al) Si sites. The deconvoluted Si/Al ratios were found to be consistent with the nominal values as depicted in Figure 2.14.

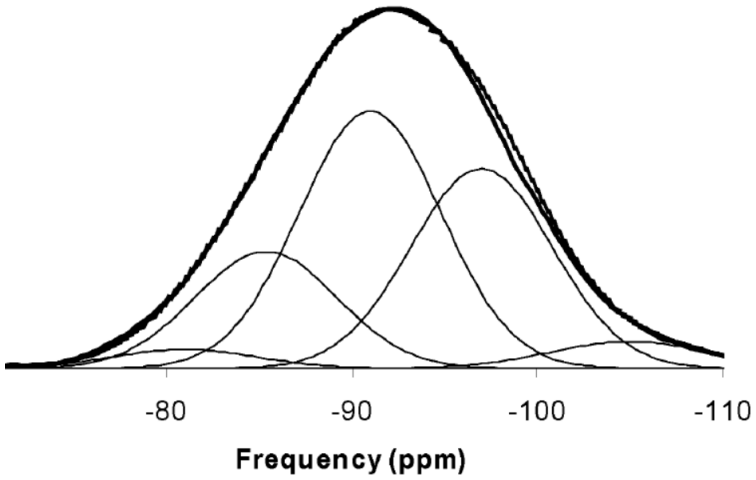

Figure 2.13. Deconvolution results for a metakaolin-based Na-geopolymer with Si/Al of 2.15. Heavy and faint lines are experimental spectra and fitted peaks, respectively (Duxson et al. 2005d).

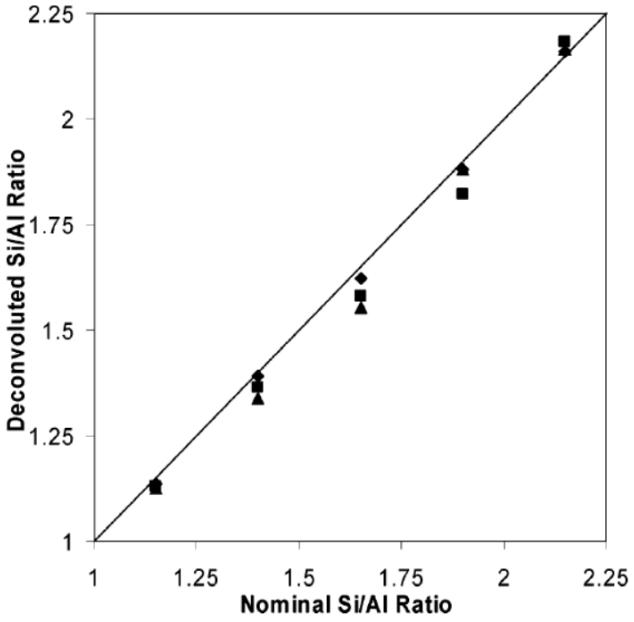

Figure 2.14. Comparison of deconvoluted and nominal Si/Al ratios for Na-, K- and NaK-geopolymers (Duxson et al. 2005d).

2.4 Setting and structural evolution of geopolymers

2.4.1 Non-calcium mixes

The conceptual model (Figure 2.15) of nanostructural evolution has been developed by Duxson et al. (2007a). Dissolution of the aluminosilicate precursor liberates aluminates and silicates into the liquid, resulting in a supersaturated aluminosilicate solution. The species then undergo gelation process to form aluminosilicate gel, which continues to rearrange and reorganize to form the three-dimensional geopolymer network. However, this model does not specifically identify the step associated with set. Supporting evidence and its correlation with setting are reviewed in the following subsections.

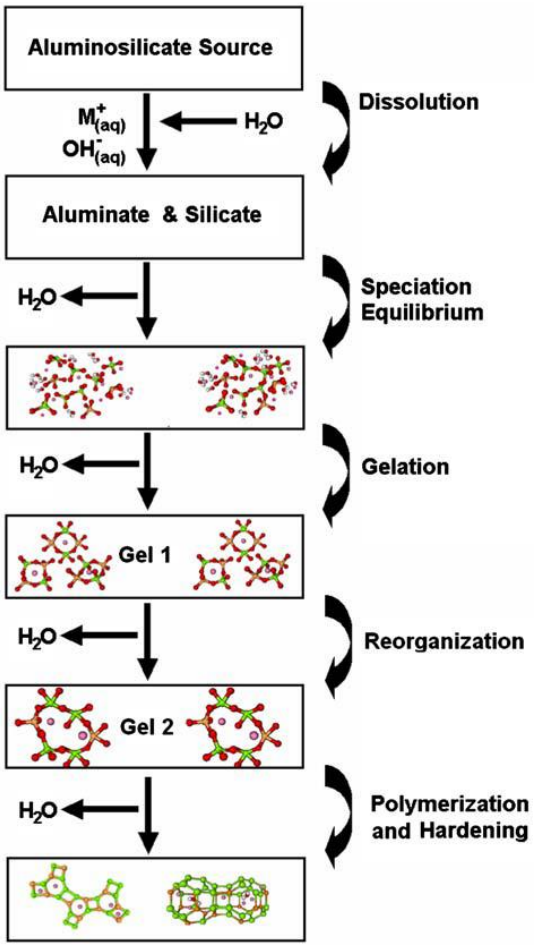

Figure 2.15. Conceptual model for nanostructural evolution of non-calcium geopolymers by Duxson et al. (2007a).

2.4.1.1 Dissolution

The dissolution of the precursor affects the concentrations of Si and Al and thus the geopolymerization kinetics. Leaching tests have been used to measure dissolution kinetics. In one study (Feng et al. 2004), 100-ml leaching solution was added to 50-g metakaolin or fly ash (with and without ultrasonication), and the Si and Al concentrations were measured as a function of time. Ultrasonication was found to enhance the dissolution. However, results here were said to be

confounded by gel precipitation (Provis and Van Deventer 2009). In another study (Chen et al. 2011), leaching kinetics of a fly ash was examined at a water-solid mass ratio of 40 g/g. The rate constants at early ages (before massive gel formation) were claimed to reflect the intrinsic glass properties of the fly ashes.

Acid attack has been used to measure the degree of dissolution. An acid attack using HCl solution (with 1:20 ratio of 37wt%-HCl solution to water by volume) was used to dissolve the reaction product and leave the unreacted fly ash in the hydroxide-activated geopolymers (Fernández-Jiménez et al. 2006b). The mass loss and the concentration of dissolved Al were measured. The HCl extractions were also conducted in other studies for both fly ash and metakaolin geopolymers (Granizo et al. 2002, Fernández-Jiménez et al. 2006a). For the silicate-activated mixes, the HCl extraction does not measure the degree of dissolution as the removed gel contains Si from the external silicates. Additionally, this time-consuming analysis can only be conducted at discrete times and can easily result in experimental errors.

Some characterization techniques have been used to examine the dissolution process. In a pair distribution function (PDF) analysis of both hydroxide- and silicate-activated metakaolin (White et al. 2011b), structural changes were suggested to mainly involve dissolution with limited polymerization and gelation in the initial 17 hours, and the dissolution in the hydroxide mix was found to be faster as attributed to the higher pH than in the silicate mix. In another study by FTIR (Rees et al. 2007b), rate of dissolution was low at low alkalinity but kept relatively constant in moderate and high alkali hydroxide-activated fly ash specimens.

The ^{27}Al NMR tests have also been carried out to examine the dissolution process. The 'detectable' Al in the liquid-state ^{27}Al NMR spectrum was quantified to examine the reaction kinetics (Rahier et al. 2007). In some other studies (Favier et al. 2013, Favier et al. 2015), the amount of Al detected by liquid-state ^{27}Al NMR tests increased and then decreased as the reaction proceeded. These liquid-state ^{27}Al NMR studies do not directly measure the dissolved Al species as some may precipitate and become invisible, nor probe structural connectivity of the Al species during dissolution. Solid-state ^{27}Al spectra have confirmed that dissolution of metakaolin is associated with the conversion of 5- and 6-coordinated to 4-coordinated Al (Duxson et al. 2005a, Provis and Van Deventer 2009), but this coordination evolution has not been systematically monitored. The solid-state ^{27}Al NMR spectroscopy seems to be the most promising method to study the dissolution, considering its capability to monitor the changes in structural connectivity and also to avoid the confusion by geopolymer gel precipitation encountered in the liquid-state tests (because Al in the gel and dissolved Al are both 4-coordinated). It should be noted that quantitative interpretation of ^{27}Al NMR spectra is not straightforward because the ^{27}Al nucleus is quadrupolar (Man and Klinowski 1988, Massiot et al. 1990b).

2.4.1.2 Condensation

In general, factors including (not limited to) the Si/Al ratio, curing temperature, presence of nucleation sites affect the condensation rate. Condensation can take place between silicate species themselves or between aluminate and silicate species, and the latter has been shown to be more likely and proceed faster at a lower Si/Al ratio (Silva et al. 2007). A higher curing temperature was found to increase the early-age compressive strength of the metakaolin geopolymers (Rovnaník 2010), a phenomenon expected to be related to enhanced condensation. The addition of the high

surface area Al_2O_3 nanoparticles was found to eliminate the induction period normally seen in the hydroxide activated fly ash geopolymer (Rees et al. 2008), but its effect was not investigated in silciate-activated fly ash and also in metakaolin geopolymers.

Among various techniques, in situ FTIR has been used to monitor the structural evolution. For a hydroxide-activated fly ash geopolymer, the functional groups corresponding to the geopolymer gel (around 958 cm^{-1}) and the unreacted fly ash (around 1055 cm^{-1}) were monitored with time as shown in Figure 2.16 (Rees et al. 2007b). The geopolymer curve shows an induction period followed by gel formation. In the same study, rate of gel formation increased with alkalinity to a maximum value and then decreased. The reduced rate at high alkalinity was attributed to multiple factors including ion pairing in solution, gel dissolution at high alkali-concentration and the amount of water available for hydrolysis. This methodology was only applied to hydroxide-activated rather than also silicate-activated mixes.

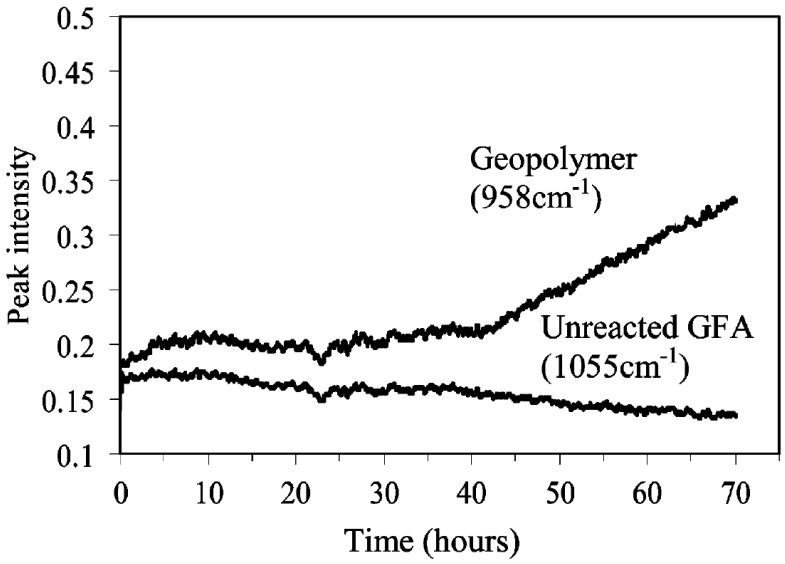

Figure 2.16. Functional group analysis of a hydroxide-activated fly ash geopolymer by in-situ FTIR (Rees et al. 2007b).

Additional information has been obtained from other tests. By in-situ neutron based PDF analysis, structural changes from early ages to 90 days of reaction were seen to transit from initially formed geopolymer gel to more ordered gel via cross-linking (White et al. 2011b). By X-ray scattering based PDF analysis, the reaction extent was estimated for both hydroxide and silicate-activated metakaolin with or without slag (White et al. 2013). By calorimetry, effects of alkalinity on the reaction kinetics, i.e., lengthened induction period and higher total heat with increasing alkalinity, were seen in metakaolin geopolymers (Granizo and Blanco 1998).

Structural evolution in the above reviewed studies has not directly correlated with setting. Recently, several studies have investigated nanostructural evolution and setting more directly. Favier and colleagues (2013) conducted rheology and NMR studies on fresh properties of sodium silicate activated metakaolin geopolymers. The flow properties at very early ages (less the 15 minutes after

mixing, stage I shown in Figure 2.17) were attributed to formation of an aluminosilicate gel with Si/Al<4.5, based on comparison of flow properties with synthesized gels. Another study by Favier et al. (2015) focused on a later age (a few hours after mixing, stage II shown in Figure 2.17). The concentrations of static-NMR-observable Al and Na both decreased at a few hours after mixing, a phenomenon attributed to the incorporation of Al as framework-site and Na as charge-balancer in the gel with low mobility. The authors therefore concluded a denser "Gel 2" was formed from the Al-rich gel and oligomers, as also supported by the appearance of a shoulder at around -105 ppm in the static ^{29}Si NMR (i.e., without magic angle spinning and mainly liquid species are detected) spectra at the same time. This "Gel 2" was claimed to be static-NMR-invisible and contribute to substantial strength development. However, no attempts were made to directly probe the structures of the gel, for example, the changes in structural connectivity of the Si and Al species involved in the gel formation.

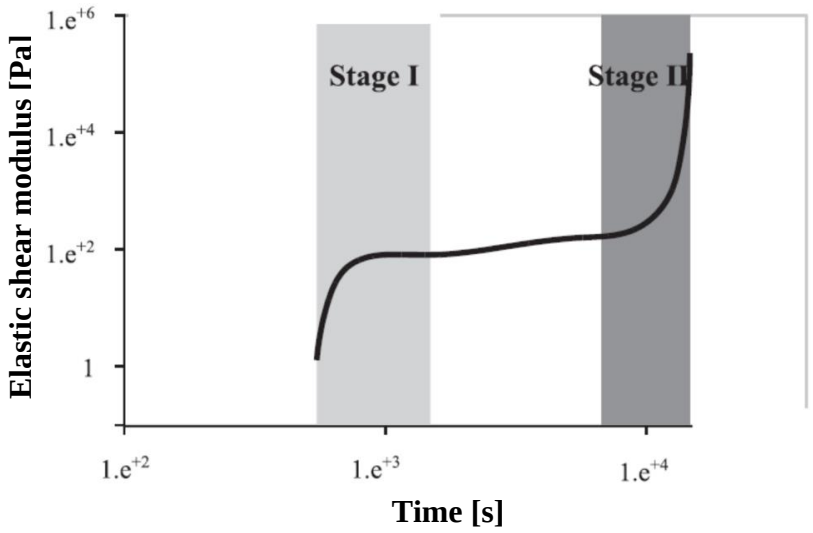

Figure 2.17. Elastic shear modulus as a function of time for a geopolymer specimen from rheology tests (Favier et al. 2015).

Another recent study by Rouyer and Poulesquen (2015) provided evidence to support geopolymerization as a fractal percolation process. A criterion used to assess the gel point of organic polymers was used for the geopolymers. The gel point is defined as the time when the elastic and viscoelastic moduli tended to become parallel, a phenomenon that indicates a percolating solid phase has formed. For the metakaolin geopolymer, this assessment of gel point from the rheology tests coincided with the time when percolating network starts to form as indicated by the SAXS tests. However, no direct nanostructural characterization of the gel was presented in this work.

Generally, 10-20 hours is needed to collect a quantitative ^{29}Si MAS NMR spectrum. This period is too long to monitor the early age structural changes. One way is to suspend the reaction and freeze the structures at different early ages prior to the quantitative ^{29}Si MAS NMR tests. In Chapter 4, methods for stopping the reaction are reviewed for cementitious materials, and an effective method has been developed and validated for geopolymers. Another way to characterize the early age structures by ^{29}Si NMR is to conduct liquid-state tests, for which less than 1-hour data collection is generally sufficient. The liquid-state spectra of a metakaolin-based Na-geopolymer in Figure 2.18 were shown to evolve with time but with little interpretation (Barbosa et al. 2000). With careful examination of these changes associated with the reactive species, more insight would be gained into the nanostructural evolution.

In summary, the condensation is affected by a few factors including the Si/Al ratio, curing temperature and presence of nucleation sites. Different techniques have been conducted to examine the nanostructural evolution during the condensation process. The combination of rheology and static NMR tests indicated formation of Al-rich gel and gel with high stiffness, with the latter

coincided with substantial strength development. A study based on rheology and SAXS tests indicated the nanostructural evolution is a percolation process. However, none of these studies has probed the evolution of the structural connectivity, which would provide more insight into setting. The liquid-state ^{29}Si NMR tests show potential to probe the evolving structures.

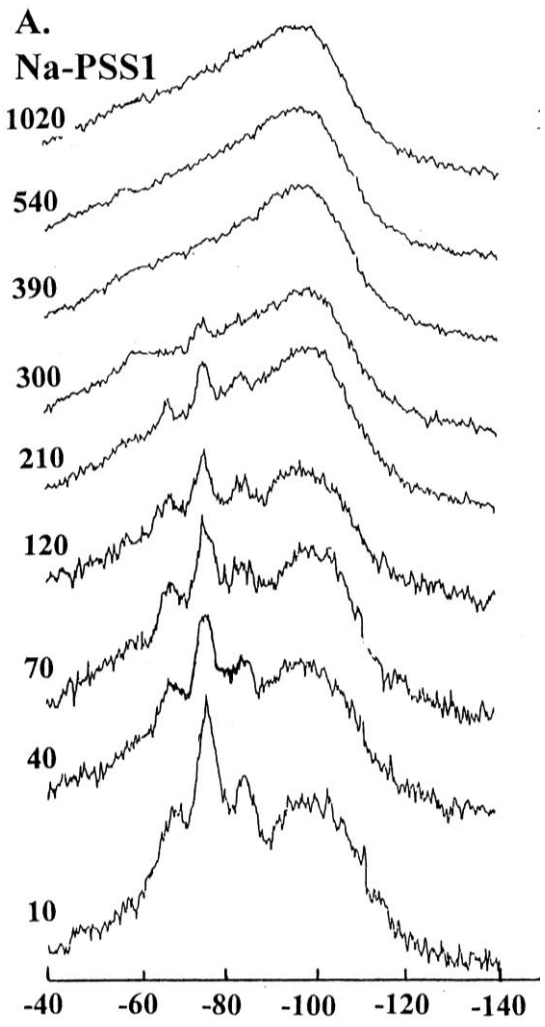

Figure 2.18. Liquid-state ^{29}Si NMR spectra of a metakaolin-based Na-geopolymer (Si/Al = 1.65, Na_2O/SiO_2 = 0.25 and H_2O/Na_2O = 10) collected at indicated times (in minutes) after mixing (Barbosa et al. 2000).

2.4.2 Calcium mixes

Some hypotheses have been proposed to explain the accelerated setting in the calcium mixes as mentioned earlier in this chapter. One is the enhanced dissolution of the precursor by calcium. In one study (Temuujin et al. 2009), with no experimental evidence, consumption of H_2O by the formation of C-A-S-H is believed to locally increase pH and thereby enhance dissolution of the precursor. This proposal explains the strength increase at ambient temperature. When slag was added to fly ash geopolymers, the enhanced dissolution of fly ash was suggested by SEM micrographs and attributed to both the increase of local pH and the need to maintain the Si concentration after consumed by forming C-A-S-H (Puligilla and Mondal 2013).

Another hypothesis is that C-A-S-H formation would itself cause setting. In portland cement, initial setting occurs approximately at the end of induction period and the beginning of rapid hydration (Mindess et al. 2003). More critically, set is defined as the point when solids in the microstructure are connected to form a rigid backbone with a non-zero stiffness (Bentz and Garboczi 1991). Similar as the cement system, the formation of C-A-S-H was claimed to cause setting of fly ash/slag geopolymers, as the calcium ions in the liquid would preferentially condense with Si ions to form C-A-S-H (Puligilla and Mondal 2013), which is supported by their more recent study (Puligilla and Mondal 2015).

The nucleation effects have also been proposed. The Ca salts in solution were found to increase the yield stress of the fly ash geopolymers before setting, and were believed to provide heterogeneous nuclei for gel formation (Lee and Van Deventer 2002). In metakaolin geopolymers with different calcium sources, the precipitates of calcium hydroxide and C-S-H were proposed to

act as nucleation sites and enhance rapid formation of geopolymer gel (Yip et al. 2008). The nucleation effects have been studied experimentally, though not directly on calcium. Addition of Al_2O_3 oxide nanoparticles eliminated the induction for geopolymer formation (Rees et al. 2008). Nucleation effects were found to influence both the reaction kinetics and the homogeneity of the nanostructures in different geopolymers (Hajimohammadi et al. 2010, Hajimohammadi et al. 2011a, Hajimohammadi et al. 2011b). The nucleation effects on the geopolymerization kinetics were incorporated in a mathematical model by Provis and van Deventer (2007).

2.5 Summary

To promote applications of geopolymers in construction, setting has to be well predicted and controlled. Setting of geopolymers has been measured by UWR and penetration resistance methods including the Vicat and Proctor tests. The Si/Al ratio, presence of calcium and other factors all affect the setting times.

Setting is believed to be controlled by the structural evolution during the geopolymerization. Structures of geopolymers have been examined by SEM, XRD, FTIR, NMR and other techniques. For the non-calcium mixes, the structural evolution during dissolution of the precursor has not been well studied. There remains lack of information, especially regarding the evolution of structural connectivity of species involved in the geopolymerization. For the calcium mixes, several hypotheses have been proposed to explain the accelerated setting. However, none has been supported by direct experimental evidence. A quantitative characterization at early ages in terms of dissolution and product formation is needed.

Chapter 3. Experimental methodology

In this chapter, the raw materials and synthesis procedure for geopolymers with and without calcium are summarized. The experimental procedures for various characterization tests are also summarized. When a technique is used in only one of the following chapters, such as FTIR and SEM, the experimental details are described in the corresponding chapter later.

3.1 Synthesis of geopolymers

Geopolymer mixtures were synthesized using metakaolin (MetaMax®, BASF, Ludwigshafen, Germany) as the precursor. The chemical composition and the size distribution of the metakaolin (both based on datasheet from the manufacturer) are shown in Table 3.1 and in Figure 3.1, respectively. The molar ratio of SiO_2/Al_2O_3 is around 2.05. The activating solution was prepared using reagent-grade sodium hydroxide (Fisher, Waltham, MA, USA) and fumed silica powder (Keanetech LLC, Champaign, USA) with average particle size of 0.2-0.3 microns based on datasheet from the manufacturer. Calcium hydroxide (≥95%, Sigma-Aldrich, Saint Louis, MO, USA) was the calcium source for the geopolymers with calcium. In mixes presented in Chapter 4 and 8, a commercial sodium silicate solution (Fisher, Waltham, MA, USA) was used as the external Si source instead of the solution prepared by fumed silica and sodium hydroxide. The weight percentages of SiO_2, Na_2O and H_2O in this solution were 29.02%, 9.00% and 61.98%, respectively.

Table 3.1. Chemical composition of the raw metakaolin.

Composition	SiO_2	Al_2O_3	Na_2O	K_2O	TiO_2	Fe_2O_3	CaO	MgO	P_2O_5	SO_3	LOI
Percent (wt%)	53.0	43.8	0.23	0.19	1.70	0.43	0.02	0.03	0.03	0.03	0.46

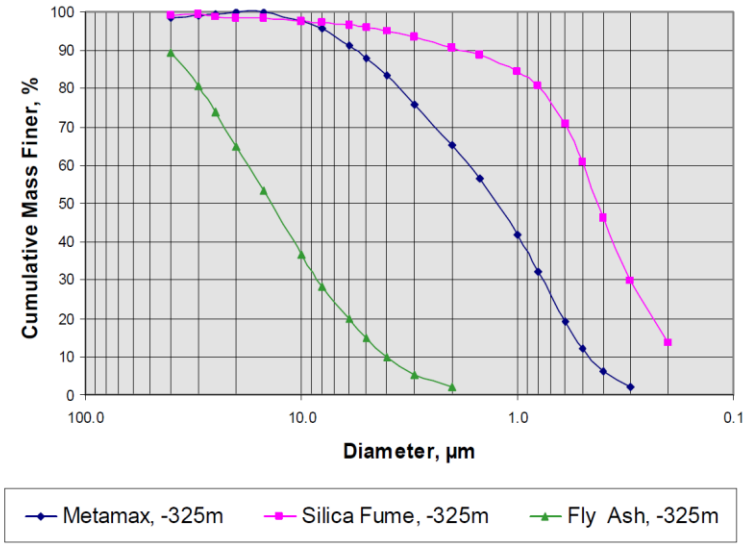

Figure 3.1. Particle size distribution for the Metamax (i.e., the raw metakaolin), and silica fume and fly ash for comparison.

The composition of the non-calcium mix (expressed as molar Na_2O:Al_2O_3:SiO_2:H_2O) was 1:1:4:11, and different compositions were specified in Chapter 4 and 8. During mixing, both the activating solution (either the commercial sodium silicate solution with some water or that prepared from fumed silica and sodium hydroxide), and the metakaolin were placed in a paddle mixer after having kept at room temperature (~23°C) for 24 hours. They were mixed at a lower speed for 2.5 minutes, then stopped for 1.0 minute while the paste was scraped off from the container, and finally mixed

for another 2.5 minutes at a higher speed. To synthesize geopolymers with calcium, the calcium hydroxide was mixed with the metakaolin precursor, and the mixture was then mixed with the activating solution in the same way as the non-calcium mix. The molar ratio of the calcium mix (expressed as $CaO:Na_2O:Al_2O_3:SiO_2:H_2O$) was 0.4:1:1:4:12.1. Both mixes have the same water/solid ratio. Samples were prepared and tested both at room temperature (~23°C).

3.2 Setting measurement

Two setting tests were conducted, the Proctor penetration resistance and UWR. In the Proctor test, different sized needles are used to monitor the evolution of penetration resistance pressure. For cement pastes, the initial and final set times were assigned to the pressure of 2 and 14 MPa, respectively (Chung et al. 2010). Since geopolymers are being promoted as construction materials, the same values were assigned for geopolymer setting (Suraneni et al. 2014). In UWR tests, the intensity of the wave reflected at the interface of a buffer and sample is monitored as a function of time. Because shear waves (S-waves) do not propagate in fluids, there is a marked decrease in the intensity of the reflected wave as setting takes place (Chung et al. 2012, Suraneni et al. 2014).

3.3 Selective chemical extractions

To stop reaction of geopolymers at early ages, a combined water and alcohol extraction, presented in Chapter 4, was conducted. For quantitative analysis, HCl extractions (Granizo et al. 2002, Palomo et al. 2004, Fernández-Jiménez and Palomo 2005, Fernández-Jiménez et al. 2006a) were conducted to remove the geopolymer gel for both metakaolin and fly ash geopolymers. Two concentrations of HCl (1:20 and 1:9, volume ratio of 37-wt%-HCl solution with H_2O) have been used. Preliminary tests in this study indicated the same mass loss upon extractions with the two

concentrations. To minimize the effects on the other phases, the 1:20 HCl solution was used in this study. During the extraction, mixture of 1-g sample and 250-ml HCl solution was stirred for 3 hours, followed by filtration using a 0.2-µm filter and then washing with deionized (DI) water. The residue was then dried in a vacuum desiccator for 24 hours. The weights before and after the extraction were recorded.

In calcium-mixes, the C-A-S-H phase forms in addition to the geopolymer gel. The salicylic acid methanol (SAM) extraction, initially developed by Takashima, is commonly used to dissolve the C-S-H phases in cements and blended cements (Struble 1985, Luke and Glasser 1987, Stutzman 1996, Kocaba et al. 2012) and also in geopolymers (Alonso and Palomo 2001b, Granizo et al. 2002, Puligilla and Mondal 2015). In this study, a mixture of 2-g sample and 8-g salicylic acid in 120-ml methanol was stirred for 2 hours, followed by filtration using a 0.2-µm filter and then washing with DI water. The residue was dried in a vacuum desiccator for 24 hours prior to the further HCl extractions. The weights before and after the extraction were recorded.

3.4 NMR tests

3.4.1 Experimental parameters

To estimate the metakaolin dissolution rate and extent, solid-state ^{27}Al NMR tests were conducted using a Varian Unity Inova spectrometer with magnetic field of 7.04 T at a resonance frequency of 78.2 MHz. Right after mixing, the specimen was packed into a 4-mm magic angle spinning (MAS) rotor and allowed to react there at a spinning rate of 12 kHz. The ^{27}Al pulse width was 0.725 µs, a 30-degree pulse. Recycle delay was 1.0 s and 2048 scans were acquired for each test unless otherwise described. The experimental chemical shift referencing, pulse calibration and

setup were performed using a 1-M $Al(NO_3)_3$ solution (chemical shift 0.00 ppm). A few other solid-state ^{27}Al NMR tests were conducted at selected times both before and around setting using a Varian NMR spectrometer at 17.6 T with 195.4 MHz resonance frequency. Experimental conditions were similar to the lower field tests, but 16-kHz MAS spinning rate and 1.25-μs (15 degree) pulse were used. Quantitative measurements of ^{27}Al spectra are difficult because the ^{27}Al is a quadrupolar nucleus. Based on earlier publications, it is believed that quantitative measurements were obtained in the latter set of tests using the spectrometer with the high field (Fyfe et al. 2000) and short pulse width (Massiot et al. 1990b). From tests at both fields, relative amounts of 4-, 5- and 6-coordinated Al were thus measured at different times of reaction, and the dissolution extent (i.e., the percent of 5- and 6-coordinated Al converted to 4-coordinated Al) was estimated.

To monitor nanostructural evolution of aqueous Si species, liquid-state ^{29}Si NMR tests were carried out using a Varian Unity Inova spectrometer with magnetic field at 14.1 T at a resonance frequency of 119.2 MHz. Right after mixing, the specimen was packed into a 5-mm glass tube and allowed to react there. A 90-degree pulse of 6 μs was used. Recycle delay was 30 s and number of scans was 64 for each test.

To quantify phases at selected times before and around setting, solid-state ^{29}Si NMR tests were conducted using the Varian Unity Inova spectrometer operating at 7.04 T with resonance frequency of 59.6 MHz. The pulse width was 2.5 μs, a 90-degree pulse. Recycle delay was 30 s and number of scans was 2048. Each quantitative ^{29}Si test took around 17 hours, and thus the specimens were treated to stop the geopolymer formation. The protocol for stopping reaction is

presented in Chapter 4. Additionally, chemical extractions were used to separate phases for unambiguous peak assignments of the spectra and for quantitative analysis.

3.4.2 Spectrum analysis

Deconvolutions of the NMR spectra were conducted to separate overlapped peaks. The ^{27}Al spectra were deconvoluted using WSolids (Eichele 2015), a program that simulates quadrupolar nuclei (Ashenhurst et al. 2000, Chen and Huang 2006, Sutrisno et al. 2012). During simulation of the ^{27}Al NMR spectra, quadrupolar coupling (C_q), asymmetry (η), and isotropic chemical shift were considered, and their values were set within ranges suggested for kaolin (Rocha 1999) and geopolymers (Brus et al. 2012). The ^{29}Si NMR spectra were deconvoluted using MestReNova, an NMR processing software. A Gaussian peak shape was assigned for each site, as also in previous studies (Massiot et al. 2002, Walkley et al. 2016). During the deconvolution, peak width and position were generally kept consistent among similar spectra.

The Si/Al ratios were estimated based on the intensities of deconvoluted peaks. The deconvoluted peaks were assigned to connectivities based on previous work on zeolites (Engelhardt & Michel, 1987) and geopolymers (Bernal et al., 2013). By measuring intensities of the peaks whose chemical shifts reflect replacement of Si by Al, the Si/Al of the geopolymer gel can be quantified using Equation 2.1, used previously for zeolites (Engelhardt & Michel, 1987) and for geopolymers (Fernández-Jiménez et al. 2006a, Kim 2012).

Chapter 4. Stop geopolymer reaction

4.1 Introduction

4.1.1 Motivation to stop geopolymerization

Magic-angle spinning nuclear magnetic resonance (MAS-NMR) has been shown to be a powerful technique to quantify structures of geopolymers. It has been used successfully to probe the short-range structure of geopolymers. ^{29}Si NMR is routinely used to measure the interconnectedness (i.e., the Q-value) of SiO_4 tetrahedra and the level of replacement of Si by Al and has been used to compute the Si/Al ratio of zeolites (Engelhardt and Michel 1987), crystalline aluminosilicates with similar structures. For geopolymers with calcium, there is coexistence of C-A-S-H (the principal product of portland cement hydration, in this case containing appreciable alumina and therefore abbreviated as C-A-S-H) and geopolymer gel (Yip et al. 2005). Using this NMR method, the amount and Si/Al ratio of geopolymer gel and the amount of C-A-S-H have been determined for calcium-containing geopolymers aged 7 days, and the results have been validated using chemical extraction methods (Kim 2012). More recently, NMR was used successfully to characterize the structures of mature alkali-activated slags and fly ashes, both qualitatively and quantitatively (Bernal et al. 2013).

However, structures have not been quantitatively characterized at early ages. ^{29}Si NMR has also been used to examine the early-age geopolymer reaction (Singh et al. 2005) but only qualitatively, perhaps because each quantitative ^{29}Si NMR test takes around 15 hours or longer. The ^{27}Al NMR, which is much faster, has mainly been used to measure the release of Al from precursors (Singh et al. 2005, Rahier et al. 2007), but also only qualitatively, probably because the quadrupolar effect confounds reliable quantitative interpretation. Fourier transform infrared spectroscopy (FTIR),

also quite fast, has been used to probe the in situ early-age structures, and the intensity of the Si-O-T (Si or Al) peaks was used to estimate the reaction rate (Rees et al. 2007b). But FTIR is not used for quantitative analysis of silicate-activated geopolymers because the overlap between the dissolved silicate species and the geopolymer gel renders the results highly uncertain (Rees et al. 2007b), and also probably because the peaks are not as spread out as those of NMR and so deconvolution is more difficult. In situ neutron pair distribution function analysis has also been used to examine the structural evolution during geopolymerization, and the dissolution of metakaolin was found to be faster in hydroxide-activated than in silicate-activated solution (White et al. 2011b), but this test could not provide information concerning atomic connectivity of geopolymers. In addition to these experimental methods, modeling has been used to simulate geopolymerization and provide quantitative understanding of the early-age molecular structure (Provis and van Deventer 2007), but the study is limited by its assumption that the kinetics of reaction is determined by its stoichiometry. The ^{29}Si NMR is powerful to obtain quantitative information about the early-age geopolymer reaction, but this method requires a procedure to stop the reaction.

4.1.2 Literature review: stop geopolymer formation

Methods to stop cement hydration have been reviewed in a paper (Zhang and Scherer 2011). Both direct drying techniques including oven, microwave, D-drying, P-drying and freeze drying, and indirect drying such as solvent exchange methods have been summarized and compared. For geopolymers, only a few studies have attempted to stop the reaction, by solvent treatment either using acetone (Oh et al. 2010, Chindaprasirt et al. 2012) or an alcohol/acetone mixture (Khater et al. 2011, Khater 2013).

However, none of these studies has validated the efficacy of the procedure in early age geopolymers. A study on 40-day alkali-activated slag/fly pastes treated using acetone to remove water indicated that the gel structures and pore network were preserved (Ismail et al. 2013). For early age specimens, the preliminary attempts indicated that the reaction was not stopped.

4.1.3 Objectives in this chapter

The initial objective of this part of study therefore was to develop a solvent extraction procedure that effectively stops the geopolymer reaction. It was focused on removal of water because the reaction proceeds via dissolution of precursor in water and condensation of the resulting dissolved molecular species to form gel (Duxson et al. 2007a). The procedure must not alter the reaction products, which are known to be sensitive to temperature, so heating to remove water was not considered.

Furthermore, precipitation of water-soluble silicate species was observed upon addition of the solvent to early-age specimens, confounding the interpretation of spectra, so the procedure was modified to include extraction with both water and solvent. This combined extraction was seen to reliably stop reaction without altering the reaction product. Results are presented of changes during extraction and efficacy of stopping reaction for the two extraction methods (solvent and combined water-solvent) in different subsections. In the first subsection, both preliminary and the final solvent extraction are included.

Setting behaviors were monitored so that extraction could be performed both before and after setting. The structural changes during extraction were determined by comparing spectra immediately before and after extraction. Efficacy was determined by comparing spectra at

different times after extraction. Because the focus of the broader study in thesis research is the setting behavior associated with the formation of C-A-S-H, the work reported here includes geopolymers made with and without calcium. Both NMR and FTIR methods were used, NMR for detailed understanding of molecular structure and FTIR for rapid analysis.

4.2 Experimental procedure

The raw materials used to synthesize geopolymers are described in Chapter 3, including metakaolin, sodium hydroxide, and calcium hydroxide. For mixes in this chapter, reagent-grade sodium silicate solution (Sigma-Aldrich, St. Louis, MO, USA) instead of the fumed silica was used as the external Si source. The mix without calcium (Mix A) had the following proportions: SiO_2/Al_2O_3 (mol) 3.0, H_2O/Na_2O (mol) 15, and water/solid (wt) 0.59; while the mix with calcium (Mix B) had: SiO_2/Al_2O_3 (mol) 3.0, H_2O/Na_2O (mol) 20, water/solid (wt) 0.70 and $CaO/(SiO_2+Al_2O_3+CaO)$ (wt) 0.10. In Mix B, higher H_2O/Na_2O was used to counteract the rapid setting associated with the addition of calcium, and the higher water/solid was used to achieve a certain workability. To determine set times, both penetration resistance and UWR were conducted.

As mentioned in the introduction of this chapter, prior to developing methods for solvent extraction to remove water and the combined extraction to also remove any soluble species, some preliminary extractions were carried out. Specimens (if they had set) were first ground to micron-sized particles using a mortar and pestle. Solvent was added, a 50/50 (vol) methanol/acetone mixture, and the resulting suspension, around 2.0 g specimen and 80 ml solvent, was further ground with the pestle so that all particles would contact the solvent. After 5 minutes, the solvent was removed using

vacuum-filtration and new solvent was added. This procedure was repeated for 3 times (i.e., totally 240 ml solvent was used).

Based on the preliminary results, the experimental details of solvent extraction were adjusted. The sequence of the procedure did not change, but the amounts of specimen and solvent were changed substantially. In the final procedure, around 80 ml solvent was added to around 0.8 g specimen and the suspension was ground and filtered 5 times rather than the previous 3 times (i.e., 400 ml rather than 240 ml solvent was used).

In early-age specimens, evidence of precipitation of soluble silicate species was observed during extraction (as presented later in this chapter), so the procedure was modified to include both water extraction and solvent extraction. In this combined extraction, around 0.8 g of specimen was stirred with 50 ml deionized water and the liquid removed by centrifuging (which required about 5 minutes). Soluble silicate species could be observed in the liquid layer upon addition of methanol (using a volume twice that of the collected liquid) because the alcohol reduces the solubility of silicate species (Iler 1979) and causes their precipitation. Water extraction of the geopolymer sample was repeated until no precipitation was observed in the collected liquid upon addition of methanol and then once more. This water extraction was then followed by the solvent extraction as described previously.

To examine changes during the extraction, FTIR spectra of extracted and non-extracted specimens were compared. The FTIR spectra were collected using a Bruker IFS 66v/S spectrometer with a SpectraTech horizontal attenuated total reflectance accessory. The specimen was scanned from 600 cm^{-1} to 4000 cm^{-1} with 2-cm^{-1} resolution. The ^{29}Si MAS-NMR was conducted using the Varian

Unity Inova 300 spectrometer with a magnetic field strength of 7.05 T. In total 1024 scans were carried out. In some cases, a 2-second relaxation delay and 2048 scans were used, giving spectra that did not provide quantitative information but could be analyzed qualitatively for changes over time. For the solid state ^{27}Al tests, the Varian Unity Inova 750 spectrometer with a magnetic field strength of 17.6 T was used. The total scan was 250 times for each specimen. More details for these tests are described in Chapter 3.

4.3 Setting behavior

Setting curves are shown in Figure 4.1. Mix A set at around 116 minutes (by penetration) or 180 minutes (by UWR), and Mix B set at around 20 minutes (by both methods). Setting here was defined when the reflection coefficient drops to 0.83 in the UWR test, based on a previous study (Suraneni et al. 2014), and defined when penetration strength increases to 2 MPa in the penetration resistance tests, based on a study for cement pastes (Chung et al. 2010). The different setting times by different methods for Mix A but not for B suggest the same penetration strength corresponds to different extent of gelation for the two mixes. The setting times of Mix A by the two methods were shorter than those of the same mix in the previous work (Suraneni et al. 2014), a difference that is attributed to changes in properties of the raw materials. Based on these results, Mix A was extracted at 100 minutes, a bit before set, and at 30 hours and 6 days, well after set when it was expected to be mature and stable. Mix B was extracted at 20 minutes, coincident with set, and at 3 hours and 8 hours, well after set. The more rapid set with addition of calcium was consistent with our previous work (Suraneni et al. 2014) as well as results of others (Lee and Van Deventer 2002, Puligilla and Mondal 2013).

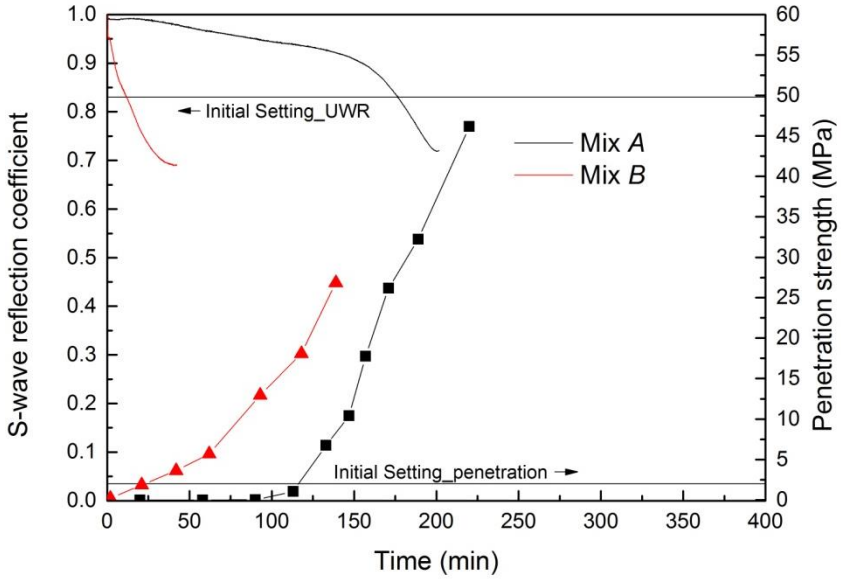

Figure 4.1. UWR and penetration curves of Mix *A* (without calcium) and *B* (with calcium).

4.4 Solvent extraction

4.4.1 Preliminary extraction

As a preliminary study, the efficacy of solvent extraction to stop reaction was determined. Around 2.0-g specimen was extracted using around 240 ml solvent. Both ^{27}Al and ^{29}Si NMR were used to examine the raw metakaolin (MK) and the extracted geopolymers. Mix A was extracted at 100 minutes (a little before set) and tested at 1 day and 7 days after extraction, and also extracted at 7 days and tested at 1 day after extraction. The specimens were stored in a desiccator under a vacuum.

Both ^{27}Al and ^{29}Si NMR indicated that the dissolution was stopped but condensation continued after this extraction. In Figure 4.2 (a), the three peaks in the ^{27}Al spectrum were assigned as 4-, 5- and 6-coordinated aluminum. The relative amount of 5- and 6-coordinated aluminum was 71% for the unreacted MK, 58% for both specimens extracted at 100 minutes, and 0% for the specimen

extracted at 7 days (calculated from the peak areas). It is recognized that the percentage values are not highly accurate because of the quadrupolar effects of the ^{27}Al method, but the comparison is useful. The fact that the two specimens extracted at 100 minutes but tested at different times had the same value indicates that MK dissolution was stopped by the extraction. However, the position of the 4-coordinated aluminum peak shifted from 59.6 ppm for the specimen tested at 1 day to 58.0 ppm for the specimen tested at 7 days, a type of shift generally associated with a higher extent of polymerization in aluminosilicates (Merzbacher et al. 1990). This peak shift is consistent with the changes seen in the ^{29}Si NMR spectra discussed below.

Additional and stronger evidence that condensation continued after extraction was provided by the ^{29}Si NMR spectra in Figure 4.2 (b). Spectra for the two specimens extracted at 100 minutes were substantially different, and both are different from the spectra for raw metakaolin and the specimen extracted at 7 days. The peaks (around -90 ppm, marked with an ellipse in the figure) assigned to silicate species with low connectivity (i.e., Q^1, Q^2 and Q^3 structures) decreased greatly in intensity in the specimen tested at 7 days (100 min_7 d) compared to the specimen tested at 1 day (100 min_1 d). At the same time, the peaks (around -105 ppm, marked with a rectangle in the figure) assigned to geopolymer gel (i.e., Q^4 structures) increased in intensity in the specimen tested at 7 days (100 min_7 d) compared to the specimen tested at 1 day (100 min_1 d). These differences indicate that condensation (i.e., polymerization) continued during this period. Compared to the 100-minute specimen tested at 7 days (100 min_7 d), the peak corresponding to the product in the specimen extracted at 7 days and tested 1 day after extraction (7 d_1 d) shifted to the left side, probably because of the lower Si/Al ratio as more Al was released by dissolution from 100 minutes to 7 days.

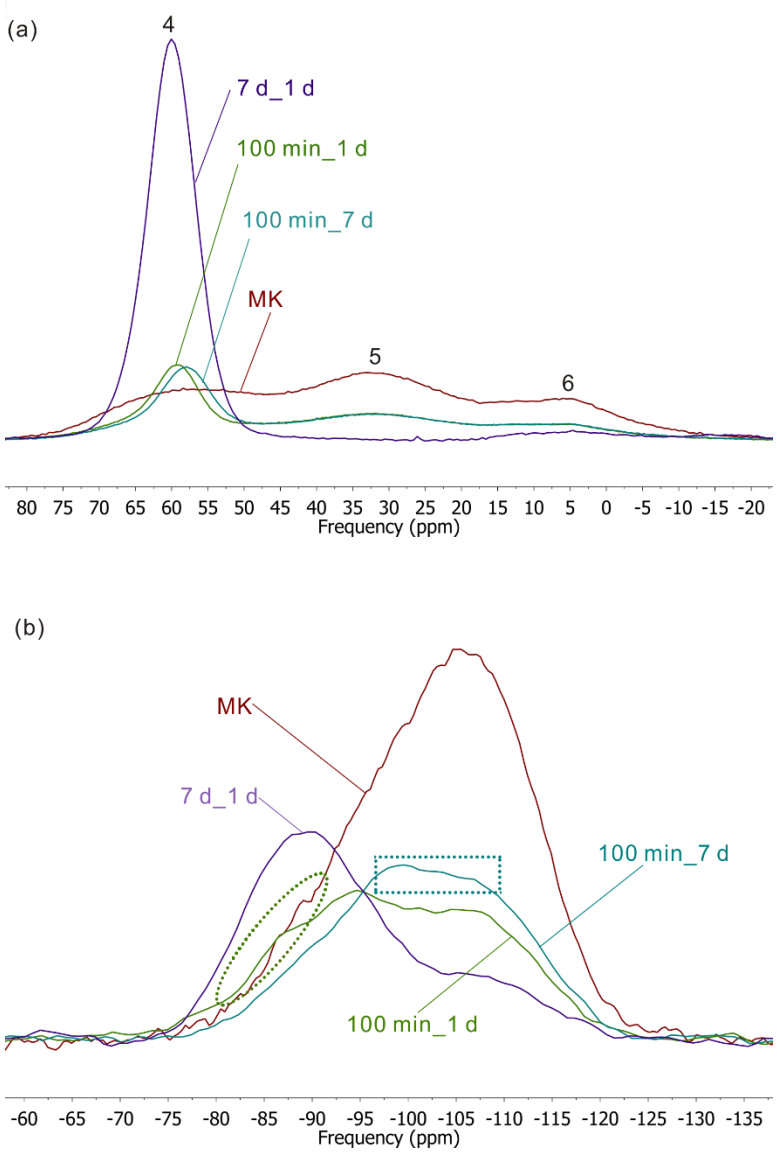

Figure 4.2. ^{27}Al (a) and ^{29}Si (b) NMR spectra of raw metakaolin, untreated geopolymer specimens, and specimens treated by solvent extraction. MK is the raw metakaolin precursor, 100 min_1 d and 100 min_7 d are Mix A geopolymers extracted at 100 minutes and tested at 1 day and 7 days after extraction respectively, and 7 d_ 1 d is the same mix extracted at 7 days and tested at 1 day after extraction.

Based on the preliminary extraction results, it is expected that solvent extraction, the method used in many papers to stop geopolymerization, if not well controlled, may be ineffective. Therefore, it is critical to develop an effective protocol and validate it.

4.4.2 Final protocol

Based on the preliminary extraction results, it seemed reasonable to use more solvent in the extraction. The amount was adjusted several times, followed by similar examination of efficacy, until the amounts given in the experimental section were settled upon. The resulting solvent extraction was then investigated in more detail. The structural changes during the solvent extraction were examined by comparing spectra right after extraction with those before extraction, and the efficacy of stopping reaction was investigated by examining any changes as a function of time after the extraction.

4.4.2.1 Changes during extraction

Spectra of Mix A were examined before and after the solvent extraction to investigate structural changes during the extraction. Extractions were made at 3 hours (around set), 30 hours and 6 days (both well after set) after mixing. FTIR spectra of metakaolin and of specimens before and after extraction are shown in Figure 4.3. The peaks at 1060 and 788 cm^{-1} in metakaolin are attributed to asymmetric stretching of Si-O-T (Si or Al) and bending of O-Al-O in the AlO_4 tetrahedra, respectively (based on the literature[27]). Extraction caused the main peak to shift from 977 to 1025 cm^{-1} at 3 hours and from 961 to 987 cm^{-1} at 30 hours, and did not cause changes at 6 days. For specimens extracted at 30 hours and 6 days, a slight carbonation was observed, which was removed by the extraction and which is therefore thought to be sodium carbonate (as there is no calcium in

this mix and sodium seems to be the only possible source for carbonation). In addition, peaks assigned to water were not as evident after extraction, further indicating that the extraction has the potential to stop geopolymer reaction as condensation, if any, is much slower with less water.

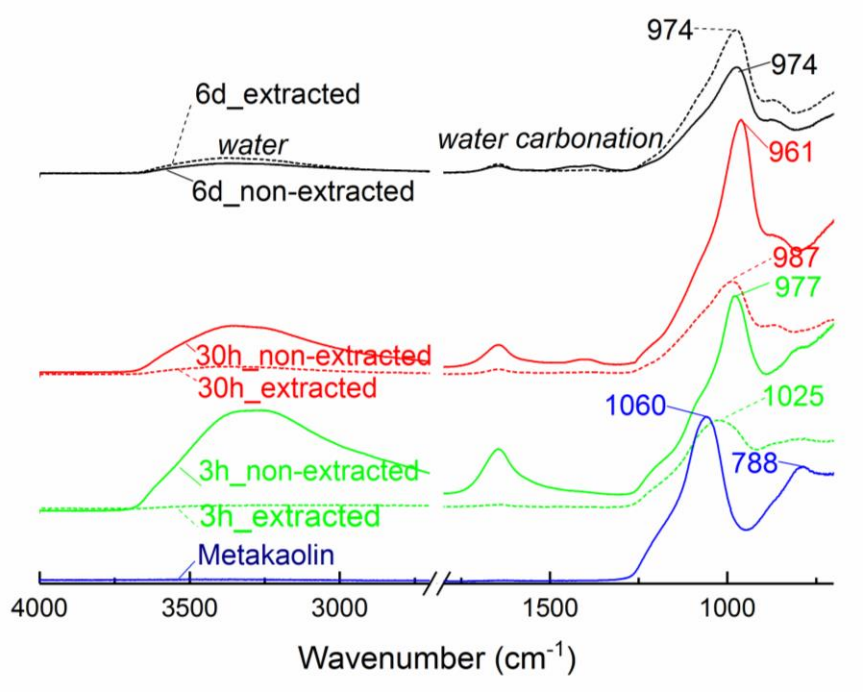

Figure 4.3. FTIR spectra of Mix A both before and right after extraction and metakaolin.

These peak shifts in the early age specimens (3 and 30 hours after mixing) in Figure 4.3 appear to be associated with the soluble silicate species. At these early times, samples contained unreacted metakaolin, some geopolymer gel, and sodium silicates. The latter are soluble, are consumed during geopolymerization, have very low molecular weight, generally have lower Q values than the geopolymer gel, but cannot be identified in the NMR spectra. The peak shifts observed in these specimens during solvent extraction cannot be attributed to metakaolin because no shifts were observed during solvent extraction of the raw metakaolin (results also not shown here). Neither

can these shifts be attributed to geopolymer gel, as they were not seen in the 6-day specimen, which contained mostly geopolymer gel. For an earlier-age geopolymer gel (mainly but not all Q^4), we did not have evidence to show if it is affected by the solvent, but this effect, if any, would not be as significant as that for the aqueous Si species. Apart from the unreacted metakaolin and the geopolymer gel, the only possible constituent to associate with the peak shifts appears to be the soluble silicate species. In a similar solvent-extraction study, these soluble species were not observed because the investigated specimen was more mature (40 days) (Ismail et al. 2013).

Soluble silicate species interact with the solvent used to extract water to cause a shift in the peaks. Soluble silicate species are known to precipitate in alcohol and/or acetone--addition of alcohol or acetone to a solution of sodium silicate has been reported to cause formation of two layers, with initially soluble silicate species precipitating in the bottom layer and sodium concentrating in the liquid layer on the top, a process called "salting-out" (Iler 1979). In the current study, precipitation was observed upon addition of methanol to a sodium silicate solution. Soluble silicate species in the sample would precipitate out during solvent extraction. Furthermore (and unexpectedly), there was evidence that some of the soluble silicate dissolved during the solvent extraction. During solvent extraction of a geopolymer sample at early age, the filtrate was clear. But precipitation was observed when methanol was added to this filtrate, indicating the presence of the soluble silicate species in the filtrate. Thus, some of the soluble species were removed by the solvent extraction and some were precipitated. These interactions are presumed to account for the peak shifts shown in Figure 4.3, although a more detailed analysis to verify dissolution and precipitation is not possible with methodology used here because peaks of soluble silicate species overlap with those of geopolymer gel in both ^{29}Si NMR and FTIR spectra, as reported in the literature (Engelhardt

and Michel 1987, Rees et al. 2007b). Such changes, whether due to precipitation or dissolution or both, would alter the spectra in the geopolymer region and thus confound interpretation of the spectra. The solvent extraction is therefore only suitable for mature geopolymers that contain little or no soluble silicate species.

4.4.2.2 Efficacy of extraction

The efficacy of the solvent extraction to stop reaction was investigated using ^{29}Si NMR. Figure 4.4 shows spectra of Mix A extracted at 100 minutes and tested every 5 hours until 53 hours after extraction. No changes were observed throughout this time, indicating that the geopolymer reaction was stopped for this time period by this treatment. It should be noted that this NMR test was only qualitative because of the limited testing time (5 hours for each spectrum), but it would indicate if any structural changes were taking place. The low signal-to-noise level reflects the short testing time.

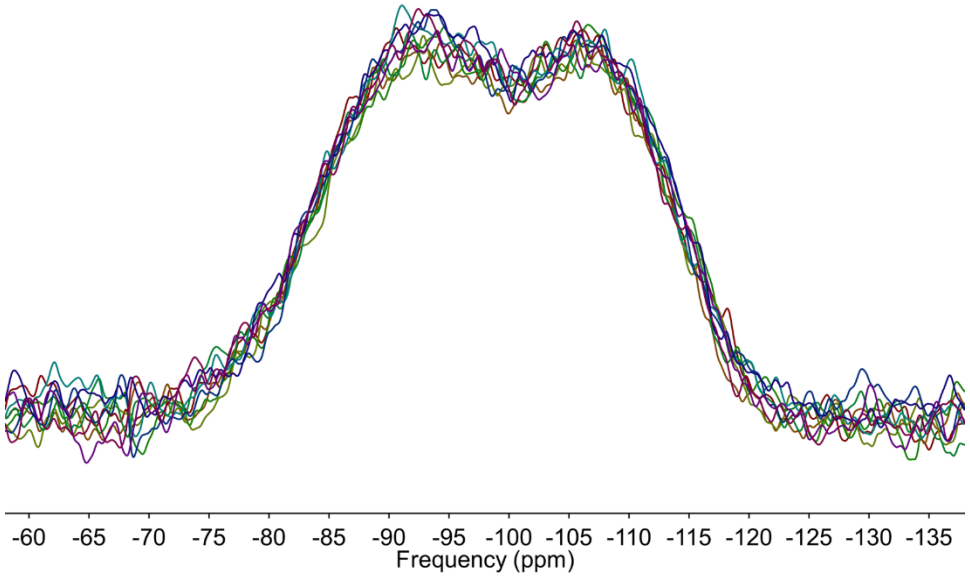

Figure 4.4. ^{29}Si NMR spectra of Mix A solvent-extracted at 100 minutes and tested every 5 hours from 3 hours until 53 hours after extraction.

4.5 Combined water and solvent extraction

Based on results of solvent extraction, using water treatment was explored to extract any soluble species prior to the solvent extraction in order to study structures at early ages in the geopolymer reaction. The specimens were mixed with water and then the resulting liquid was separated using centrifugation. This water extraction was repeated until the centrifugation liquid contained no detectable silicate species, as indicated by lack of precipitation upon addition of methanol, then one final water extraction was conducted to remove any remaining soluble silicate. The lab results showed that the addition of methanol as described in the experimental section (i.e., double amount of the amount of centrifugation liquid) provided observable precipitation in the centrifugation liquid from the extraction of a specimen containing sodium silicate equivalent to 30 wt% of the

total solid or paste material (i.e., 0.25 g sodium silicate out of the 0.8 g specimen). The addition of methanol was therefore regarded as sensitive enough to confirm that almost all soluble species were removed. Following subsections presented results on structural change during this combined extraction and the efficacy of stopping reaction.

4.5.1 Changes during extraction

FTIR spectra of non-extracted and combined-extracted specimens at 6 hours after mixing (after set) are shown in Figure 4.5. The main peaks were at 958 and 1022 cm^{-1} for non-extracted and combined-extracted specimens, respectively, and were attributed (also respectively) to soluble silica and geopolymer gel. After combined extraction, the peak for soluble silica at 958 cm^{-1} was lost, and the only remaining peak was at 1022 cm^{-1} and was attributed to geopolymer gel, probably mixed with unreacted metakaolin. The results here indicate that the combined extraction effectively removes soluble species and therefore provides a viable procedure to study structural changes associated with geopolymer setting without any uncertainties caused by the soluble species.

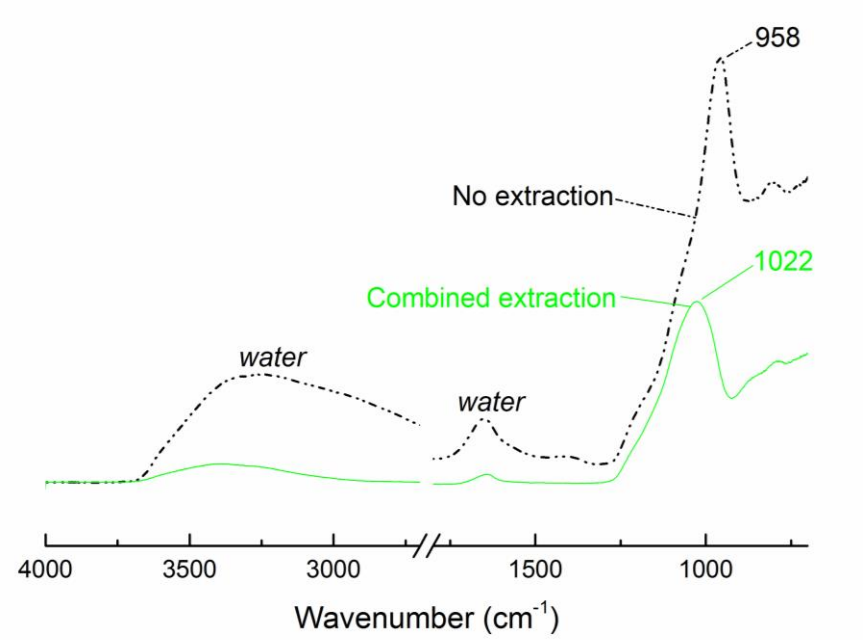

Figure 4.5. FTIR spectra of Mix A both before and after combined extraction at 6 hours.

4.5.2 Efficacy of extraction

4.5.2.1 No-calcium-containing mix

The efficacy of the combined method was examined using both FTIR and NMR, including specimens both without (Mix A) and with (Mix B) calcium. Figure 4.6 shows FTIR spectra of Mix A extracted using the combined method at different times (corresponding to bottom, middle and upper series of spectra) and tested at different times (corresponding to each spectrum in the corresponding series) after extraction. For the specimens extracted at 100 minutes (bottom series, a little before set), when tested immediately, 3 days, and 8 days after extraction, the peak associated with Si-O-T was at 1052 cm^{-1}, and did not change position in this testing period. Similarly for specimens extracted at 6 hours and 8 hours (spectra in the middle and upper part, both after set)), the peak did not shift over the few days of the testing period. Even the sample extracted at 6 hours

and tested after 90 days showed only a slight shift in this peak (around 8 cm^{-1}, from 1022 to 1014 cm^{-1}). Thus the combined method is regarded as effective to stop the geopolymerization for the specimen without calcium. Another interesting point is the presence of water in the specimens extracted at 6 hours and 8 hours, as shown in the middle and upper spectra. Similar water after acetone extraction was referred as zeolitic water (Ismail et al. 2013). The absence of water in the specimen extracted at 100 minutes indicates that the sample prior to set contained little or no geopolymer gel.

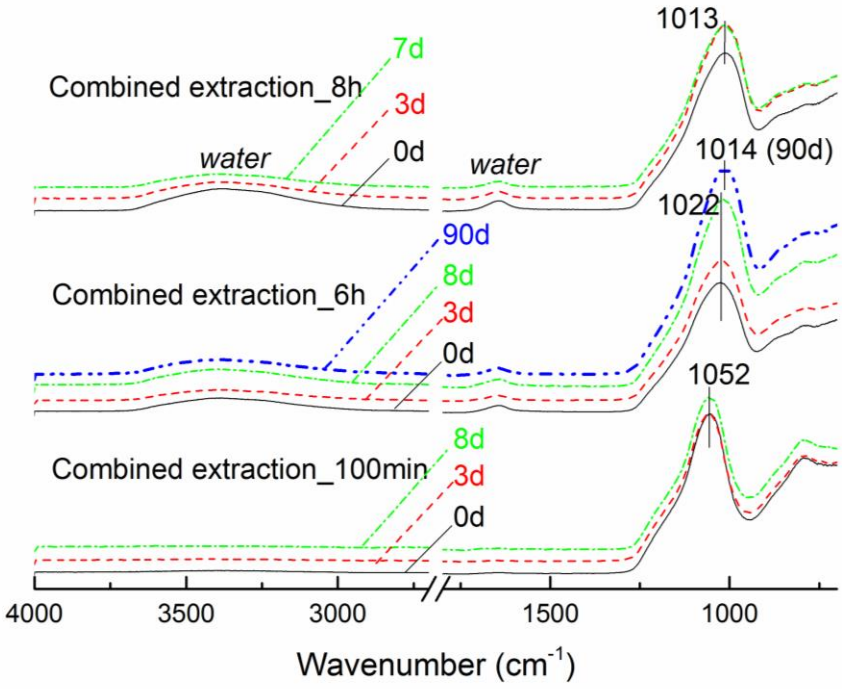

Figure 4.6. FTIR spectra of Mix A treated using combined extraction at 100 minutes, 6 hours and 8 hours, and tested at times up to several days or even 90 days after extraction.

To further validate the efficacy of this combined extraction when conducted at a later age, the Mix A was extracted at 24 hours after mixing and tested using ^{29}Si NMR right after extraction (within

1 day) and at 34 days after extraction. Results are shown in Figure 4.7. The peaks around -90 ppm and the shoulders around -108 ppm were assigned to geopolymer gels and unreacted metakaolin, respectively. No significant changes between these two spectra were observed. It is therefore concluded that the combined extraction effectively stopped reaction at 24 hours for an extended time.

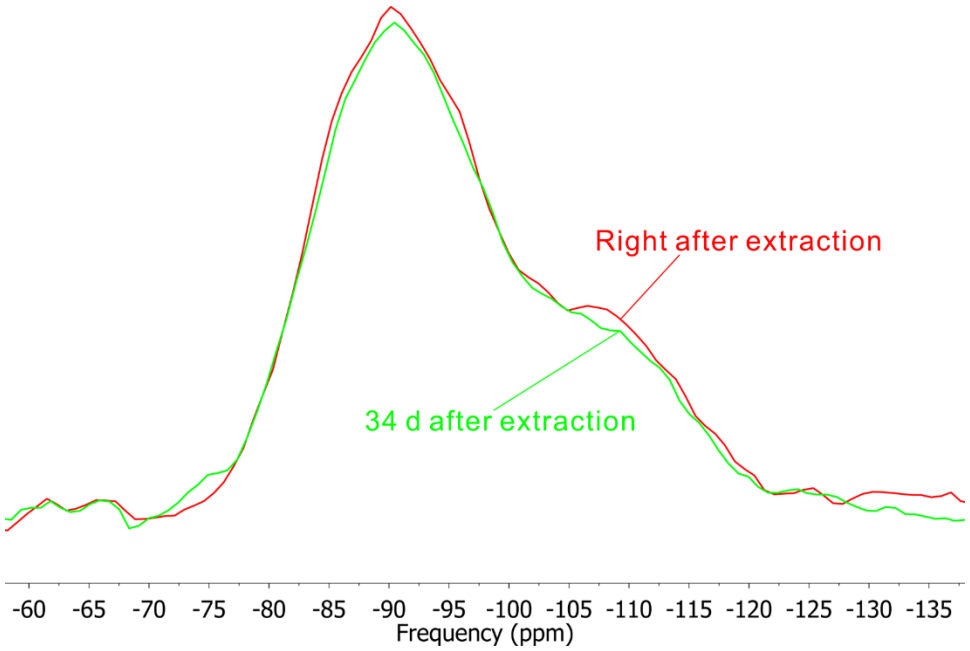

Figure 4.7. ^{29}Si NMR spectra of Mix A extracted using combined extraction and tested right after (within 1 day) and at 34 days after extraction.

4.5.2.2 Calcium-containing mix

The addition of calcium complicates the situation because C-A-S-H forms in addition to the geopolymer gel. Figure 4.8 shows spectra of Mix B (with calcium) treated using combined extraction and tested at different times after extraction. In the specimen extracted at 20 minutes

(around set), there were two peaks in the Si-O-T region, at 1032 and 967 cm^{-1}. SAM extraction (not shown here), which removes C-A-S-H but leaves geopolymers, indicated that the 967 cm^{-1} peak was associated with C-A-S-H and the 1032 cm^{-1} peak was associated with geopolymer gel. The peak at around 790 cm^{-1} was attributed to the O-Al-O peak in the precursor as shown in Figure 4.3, indicating the presence of unreacted metakaolin at 20 minutes. When tested up to 7 days after extraction, the positions of the two Si-O-T peaks (geopolymer gel and C-A-S-H) did not change, but the intensity of the C-A-S-H peak decreased. The small peaks at around 1410-1470 cm^{-1} and the one at 875 cm^{-1} in specimens extracted at 3 and 7 days were all attributed to carbonates, based on a previous study (Garcia-Lodeiro et al. 2007). The carbonation was not likely to involve the geopolymer gel, as there were no carbonation peaks in specimens without calcium (Figure 4.6). The carbonation was not likely to involve calcium hydroxide either. There was a small amount of calcium hydroxide in the 20-minute sample before extraction, as indicated by the peak at 3639 cm^{-1}, but the peak was removed by the extraction, as shown in the bottom series of spectra (Figure 4.8). So the carbonation appears to involve the C-A-S-H, not the geopolymer gel. It may be that the decrease in intensity of the C-A-S-H peak with extraction is associated with this carbonation. As a matter of fact, carbonation is common during synthesis of C-A-S-H (Hunnicutt 2013). Similar carbonation was observed for specimens extracted at 3 hours and 8 hours (middle and upper series of spectra, both after set). Other than these, no changes were observed after extraction for either geopolymer gel or C-A-S-H peaks up to 7 days, indicating that these phases did not undergo further structural evolution after the combined extraction.

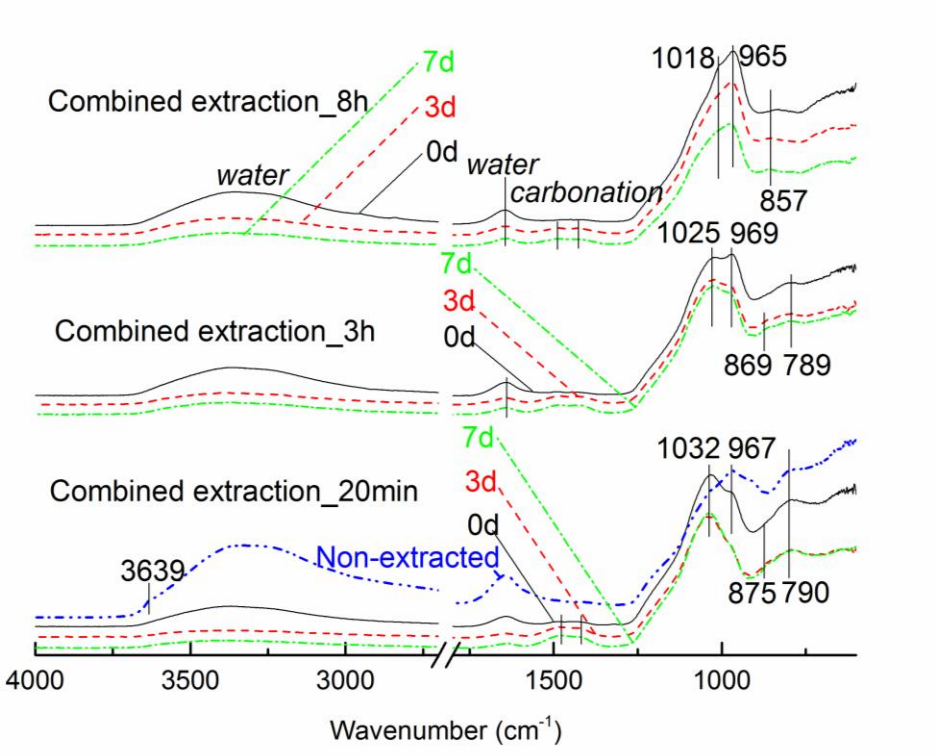

Figure 4.8. FTIR spectra of Mix B treated using combined extraction at 20 minutes, 3 hours and 8 hours, and tested at times up to several days after extraction.

4.6 Conclusions

To allow characterization of geopolymerization systems for setting studies, a procedure has been developed to stop the geopolymer reaction. Solvent extraction was suitable for mature geopolymers, and combined water and solvent extraction was required for early-age specimens.

1. Extraction using the methanol/acetone solvent was not effective to stop geopolymer formation when the amount of the solvent is not carefully selected.
2. Solvent extraction suspended the reaction up to at least 53 hours.

3. In early-age specimens, soluble silicate species precipitated during this treatment, confounding the interpretation of the geopolymer gel structure, so simple solvent extraction is suitable only for mature geopolymers.
4. A combination of water and solvent extraction removed soluble species that would otherwise precipitate in solvent extraction and thereby stopped reaction without the confounding effects noted above.
5. For specimens without calcium, combined extraction both before and a few hours after set stopped the geopolymer reaction for up to at least 1 week.
6. Specimens with calcium were seen to contain both geopolymer gel and C-A-S-H. The combined extraction both before and a few hours after set stopped the geopolymer reaction for up to at least 1 week.

Chapter 5. Quantification of early-age geopolymer nanostructures

5.1 Introduction

As reviewed in Chapter 4, NMR shows to be a powerful technique to probe structures of geopolymers. Compared to Fourier transform infrared spectroscopy (FTIR) and X-ray photoelectron spectroscopy (XPS), NMR shows major advantages in quantification as reviewed in Chapter 2. However, current published studies using NMR are limited to mature geopolymers when the structures are relatively stable. This is probably because each quantitative ^{29}Si NMR test usually takes around 10-20 hours, too long for specimens with evolving structures. The objective of this chapter is to mainly use ^{29}Si NMR to quantify phases in geopolymers with evolving structures.

The combined extraction method for stopping geopolymer formation, developed in Chapter 4, was conducted prior to each quantitative ^{29}Si NMR test. In the combined extraction, water and alcohol were used sequentially to remove the soluble species and any free water, thereby stopping the geopolymer reaction.

Before studying geopolymers, the Si/Al ratio of a zeolite specimen was quantified by ^{29}Si NMR tests and validated. With this confidence, structures of mature geopolymers and then earlier age specimens were probed by the NMR tests.

In each NMR analysis, for unambiguous peak assignment in deconvolution, the residue from the combined extraction was treated by HCl extraction to remove the geopolymer phase to reduce/avoid the confusion if any peaks of the geopolymer gel overlap with the other phases. The

mass was recorded before and after, both tested by the quantitative ^{29}Si NMR and the Si/Al ratio of geopolymer gel estimated from the deconvoluted NMR spectra. For comparison, the Si/Al ratio was also estimated based on intensity of both ^{29}Si and ^{27}Al NMR spectra. The Si/Al ratios of geopolymer gel based on both NMR deconvolution and intensity analysis were validated by the quantitative extraction.

5.2 Experimental procedure

5.2.1 Materials

To validate effectiveness of ^{29}Si NMR to quantify structures of aluminosilicates, a natural zeolite was tested. This specimen is clinoptilolite, from St. Cloud Mining Co., New Mexico. This is a typical type of zeolite with variety of Q^4(nAl) Si sites. The bulk molar ratio of Si/Al was 4.9 based on the materials data sheet. The chemical analysis results in weight percent are presented in Table 5.1.

Table 5.1. Composition of the clinoptilolite specimen based on product information (2007).

Oxides	wt %
SiO_2	70.0
Al_2O_3	12.1
CaO	3.4
K_2O	3.0
Fe_2O_3	1.6
MgO	1.5
Na_2O	0.3
P_2O_5	0.1

To synthesize geopolymers, the raw materials including metakaolin, sodium hydroxide and fumed silica powder, as well as the mixing procedure are described in Chapter 3. The composition (expressed as $Na_2O:Al_2O_3:SiO_2:H_2O$) of this mix is 1:1:4:11. The specimens were kept in sealed condition at around 23^oC until direct testing or treatment (stopping reaction or chemical extraction).

Specimens at two different ages (51 hours and 19 days) were extracted prior to the ^{29}Si NMR tests. The two ages were chosen so that the Si sites in the geopolymer product are not all Q^4 and thus are different compared to the mature geopolymer gel. A weighed sample (about 2.0 g) was treated with combined extraction as developed in Chapter 3. The residue, expected to be unreacted metakaolin and geopolymer gel, was vacuum dried for about 24 hours and weighed. Around 1 g of dried residue was then further extracted in 250 ml HCl (1:20 ratio of water to 37-wt% HCl solution by volume) by stirring for 3 hours to remove the geopolymer gel. The HCl residue was

dried in the same manner and its residue mass was measured to determine the mass of unreacted metakaolin.

5.2.2 Characterization

To examine impurity phases in the zeolite, XRD (Siemens/Bruker D-5000) was used, with a scanning rate 1.0 degree/minute and step size 0.02 degree. For both the zeolite and geopolymers, quantitative ^{29}Si NMR tests were conducted, recycle delay and scan number are 30 seconds and 1024, respectively. More detailed parameters are described in Chapter 3.

For geopolymer specimens, a mature specimen (~ 3 month old) was tested using the quantitative ^{29}Si NMR. The spectrum was deconvoluted, during which Gaussian-line-shape peaks were assigned at positions at shoulders or peaks. The Si/Al ratio of the mature specimen was estimated based on intensities of deconvoluted peaks, and was compared with the known bulk ratio to validate the deconvolution.

For earlier age specimens, spectrum of the HCl residue was subtracted from that of the combined extraction residue, and obtained spectrum was expected to be the geopolymer phase. To estimate the Si/Al of the geopolymer phase, this obtained spectrum was deconvoluted. In this deconvolution, this early age specimen may contain lower Q species. The solid-state ^{1}H/^{29}Si cross-polarization (CP) NMR tests provided peak width and position of these low-Q sites, which were then incorporated in deconvolution of the subtracted spectrum of the geopolymer phase. In deconvolution, the minimum possible number of component peaks was used to describe each spectrum (Bernal et al. 2013).

To validate the Si/Al ratio from above procedure, this ratio was estimated independently by NMR intensity analysis. The moles of Si and Al in geopolymer phase were calculated by subtracting those in unreacted metakaolin and soluble aluminates and silicates from the total moles in the specimen by following the following procedures. (1) The total moles of Si and Al in the specimen were computed based on the mass of the specimen and the mix design. (2) The moles of Si and Al in the HCl residue were estimated: (a) amount of Si in the HCl residue was estimated by comparing its ^{29}Si NMR intensity with the intensity of a raw metakaolin specimen with known amount of Si; (b) amount of Al was calculated based on this Si amount and the Si/Al ratio of the HCl residue; and (c) this Si/Al ratio was estimated by comparing the I_{27Al}/I_{29Si} (i.e., the intensity ratio of the ^{27}Al and ^{29}Si NMR spectra) ratio of this residue with the intensity ratio of metakaolin (with known Si/Al ratio) with both specimens activated by the same relative amount of excessive NaOH (10 M) solution. This activation converts any 5- and 6-Al to 4-Al for quantitative comparison, as the intensity per mole of Al is different in different coordination environments (Massiot et al. 1990b). Compared to the raw metakaolin, the Si/Al ratio in the NaOH-activated metakaolin is the same but the moles of Al pre unit weight is not. Therefore, the Si/Al ratio was used to indirectly estimate the amount of Al. (3) The moles of Si and Al of soluble aluminates and silicates were estimated in a similar manner. (4) The Si and Al in the geopolymer phase were computed by subtracting those of the unreacted metakaolin and soluble species from the total.

Based on the computed moles of Si and Al, weights were computed and were compared with measured extraction residues. Formulas were assumed to be $(SiO_2)_x \cdot (Al_2O_3)_y$ for the HCl residue, and $(SiO_2)_m \cdot (Al_2O_3)_n \cdot (Na_2O)_n$ for the geopolymer gel, where x, y, m and n are related to the moles of Si and Al in each phase.

5.3 Nanostructure of zeolite

5.3.1 Identification of phases in the zeolite specimen

XRD pattern of this zeolite is presented in Figure 5.1. In addition to the main phase clinoptilolite, two zeolites heulandite and mordenite together with quartz were identified. Peaks of the three zeolite phases are mostly overlapped, but not at a few positions.

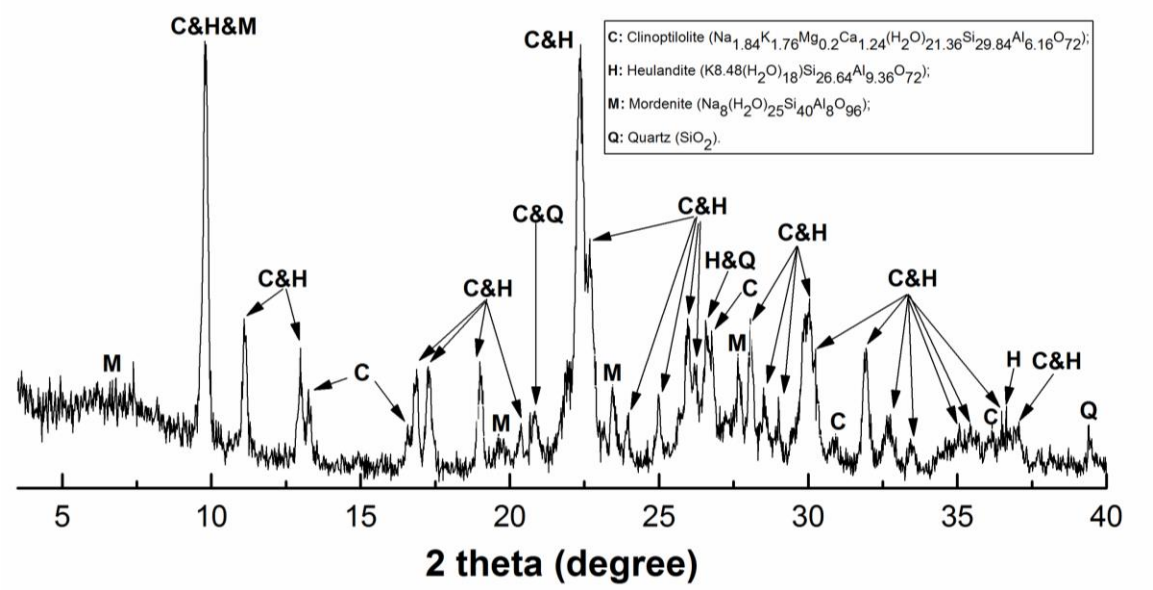

Figure 5.1. XRD pattern of the natural clinoptilolite specimen.

5.3.2 NMR deconvolution to estimate Si/Al

Two versions of deconvolution were carried, with only clinoptilolite shown in Figure 5.2 (a) by assuming only this zeolite phase is present and with all phases identified in the XRD pattern shown in Figure 5.2 (b). For the deconvoluted peak at -107.1 ppm in Figure 5.2 (a), there is an inconsistency in assignment, as both Q^4(1Al) and Q^4(0Al) were assigned in different papers (Lippmaa et al. 1981, Rivera et al. 2003). The corresponding peak in Figure 5.2 (b) is at -106.2

ppm. In both versions of deconvolution, the residue was less than 1% of the total intensity of the spectrum.

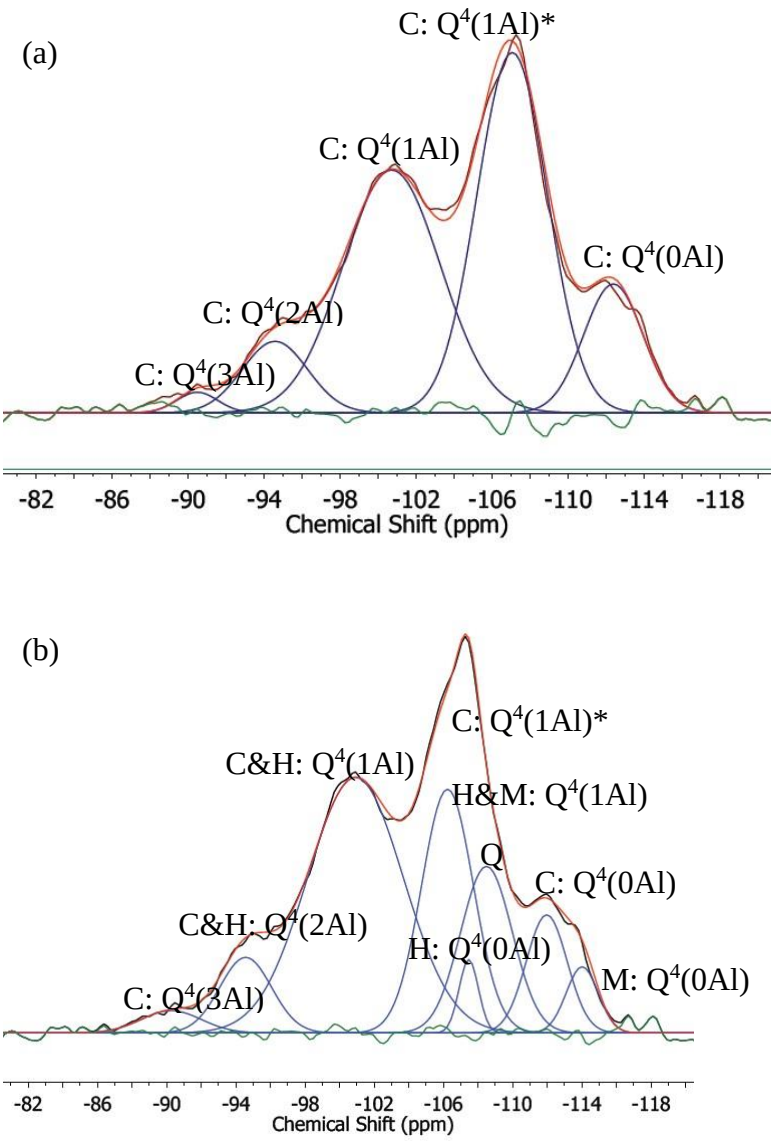

Figure 5.2. Deconvolution and peak assignments of the clinoptilolite specimen, with only clinoptilolite phase (a) and with all the phases identified in XRD (b). The C, H, M and Q are the same as those in Figure 5.1 (* indicates inconsistent assignment from literature).

Peaks were assigned and the Si/Al ratio was estimated for both deconvolutions, as shown in Table 5.2. The debatable peak at around -106 ~ -107 was assigned to Q^4(0Al) or Q^4(1Al) in clinoptilolite phase, and the corresponding Si/Al ratios were calculated. For deconvolution (a) shown in Figure 5.2 (a), assignment of the Q^4(1Al) structure yielded Si/Al ratio of 4.08, and the Q^4(0Al) yielded 7.00. Neither of values is consistent with the bulk Si/Al ratio. For deconvolution (b) shown in Figure 5.2 (b), assignment of the Q^4(1Al) structure yielded Si/Al ratio of 4.85, and Q^4(0Al) yielded 6.53. The value 4.85 is consistent with the bulk ratio 4.9. This consistency suggests the quantitative NMR analysis was able to provide reliable estimation of Si/Al ratio if peaks are appropriately assigned.

Table 5.2. Peak assignment and estimation of Si/Al for deconvolution (a) and (b) in Figure 5.2.

Deconvolution (a)			Deconvolution (b)		
Peaks (ppm)	phase/structure		Peaks (ppm)	phase/structure	
-90.5	C/Q^4(3Al)		-90.3	C/Q^4(3Al)	
-94.6	C/Q^4(2Al)		-94.6	C&H/Q^4(2Al)	
-100.7	C/Q^4(1Al)		-100.9	C&H/Q^4(1Al)	
-112.4	C/Q^4(0Al)		-107.5	Q	
107.1	C/Q^4(1Al)	C/Q^4(0Al)	-108.4	H/Q^4(0Al)	
-	-		-111.9	C/Q^4(0Al)	
-	-		-114.0	M/Q^4(0Al)	
-	-		-106.2	Q^4(1Al)	Q^4(0Al)
Si/Al	4.08	7.00	Si/Al	**4.85**	6.53

5.4 Nanostructure of mature geopolymer

Figure 5.3 shows the ^{29}Si NMR spectrum of the 3-month geopolymer. The tail-like region of the spectrum (from -105 to -120 ppm) suggests the presence of unreacted metakaolin, as it is not observed in a more fully reacted metakaolin geopolymer (Duxson et al. 2005c). Additionally, 5- and 6-coordinated Al have been observed in the MAS ^{27}Al NMR spectrum for the same specimen as shown in Figure 5.4.

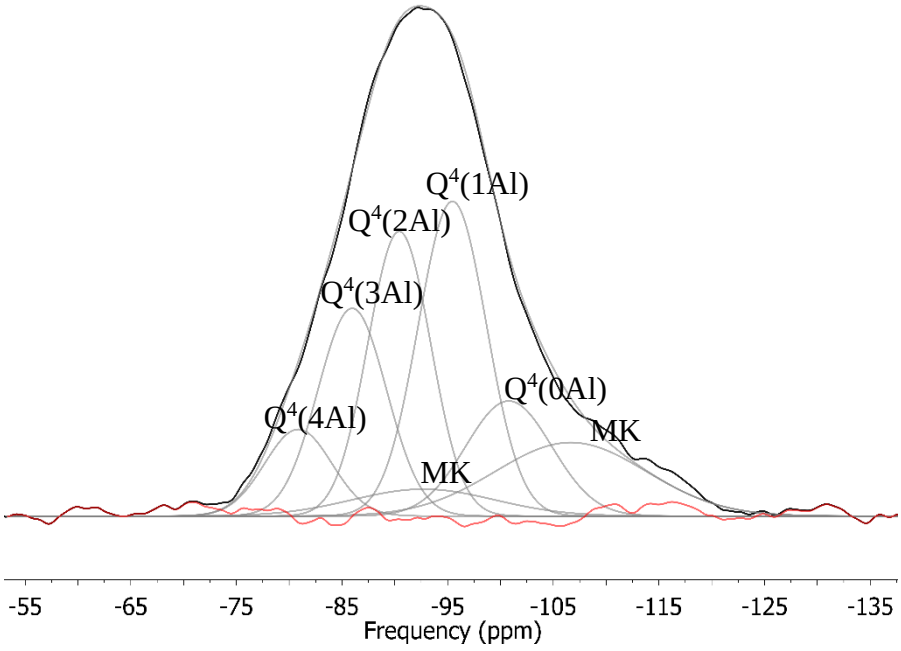

Figure 5.3. Deconvolution of ^{29}Si NMR spectrum of the 3-month geopolymer specimen with no extraction.

During deconvolution of the ^{29}Si NMR spectrum, metakaolin peaks are considered in addition to those for geopolymer gel. Peaks with the same width, position and relative intensity as the raw metakaolin were incorporated. The peak positions are -92.7 and -106.6 ppm respectively. Since no

geopolymer peaks are expected at around -106.6 ppm, this peak is used to determine the relative intensity percent in this spectrum. For geopolymer phase, the peak widths were constrained to be less than 10 ppm, the same assumption made by Bernal et al. (2013) for geopolymers. The peak position, width and the intensity of each peak are summarized in Table 5.3.

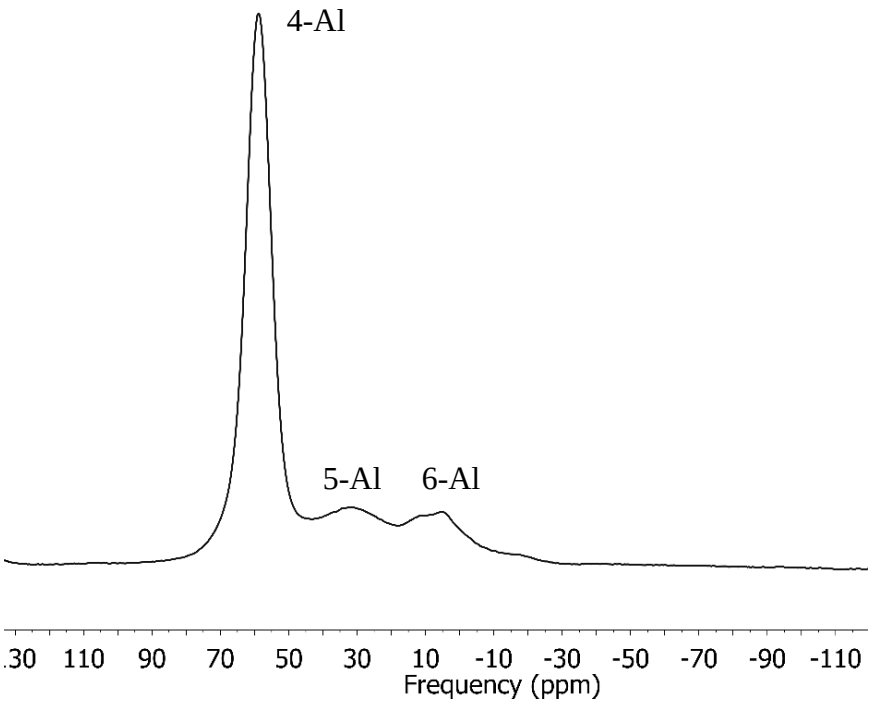

Figure 5.4. ^{27}Al NMR spectrum of the 3-month geopolymer specimen with no extraction using a 17.6-T probe.

Based on the intensity of each peak, Si/Al was estimated using Equation 2.1, derived for zeolites (Engelhardt and Michel 1987) and also used successfully for mature geopolymers (Fernández-Jiménez et al. 2006a, Kim 2012).

The Si/Al was estimated to be 1.89. This ratio is considered to be consistent with the mix design (bulk ratio is 2.0).

Table 5.3. Deconvoluted peaks of the MAS ^{29}Si NMR spectrum of the 3-month geopolymer.

Peak position (ppm)	width (ppm)	Area (%)	Peak assignment
-80.9	7.5	6.9%	Q^4(4Al)
-86.0	7.7	16.9%	Q^4(3Al)
-90.4	7.0	21.2%	Q^4(2Al)
-95.5	7.6	25.5%	Q^4(1Al)
-100.8	9.6	11.7%	Q^4(0Al)
-92.7	15.8	4.5%	MK
-106.7	16.9	13.2%	MK

5.5 Nanostructures of geopolymers at early ages

5.5.1 Specimen at 51 hours

5.5.1.1 Residue weights

The weight of the specimen right after mixing was 1.9950 g and after curing in a sealed condition for 51 hours was 1.9885 g. Before extraction, the specimen was expected to contain three phases: metakaolin, geopolymer and soluble species. This specimen was then treated using combined water and solvent extraction, as developed in Chapter 4, to remove the soluble species and free water, and the dried residue was 1.1509 g. This residue was further treated using the HCl extraction to remove the geopolymer phase, after which the residue was 0.7525 g.

5.5.1.2 Si/Al from deconvolution

The direct polarization (DP) spectra of HCl and combined extraction residues, and the ^{1}H-^{29}Si spectrum (CP) of the combined residue are shown in Figure 5.5. In deconvolution, two peaks were identified in the CP spectrum and assigned as Q^2 and Q^3. It should be noted that the HCl residue showed little intensity in its ^{1}H-^{29}Si CP spectrum, so these Q^2 and Q^3 are presumed to be from the geopolymer phase. The HCl residue (Figure 5.5a) was subtracted from that of the combined extraction residue (Figure 5.5b), with the obtained spectrum expected to be geopolymer gel. Before this subtraction, the spectra of the HCl and combined extraction residue were normalized to 0.7525 g and 1.1509 g of each residue, respectively, such that both intensities corresponded to the total initial specimen before extraction.

During deconvolution, the four Q^4(nAl) peaks were identified based on features including shoulders and peaks in the subtracted spectrum of the geopolymer gel phase. The peak widths and shifts were adjusted to be close to the parameters in the 3-month specimen. For the Q^2 and Q^3 peaks, the peak positions and widths were fixed to be consistent with those in the CP spectrum. Their intensities however were difficult to determine because they overlapped with the Q^4(nAl) peaks. To roughly estimate the relative amount of Q^2 and Q^3, the intensity of the both CP and DP spectra for the geopolymer gel was compared with that of crystalline sodium silicate pellets with 100% low-Q sites (Q^0 and Q^1) under the same NMR testing conditions (see Appendix A). Considering intensities of all the peaks and assuming the Q^2 and Q^3 structures have no aluminium replacement, the Si/Al ratio was estimated to be 3.61. The assumption of no aluminium replacement may result in certain inaccuracy, but it is believed to be acceptable because in other

alkaline-based aluminosilicate systems it has been suggested that Al is thermodynamically more likely to condense with higher-Q silicate species (McCormick et al. 1989).

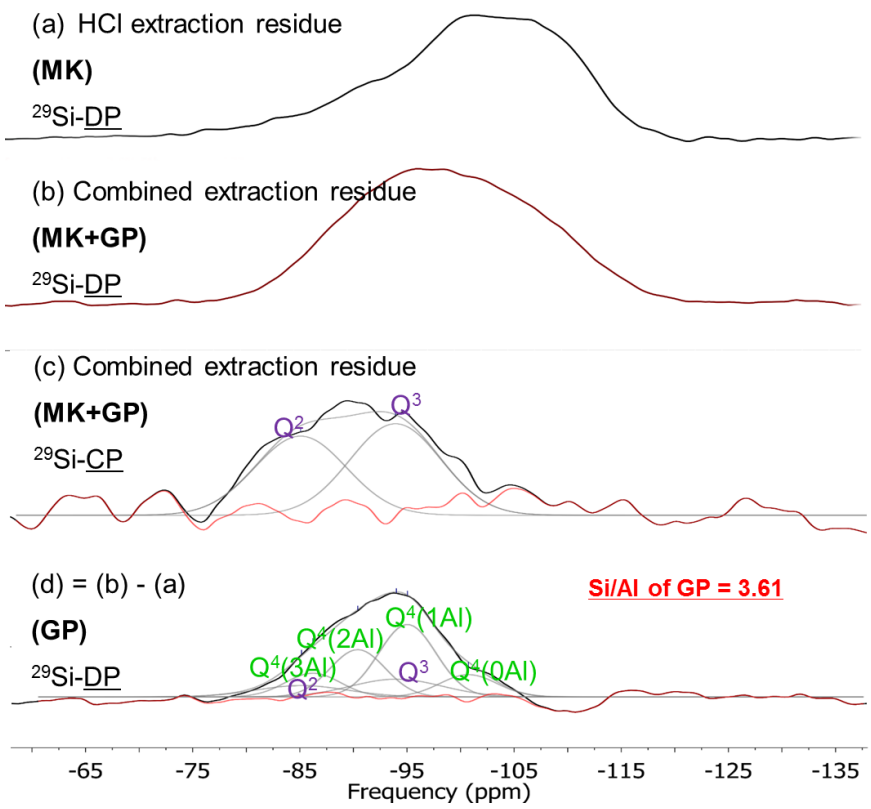

Figure 5.5. ^{29}Si spectra of 51-hour specimens: (a) DP of HCl residue, (b) DP of combined extration residue, (c) ^{1}H-^{29}Si CP of combined extraction residue and (d) deconvoluted spectrum of geopolymer phase by subtraction (a) from (b) (MK = metakaolin; GP = geopolymer).

These Q^2 and Q^3 sites might be on the surface of the geopolymer molecules. They might condense to form more crosslinked geopolymer gel in the combined extraction resideue, but no substantial changes are expected right after extraction until the NMR testing based on results presented in

Chapter 4. These sites are different from those in the solvent extraction residue where low-Q sites are precipitated from the solution due to the "salting-out" effects as discussed in Chapter 4.

5.5.1.3 Si/Al from intensity analysis

Based on the mix design of the specimen, the Si and Al in the specimen with known mass used for extraction at 51 hours were 1.32E-2 and 6.50E-3 moles. Following paragraphs aim to estimate the moles of Si, the Si/Al ratio of the HCl residue, based on both of which the mole number of Al was computed. These obtained mole numbers of Si and Al were used to estimate weights of corresponding phases in following sections.

To estimate the moles of Si of the HCl residue from its total ^{29}Si NMR intensity, the raw metakaolin was used as a standard. A raw metakaolin specimen of 58.4 mg, which contained 5.16E-4 moles of Si based on its chemical composition, showed an intensity of 4469 (arbitrary unit). The specimen of the HCl extraction residue of 60.2 mg showed an intensity of 5410 (arbitrary unit). By comparing these intensities, the Si in the HCl residue (0.7525 g in total) was computed to be 7.63E-3 moles. This comparison across specimens here and below is believed to be valid as NMR tests would yield the same intensity for the same amount of a structural site with a certain chemical environment under the same experimental conditions. The following subsection validated this method by comparing these results with weights from chemical extractions.

Then the Si/Al ratio of the HCl residue was estimated. With presence of 4-, 5- and 6-coordinated Al, it is not possible to estimate the total amount of Al by comparing the overall intensity, as intensity per mole of Al is different in different coordination environments (Massiot et al. 1990a). Therefore, the HCl residue was activated by NaOH solution so that all Al was converted to 4-

coordination. As a reference, metakaolin was also activated by the same relative amount of NaOH solution. Around 100 mg of NaOH-activated MK showed intensities of 2194 and 35346 in ^{29}Si and ^{27}Al NMR, respectively, while around 100 mg NaOH-activated HCl residue at 51 hours showed intensities of 3079 and 33690 respectively. The molar Si/Al ratio of the reference materials (i.e., raw MK activated by NaOH), however, was known to be 1.03, the same as that in the raw MK. Based on this reference, the Si/Al of the NaOH-activated HCl residue, i.e., also the non-activated HCl residue, was estimated to be 1.51.

Using the Si/Al ratio and the moles of Si estimated above, the amount of Al was computed to be 5.04E-3. The moles of Si and Al were later validated by comparing with the extraction weights.

During the combined extraction, the liquid was collected and evaporated. Its dried mass was 0.4906 g. Around 73.9 mg of this residue was tested using both ^{29}Si and ^{27}Al, and the intensities were 272 and 169, respectively. No NaOH activation was conducted, as the resulting error in the estimated amount of geopolymer phase is expected to be small. By comparing with the reference materials, the moles of Si and Al were estimated to be 3.07E-5 and 4.17E-6, respectively in this 73.9 mg specimen. In the total 0.4906 g sample, the moles of Si and Al were calculated to be 2.04E-4 and 2.77E-5.

The moles of Si and Al of the geopolymer phase were estimated by subtracting those of the HCl residue and soluble silicates from the total Si and Al, respectively. For Si, the total moles and those corresponding to HCl residue and soluble silicates were 1.32E-2, 7.63E-3 and 2.04E-4, respectively, and thus that in the geopolymer phase was computed to be 5.37E-3 moles. Similarly, moles of Al in the geopolymer phase was computed to be 1.43E-3. The Si/Al ratio was therefore

3.74, similar to that obtained from spectrum deconvolution (i.e., 3.61). These results are summarized in Table 5.4.

5.5.1.4 Estimated versus extracted weights

The moles of Si and Al were obtained from the intensity above, from which the weights of HCl residue and geopolymer phase can be reasonably estimated by assuming a formula. The moles of Si and Al for the HCl residue were 7.63E-3 and 5.04E-3, respectively. The weight of the HCl residue therefore could be estimated to be the sum of 7.63E-3 moles SiO_2 and 5.04E-3 moles of Al_2O_3, i.e., 0.72 g. This value is close to that obtained directly from weight measurements, 0.7525 g.

Table 5.4. Summary of results from extraction, intensity analysis and deconvolution.

Specimens		Total weight	NMR intensity analysis			NMR deconvolution
		Weight (g)	Si (mole)	Al (mole)	Si/Al	Si/Al
51h	Total specimen	1.9885	1.32E-02	6.50E-03	2.00	-
	Residue (HCl)	0.7525	7.63E-03	5.04E-03	1.51	-
	SS*	0.4906	2.04E-04	2.77E-05	-	-
	GP gel	0.3984	5.37E-03	1.43E-03	3.74	3.61
19d	Total specimen	1.9765	1.35E-02	6.63E-03	2.00	-
	Residue (HCl)	0.1654	1.21E-03	5.58E-04	2.17	-
	SS	-	-	-	-	-
	GP gel	1.4760	1.23E-02	6.08E-03	2.02	2.27

* SS are the soluble species including aluminates and silicates removed during combined extraction.

For geopolymer phase, the moles of Si and Al were 5.37E-3 and 1.43E-3, respectively. In Na-based geopolymers, the moles of Na_2O and Al_2O_3 should be theoretically equal to each other to balance the charge. The mass therefore can be estimated as sum of 5.37E-3 moles of SiO_2, 1.43E-3 moles of $AlO_{3/2}$ and 1.43E-3 moles of $NaO_{1/2}$, or 0.45 g. The corresponding value from weight measurement 0.3984, obtained by subtracting mass of HCl residue (0.7525 g) from that of the combined residue (1.1509 g).

For both HCl residue and geopolymer phase, the estimated mass is regarded to be close to that from weight measurement. This consistency validated the moles of Si and Al from the intensity analysis. Furthermore, the Si/Al from the intensity analysis was 3.74, close to 3.61 from the deconvolution.

5.5.2 Specimen at 19 days

5.5.2.1 Residue weights

The weight of the specimen right after mixing was 2.0355 g and after curing in a sealed condition for 19 days was 1.9765 g. This specimen was then treated using combined water and solvent extraction to remove the soluble silicates and free water, and the dried residue was 1.6414 g. This residue was further treated using HCl extraction to remove the geopolymer phase, after which the residue was 0.1654 g.

5.5.2.2 Si/Al from deconvolution

As shown in Figure 5.6, deconvolution was conducted in a similar way as for the 51-hour specimen. In this case, however, the positions of the Q^4(nAl) peaks more closely followed those seen in the 3-month specimen shown in Figure 5.3. The amount of Q^{2-3} was insignificant at 19 days and thus was not included during deconvolution of the spectrum. The Si/Al of the geopolymer gel was estimated to be 2.27, lower than in the 51-hour specimen, probably because more Al was dissolved and participated to form geopolymers.

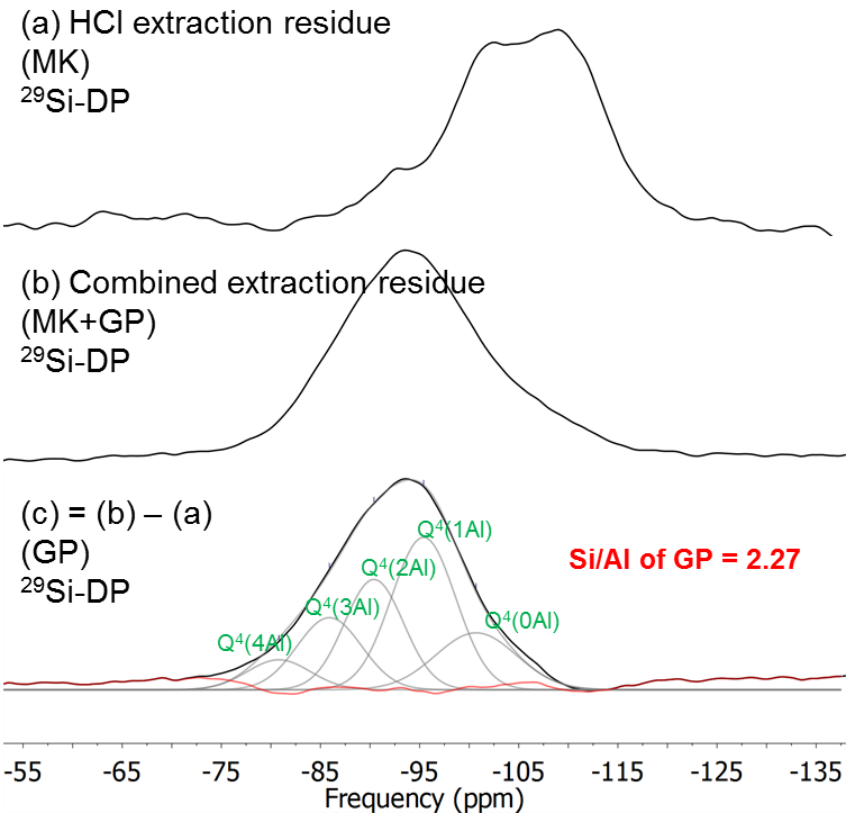

Figure 5.6. ^{29}Si spectra of 19-day specimens: (a) DP of HCl residue, (b) DP of combined extration residue, (c) deconvoluted spectrum of geopolymer phase by subtracting (a) from (b) (metakaolin = MK; geopolymer = GP).

5.5.2.3 Si/Al from intensity analysis

Based on the mix design of the specimens, the moles of Si and Al the specimen with known mass used for extraction at 19 days were 1.35E-2 and 6.63E-3. Following paragraphs aim to estimate the moles of Si and the Si/Al ratio, and based on these two values to compute the moles of Al.

To estimate the moles of Si from the total ^{29}Si NMR intensity, the raw metakaolin was used as a standard. Around 51.7 mg HCl residue at this age was tested using ^{29}Si NMR, showing intensity of 3359 (arbitrary unit). By comparing with the reference specimen, the Si in this specimen was estimated to be 3.79E-4 moles. The total mass of the HCl residue was 0.1654 g, and thus it contained 1.21E-3 moles of Si.

Then the Si/Al ratio was estimated in the HCl residue. Around 140 mg NaOH-activated HCl residue was tested using ^{29}Si and ^{27}Al NMR. The intensity of ^{29}Si and ^{27}Al were 2766 and 21083, respectively. Using the NaOH-activated raw MK as a reference, the Si/Al of the NaOH-activated HCl residue, and thus also the non-activated HCl residue, was estimated to be 2.17. This value is higher than that in the raw MK, probably related to incongruent dissolution of the MK, but more systematic investigation is needed to fully understand this difference.

Using the Si/Al ratio and the moles of Si estimated above, the amount of Al in the HCl residue was computed to be 5.58E-4. The moles of Si and Al were later validated by comparing with the extraction weights.

The amount of soluble species during the combined extraction at 19 days was insignificant. The moles of Si and Al in geopolymer gel were estimated by subtracting those of the HCl residue only

from the total moles Si and Al before extractions, respectively. For Si, the total moles and that corresponding to HCl residue were 1.35E-2 and 1.21E-3, respectively, and thus Si in the geopolymer phase was computed to be 1.23E-2 moles. Similarly, moles of Al in the geopolymer phase were computed to be 6.08E-3. The Si/Al ratio was thus 2.02, similar to that obtained from spectrum deconvolution, 2.27. These results were summarized in Table 5.4.

5.5.2.4 Estimated versus extracted weights

Similar as the calculation for the 51-hour specimens, the weight of the HCl residue at 19 days was estimated to be the sum of 1.21E-3 moles SiO_2 and 5.58E-4 moles of $AlO_{3/2}$, i.e., 0.16 g. This value is close to that obtained directly from weight measurements, 0.1654g.

For geopolymer phase, the mass was estimated as the sum of 1.23E-2 moles of SiO_2, 6.08E-3 moles of $AlO_{3/2}$ and 6.08E-3 moles of $NaO_{1/2}$, or 1.73 g. The corresponding value from weight measurement was 1.4760, based on subtracting mass of HCl residue (1.6414 g) from that of the combined residue (0.1654 g).

For both HCl residue and geopolymer phase, the estimated mass is close to that from weight measurement. This consistency indicates the moles of Si and Al from the intensity analysis are reasonable. Furthermore, the Si/Al from the intensity analysis was 2.02, close to 2.27 from the deconvolution.

5.5.3 Specimens at 51 hours versus 19 days

As summarized in Table 5.4, the Si/Al ratio is the geopolymer is higher in the 51-hour specimen than in the 19-day one. This higher ratio at 51 hours was probably due to continuous incorporation

of more Al into the geopolymer gel. Relatively more geopolymer gel was seen at 19 days than at 51 hours, suggesting reaction proceeded during this period. The Si/Al ratios of the HCl residue at both the ages were higher than 1.03, the ratio for the raw metakaolin, probably due to incongruent dissolution. The Si/Al ratio of 2.17 in the 19-day HCl residue, somewhat higher than expectation, is worth some further investigation.

5.6 Conclusions

A protocol using NMR deconvolution was developed to quantify structures of zeolites and geopolymers. Using deconvolution, the Si/Al ratios of a natural zeolite and a mature-geopolymer specimen were estimated and validated with their known bulk ratios. Then the Si/Al ratio of geopolymer phase was estimated for geopolymer specimens at 51 hours and 19 days after mixing. The amount of the geopolymer gel was higher and its Si/Al ratio was lower in 19 day-specimen than those in the 51 hour-specimen. For validation, moles of Si, Al and thus Si/Al were also estimated by analyzing the intensities of both the ^{29}Si and ^{27}Al NMR spectra, and the mass of each phase was estimated based on the moles of Si and Al, and was then compared with weights measured from different extractions. This study has demonstrated that deconvolution of ^{29}Si NMR spectra, if properly conducted, is an effective technique to quantify the structures of geopolymer specimens.

Chapter 6. Setting and nanostructural evolution of metakaolin geopolymer

6.1 Introduction

As reviewed in Chapter 2, if geopolymers are to be used in structural concrete, it is critically important to understand and control their setting. Setting is the process by which a material changes from a fluid to a solid. In structural concrete, setting controls the time during which the material can be mixed, transported, and shaped. A few studies have reported set times for geopolymers (Silva et al. 2007, Suraneni et al. 2014), and some other studies examined related stiffening behaviors by rheology tests, small-angle X-ray scattering (SAXS) and static NMR tests (Steins et al. 2012, Favier et al. 2013, Favier et al. 2015, Rouyer and Poulesquen 2015). Nonetheless, there remains lack of detailed understanding concerning the nanostructural evolution associated with set, including a sysmtematic monitoring of precursor dissolution and consumption of liquid species.

A conceptual model was proposed by Duxson et al. (2007a) to describe the geopolymerization process. It lists the following nanostructural changes: dissolution, equilibration of dissolved species, gelation, reorganization and polymerization. A key focus of the present study is to expand and improve on this model based on direct experimental evidence. The following paragraphs review evidence for this conceptual model.

Many studies have shown that geopolymerization starts with dissolution of the precursor (often metakaolin or fly ash). One study concluded that setting is controlled by the aluminate species released by dissolution (Fernández-Jiménez et al. 2006b), although setting measurement was presented in their study. Dissolution is difficult to measure independently of precipitation or condensation. Leaching tests have been used to measure the dissolution kinetics of metakaolin in

a geopolymer (Feng et al. 2004), but results were said to be confounded by precipitation (Provis and Van Deventer 2009). The amount of aluminum released by dissolution of fly ash was estimated by analyzing its concentration in the filtrate after acid attack (Fernández-Jiménez et al. 2006b), a time-consuming analysis that can only be conducted at discrete times and can easily result in experimental errors. Liquid-state ^{27}Al NMR has been used to examine reaction kinetics by probing the amount of 'detectable' Al (Rahier et al. 2007), but no direct estimation of the dissolution extent was reported. Solid-state ^{27}Al spectra have confirmed that dissolution of metakaolin is associated with the conversion of 5- and 6-coordinated Al to 4-coordinated Al (Provis and Van Deventer 2009), but the full nanostructural evolution in this conversion has not been systematically studied. Although solid-state ^{27}Al NMR spectroscopy seems to be the most promising method to study the dissolution, it should be noted that quantitative interpretation of ^{27}Al NMR spectra is not straightforward because the ^{27}Al nucleus is quadrupolar (Man and Klinowski 1988, Massiot et al. 1990b).

After dissolution, aluminate and silicate species are believed to condense to form a gel (Provis and Van Deventer 2009), although detailed experimental evidence regarding this process has been lacking. Condensation can take place between silicate species themselves or between aluminate and silicate species, and the latter has been shown to proceed faster (Silva et al. 2007). Other factors shown to influence early-age mechanical properties include presence of nucleation sites such as aggregates or added oxides (Rees et al. 2008), and curing temperature (Rovnaník 2010). Techniques including (but not limited to) FTIR (Rees et al. 2007a, Rees et al. 2007b, Hajimohammadi et al. 2010, Hajimohammadi et al. 2011b), PDF (White et al. 2011b, White et al. 2013), SAXS (Steins et al. 2012, Rouyer and Poulesquen 2015) and calorimetry (Yao et al. 2009)

have been used to probe the nanostructure evolution. Compared to these techniques, solid-state ^{29}Si NMR provides more detailed nanostructural information in terms of atomic connectivity for both zeolites and mature geopolymers. However, this experiment is too slow for probing early-age reactions in geopolymers. Nanostructural evolution has been investigated in dilute solutions with liquid-state ^{29}Si NMR (North and Swaddle 2000, Anseau et al. 2005), but not for geopolymer systems in which species are highly concentrated. One exception is a study of metakaolin-based geopolymers, in which liquid-state ^{29}Si NMR was used to probe the silicate species right after mixing until around 15 hours (Barbosa et al. 2000), and spectra were seen to evolve with time. With careful examination of these observable silicates, more insight could be obtained on condensation reactions.

A few studies have examined the structure of geopolymers at set. The conceptual model by Duxson et al. (2007a) described above did not identify the step associated with set. Fernandez-Jimenez attributed set to the formation of gel with high aluminum content (Fernández-Jiménez et al. 2006b) but, as noted above, did not report set measurements. A previous study correlated the rheology behaviors of early-age geopolymers with the size evolution of aluminosilicate using SAXS (Steins et al. 2012), and in a later study (Rouyer and Poulesquen 2015) the gel point was estimated by a rheology method used in organic polymer system. Favier et al. (2013) attributed the first increase of shear elastic modulus in rheology tests within 15 minutes after mixing to the formation of Al-rich gel by comparing rheology behaviors with synthesized gel, and attributed a second increase to the formation of gel with low mobility as it coincided with intensity drop of Al and Na detected in static NMR tests (Favier et al. 2015). At set, there still remains lack of information regarding the structural connectivity of the product. Therefore, the objective here in this chapter was to better

understand the correlation between nanostructure and setting using more detailed nanostructural information. Calcium has been found to speed up setting (Temuujin et al. 2009, Suraneni et al. 2014), an effect that is discussed in Chapter 7.

To better understand setting, it is necessary to probe the structure of aluminate and silicate precursor species as condensation proceeds, to observe formation and structural evolution of the gel, and to correlate these with measured setting behavior. In this study set was measured using both penetration resistance and UWR. Dissolution of aluminum was measured using solid-state ^{27}Al NMR spectroscopy. Liquid-state ^{29}Si NMR spectra were analyzed to provide insights on how silicate species in solution change as they undergo condensation. The liquid-state ^{29}Si NMR experiment is rapid enough for monitoring early-age changes with time and is reliably quantitative under appropriate experimental conditions; and in particular reduction in silicates in solution detected using liquid-state ^{29}Si NMR is expected to reflect their inclusion in large aluminosilicate gel species at early ages when Si from dissolution is minimum. The main objective of study presented in this chapter was to probe nanostructural changes associated with reaction, and only limited microstructural work was done.

6.2 Experimental procedure

The composition of the geopolymer mix (expressed as molar Na_2O:Al_2O_3:SiO_2:H_2O) was 1:1:4:11, chosen because it has been shown to produce high mechanical strength (Kriven et al. 2003, Duxson et al. 2007b), and to be thermodynamically stable (Criado et al. 2008). Detailed synthesis procedure is described in Chapter 3. Two setting tests were conducted, penetration resistance and UWR, both of which are described in Chapter 3. Both tests were begun right after mixing.

The solid-state ^{27}Al NMR tests were carried out to monitor the conversion of 5- and 6-coordinated Al to 4-coordinated Al in metakaolin in geopolymer gel by measuring the amount of each site at different times and examine how this conversion is associated with setting. Tests were conducted at 7.04 T using a Varian Unity Inova spectrometer. A 4-mm magic-angle spinning (MAS) probe was used at a spinning rate of 12 kHz. The specimen was packed into the rotor right after mixing and allowed to react there. The first test began at about 20 minutes after mixing. A 30-degree pulse of 0.725 μs was used. Recycle delay was 1.0 s and 2048 scans were acquired for each test. More details are described in Chapter 3.

Liquid-state ^{29}Si NMR tests were also carried out to monitor nanostructural evolution associated with setting. Tests were conducted at 14.1 T using a Varian Unity Inova spectrometer. Right after mixing the specimen was packed into a 5-mm glass tube and allowed to react there. The first test began at about 20 minutes after mixing. A 90-degree pulse of 6 μs was used, and recycle delay was 30 s and 64 scans were acquired for each test.

Deconvolutions of the NMR spectra were conducted using two types of software. The ^{27}Al spectra were deconvoluted using WSolids (Eichele 2015), a program that deconvolutes solid-state NMR spectra. Several studies have used this program to simulate quadrupolar nuclei (Ashenhurst et al. 2000, Chen and Huang 2006, Sutrisno et al. 2012). During simulation of ^{27}Al NMR spectra, quadrupolar coupling (C_q), asymmetry (η), and isotropic chemical shift were considered, and their values were set within ranges suggested for kaolin (Rocha 1999) and geopolymers (Brus et al. 2012). The ^{29}Si spectra were deconvoluted using MestReNova, an NMR processing software, as described in detail in Chapter 3.

To provide further structural information, three additional experiments were conducted. First, solid-state cross-polarization $^{1}H/^{29}Si$ NMR tests were conducted using the Varian Unity Inova spectrometer at 7.04 T. The contact time was optimized to show the highest intensity. Recycle delay was 2.0 seconds, and 8192 scans were acquired. Prior to the testing, the specimen at set was dried by solvent extraction as developed and shown in Chapter 4. Microstructure of the mix at set was also examined using a JEOL JSM-6060 LV scanning electron microscope (SEM). Prior to the imaging, the specimen was treated with the combined water and solvent extraction, as developed and shown in Chapter 4, to stop the geopolymer formation and extract water. For comparison, microstructure of the raw metakaolin powders was examined. Additionally, MAS ^{27}Al NMR tests were carried out on both silicate-activated mix (with composition 1:1:4:11) and hydroxide-activated mix (with composition 1:1:2:11) at 17.6 T using an Agilent VNMRS spectrometer operating at a resonance frequency of 195.3 MHz. A 15-degree pulse was used. Recycle delay was 1.0 s and 2048 scans were acquired for each test.

6.3 Results and discussion

6.3.1 Setting behavior

Setting behavior is shown in Figure 6.1. Set was assigned when penetration resistance reached 2 MPa, around 15-16 hours, and when two lines fitted to the UWR results (using a least squares fit) intersected (Puligilla and Mondal 2013), also around 15-16 hours. In Figure 6.1, the UWR curves decreased substantially (from unity) immediately after mixing. This drop seems to be consistent with the increase in shear elastic modulus in rheology tests reported by Favier et al. (2013) within 15 minutes after mixing, while further examination is needed to understand this phenomenon. They attributed this increase to the formation of Al-rich gel. In the UWR test of cement pastes, a less

substantial initial drop is generally observed, and is attributed to flocculation of the cement particles (Suraneni et al. 2014), although it is not expected that metakaolin would show such flocculation.

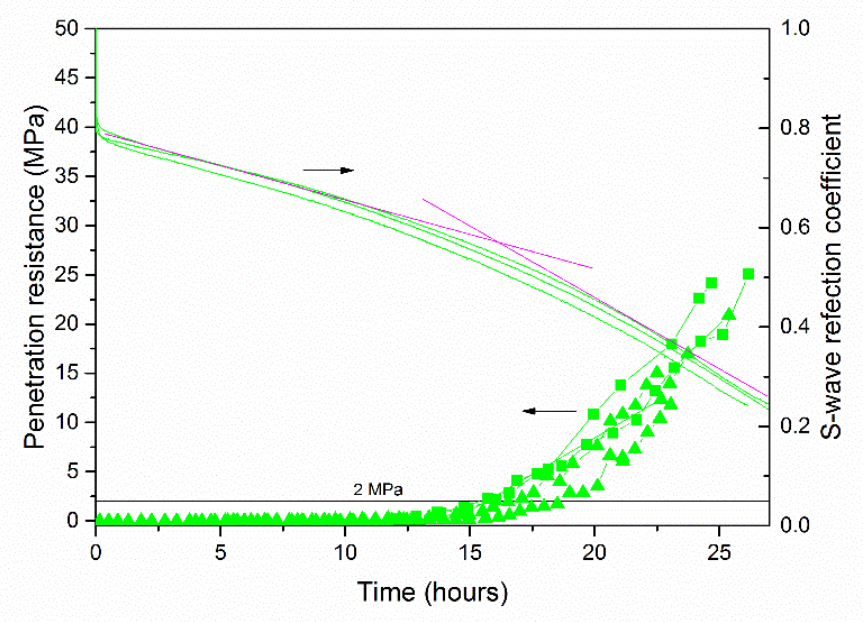

Figure 6.1. Penetration resistance and UWR curves of geopolymer with composition $1Na_2O{\cdot}1Al_2O_3{\cdot}4SiO_2{\cdot}11H_2O$.

6.3.2 Al dissolution during geopolymerization

The solid-state ^{27}Al NMR spectrum in Figure 6.2 was typical for those obtained for the study. The spectra were deconvoluted into peaks for 4-, 5- and 6-coordinated Al, as shown in this figure, and the area of each deconvoluted peak was plotted versus time in Figure 6.3. Data points at each time in this figure correspond to individual ^{27}Al NMR tests. The 4-coordinated Al increased while the 5- and 6-coordinated Al decreased with time, changes generally observed during geopolymer reaction and indicating metakaolin dissolution (Provis and Van Deventer 2009). This conversion

was rapid right after mixing up to around 10 hours, then slowed down and became immeasurable after 15 hours (although additional dissolution was observed after several months shown in Appendix B). Although ^{27}Al is a quadrupolar nucleus so quantitative interpretation is uncertain, this test provides a reliable indicator for the conversion from 5- and 6- to 4-coordinated Al. The 4-Al structure is more symmetric than those of 5- and 6-coordinated Al, and thus a higher portion of 4-coordinated Al with respect to its own amount can be detected (Fyfe et al. 2000); so the molar percentage of 4-coordinated Al estimated from the intensity percentage would be magnified, and thus also is the estimated conversion of 5- and 6- to 4-coordinated Al. Nonetheless, it can be conservatively concluded that dissolution to release Al was negligible after 15 hours.

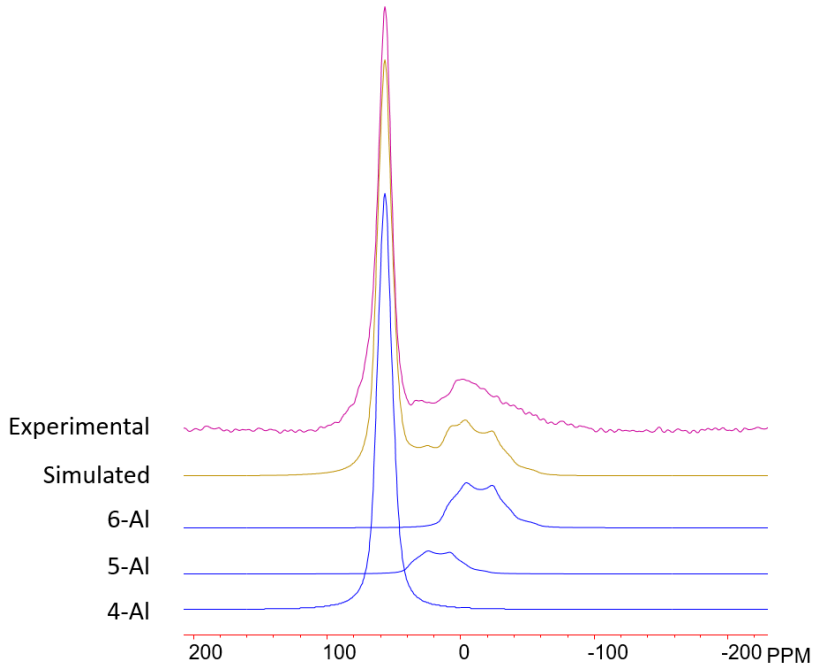

Figure 6.2. Solid-state ^{27}Al spectrum around 20 hours after mixing (experimental spectrum and deconvoluted peaks).

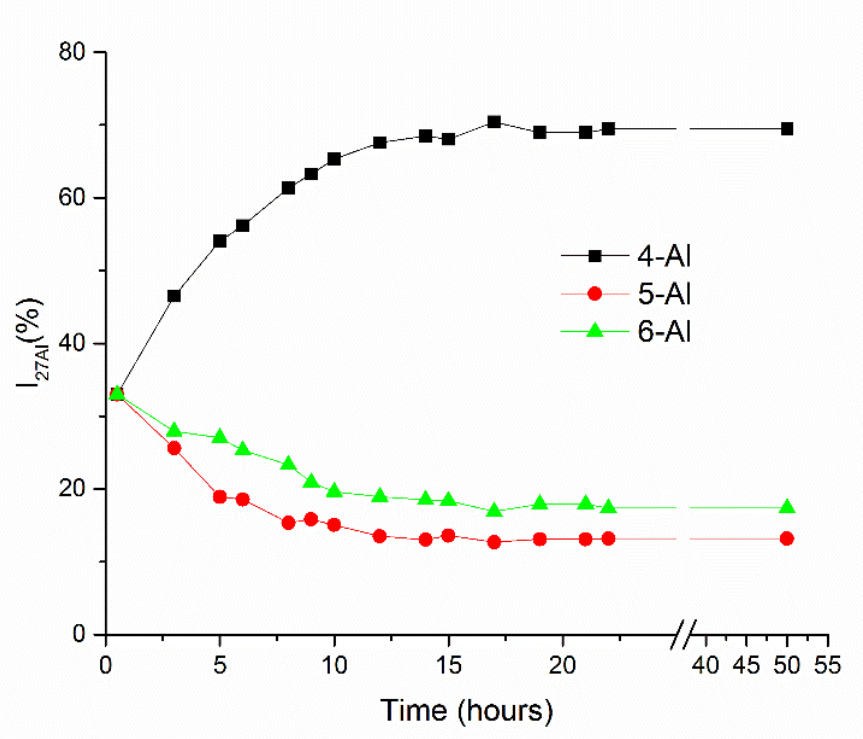

Figure 6.3. Amounts of 4-, 5- and 6-coordinated Al as geopolymerization proceeded.

6.3.3 Aqueous species during geopolymerization

The liquid-state ^{29}Si tests were carried out to examine silicates in solution. Figure 6.4, a spectrum at around 0.5 hour after mixing, was typical for study presented in this chapter. The spectra were deconvoluted based on observed shoulders, and these were assigned to Q^{0-4} silicon sites as shown. The assignments are based on those reported for aluminum-free silicates in liquid-state ^{29}Si NMR spectra (Bass and Turner 1997). The Q^4 peak is broader than the others, suggesting that the Q^4 molecules are larger and less mobile than the lower-Q molecules. The amount of silicon in each site was estimated and normalized with respect to its own amount right after mixing (i.e., from the first data collected for the specimen). Each normalized amount and the ratio Q^4/Q^3 were plotted versus time in Figure 6.5 (a) and (b), respectively. As shown in Figure 6.5 (a), intensities of Q^3

and Q^4 species decreased right after mixing up to 10 hours, and those of Q^2 and Q^3 species began to drop after 15 hours. The increase of Q^0 was rapid after 20 hours and is discussed later in this chapter. As shown in Figure 6.5 (b), the ratio Q^4/Q^3 increased progressively with time. These changes are discussed and correlated with Al dissolution results and set later in this chapter.

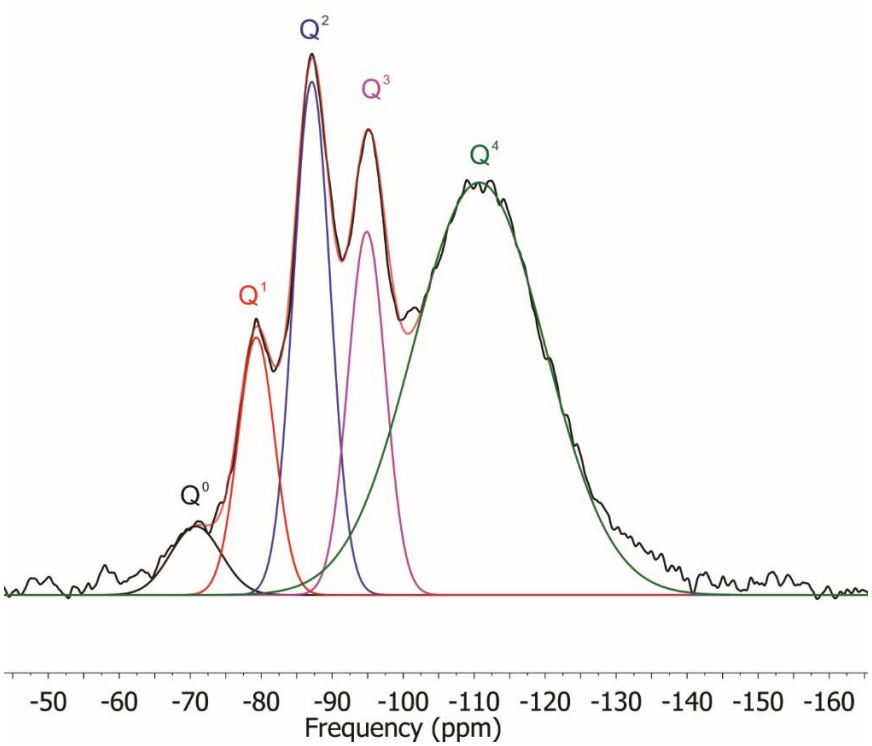

Figure 6.4. Deconvolution of liquid-state ^{29}Si NMR spectrum, 0.5 hour after mixing (experimental spectrum and deconvoluted peaks).

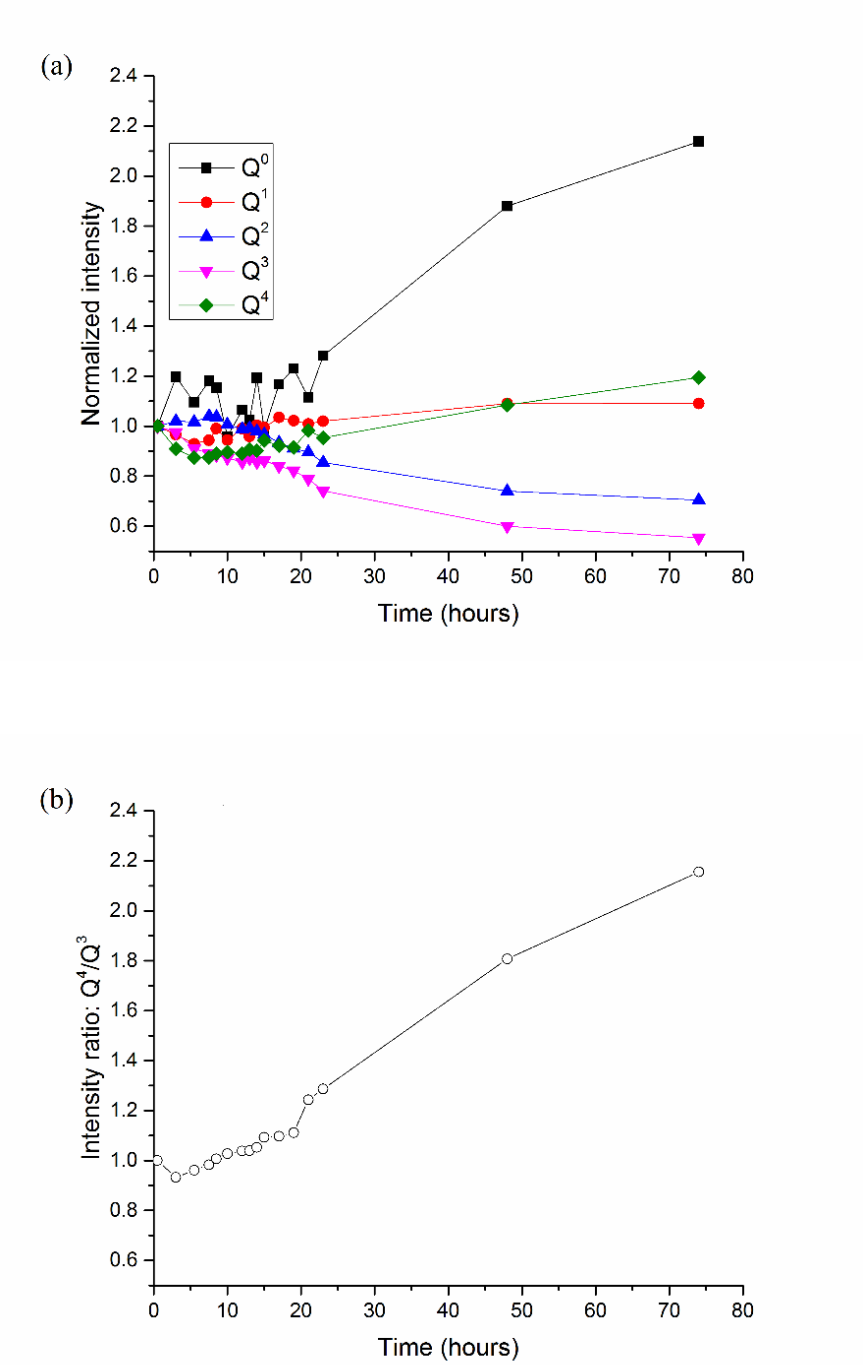

Figure 6.5. Normalized amounts of $Q^{(0-4)}$ sites (a) from liquid-state ^{29}Si NMR tests and ratio of the normalized Q^4 and Q^3 (b) as geopolymerization proceeded.

No peaks were assigned to aluminum-containing silicate species in the liquid-state ^{29}Si NMR spectra in the current study. This assignment is consistent with the literature. Here the peak positions (-71, -79, -87, -95, and -109 ppm) are no more different than 1 ppm from each corresponding Al-free silicate site (Q^{0-4}) in solution as reviewed by Bass and Turner (1997), and generally a 4-5 ppm difference in chemical shift is expected when silica is bonded to alumina (Swaddle 2001). Similarly, no aluminosilicate species were detected in an aluminosilicate solution with similar composition during zeolite formation using liquid-state ^{29}Si NMR (Ginter et al. 1992). Furthermore, the static ^{27}Al NMR tests (shown in Appendix C) indicated very little Al in solution, consistent with a recent study by Favier et al. (2013) for mixes similar to the current studied composition. It should be noted that liquid-state ^{29}Si NMR may not detect aqueous aluminosilicates at the concentration and temperature used here (Kinrade and Swaddle 1989, North and Swaddle 2000).

6.3.4 Formation of aluminosilicate gel

Upon dissolution, Al appeared to be incorporated into solid aluminosilicate oligomers. An aqueous $Al(OH)_4^-$ peak was seen in ^{27}Al spectra of hydroxide-activated metakaolin geopolymers with Si/Al around 1.0 (not shown here, can be found in Figure 6.8), and also observed in a similar study of metakaolin-based geopolymer with Si/Al less than 1.4 (Duxson et al. 2005a). However, no such peak was detected in the current mix (composition 1:1:4:11), indicating that, at this high Si/Al ratio, all Al released from the dissolution of metakaolin was condensed immediately with silicate species to form aluminosilicate oligomers. Favier and colleagues (2013) drew a similar conclusion for specimens within 15 minutes after mixing based on the rheology behavior of gels synthesized with varying Al contents.

Based on other reports, the newly formed aluminosilicate oligomers, which were not detected by liquid-state ^{29}Si NMR, are presumed to be larger than the silicate species that were detected by this method. In one such report (Granizo et al. 2014), a leaching study conducted on a metakaolin geopolymer, both liquid-state ^{27}Al and ^{29}Si NMR detected only silicate and aluminate monomers in the liquid phase and found aluminosilicates only as precipitates, separated from the liquid phase by filtration using a pore size of 3-5 μm. In a SAXS study of metakaolin geopolymers (Steins et al. 2012), aluminosilicate oligomers right after formation were estimated to be around 2 nm (11 to 12 monomeric repetitions) and then to aggregate into larger-sized species. More recently, Favier and colleagues (2015) correlated the increase of shear elastic modulus at a few hours with the decrease of intensity in static ^{27}Al and ^{23}Na NMR, and attributed to the formation of low-mobility gel, which could be considered as solid. These studies suggest the aluminosilicate oligomers tend to enlarge over time.

To provide further insight into nanostructural evolution, results from the two NMR methods were compared in more detail.

At 0-10 hours, the Q^3 and Q^4 silicates decreased, as shown in Figure 6.5 (a). This change was accompanied by a rapid release of Al due to dissolution of metakaolin, as shown in Figure 6.3. Only higher-Q silicate species were seen to decrease, consistent with the observation that aluminosilicate formation was enhanced with the ratio of $[SiO_2]/[M_2O]$ (McCormick et al. 1989), as the higher ratio results in higher polymerization degree in silicate solution (McCormick and Bell 1989). As noted above, these two changes indicated formation of aluminosilicate oligomers.

At 10-15 hours new aluminosilicate formation slowed down, indicated by the slower decrease in Q^3 and Q^4 in Figure 6.5 (a) as well as the slower dissolution of metakaolin in Figure 6.3. The Q^4/Q^3 ratio increased during this time, as shown in Figure 6.5 (b), suggesting that the size of Q^4 silicates in solution was progressively increased. At the same time, the previously-formed aluminosilicates in the system condensed to form larger structural units. Such condensation between aluminosilicates is expected, as the formation of Si-O-Al bonds is thermodynamically more favorable than formation of Si-O-Si bonds (Silva et al. 2007). White et al. found thermodynamics of reactions involving aluminate monomer depend on charge state, but they did not provide results for reactions involving aluminosilicates reactants (White et al. 2011a). The observation of condensation is consistent with the SAXS (Steins et al. 2012) observation that smaller aluminosilicate oligomers (seen right after dissolution of metakaolin) condense to form larger oligomers (that act as building blocks for further growth of geopolymer network). Once most, if not all, Al-containing species have condensed into large aluminosilicate structural units, more Al-free silicates in the solution are expected to participate in the following stages of the reaction.

Starting at 15 hours, Q^2 and Q^3 decreased and Q^4 increased, as shown in Figure 6.5 (a). The decrease should not be due to formation of aluminosilicates, as little aluminum was released by dissolution (Figure 6.3). The only possibility for these changes is that silicate ions in solution are attaching to the larger aluminosilicate structural units that were developed beforehand. This attaching process is consistent with the incorporation of Si-OH group to Al-rich gel, thereby enriching the gel in Si, proposed by Provis and Bernal (Provis and Bernal 2014) when they commented on earlier FTIR results regarding geopolymerization (Fernández-Jiménez and Palomo 2005). Such attaching was also concluded by previous simulation studies: mathematical modeling

by Provis and van Deventer (2007) concluded that aluminosilicate gel forms by consuming aluminosilicate polymer and silicate species; and multiscale modeling by White et al. (2012) concluded that gel forms by Ostwald ripening, during which larger species growth while smaller ones disappear. Medium sized Q^2 and Q^3 species are more likely to participate in this attaching process—on the one hand they have sufficient mobility, and on the other hand they are large enough to make contact with the aluminosilicate molecules. This attaching process leads to the formation of aluminosilicate gel, comprised mainly of Q^4 species. The beginning of this attaching process, i.e., right at the point when the large units have formed, coincided with set (around 15-16 hours) in Figure 6.1. At this time, the large structural units are believed to span across unreacted metakaolin particles. Another point worth mentioning is that at 15 hours after mixing and thereafter, Q^0 silicon intensity increased substantially, perhaps because, as suggested (Provis and Van Deventer 2009), at first dissolution releases aluminum more rapidly than silicon and later the silicon is catching up. Alternatively, this increase could be due to an increased pH resulting from removal of Si species from the solution, which may shift speciation towards monomers and may also enhance dissolution of metakaolin. At the same time dissolution of Al ceased or significantly slowed down, perhaps because the metakaolin, from which $Al(OH)_4^-$ is released, was covered by solid product, as proposed by Provis et al. (Provis et al. 2005) for silicate-activated metakaolin geopolymers.

6.3.5 Structure at set

The discussion above of MAS ^{27}Al and liquid-state ^{29}Si NMR results indicates at set (around 15 hours) that aluminosilicate gel coexists with silicate species in solution and unreacted solid

metakaolin particles. Here SEM and solid-state cross-polarization $^{1}H/^{29}Si$ NMR results are presented to further confirm the presence of aluminosilicate gel and silicate species, respectively.

SEM results further support presence of aluminosilicate gel at set. Figures 6.6 (a, b) show the residue after combined extraction for the mix at 15 hours (around set) and raw metakaolin, respectively. Little gel is seen, probably because little remains after combined extraction—it was noted above that the three-dimensional network structure (required to resist dissolution during the extraction) has not yet formed at set. Nonetheless, examination reveals some subtle differences. In circled areas, for example, raw metakaolin particles, Figure 6.6 (b), show plates with sharper edges, but the combined-extraction residue, Figure 6.6 (a), show plates with smoother edges. This smoothness could be due to gel coated on the unreacted metakaolin. The particles can still be distinguished from each other, suggesting that only a small amount of gel is present.

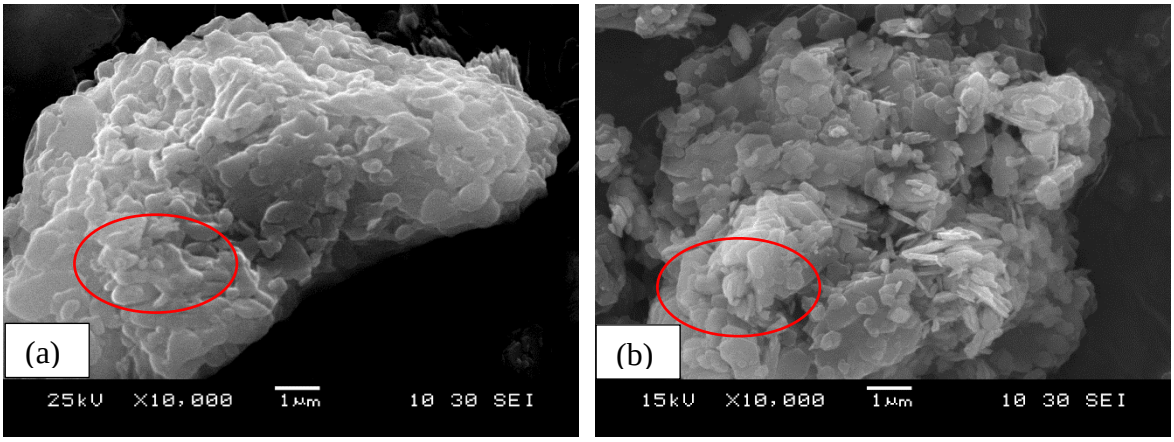

Figure 6.6. SEM micrographs of residue of the geopolymer mix after combined extraction at 15 hours (a) and raw metakaolin particles (b).

The solid-state cross-polarization $^{1}H/^{29}Si$ NMR tests were conducted to further confirm the presence of low-Q Si species at set. Specimen was dried by solvent at set. Figure 6.7 shows both the direct and cross-polarization NMR spectra. In the cross-polarization spectrum, signal of low-Q Si sites, Q^{1-3}, was enhanced. It should be noted that solvent drying might change the relative amount of low-Q species, as discussed in Chapter 4, but would not decompose Q^4 to lower-Q species. Low-Q species are thus present in specimen at set regardless of drying. Similar tests were conducted under the same condition for raw metakaolin and 3-month geopolymer mix, but no such significant signal enhancement of the low-Q sites was observed. Evidence here is consistent with the liquid-state ^{29}Si NMR and further confirms the presence of low-Q Si sites at set. Spectra of additional specimens also suggest the presence of the low-Q species, as presented in Appendix D.

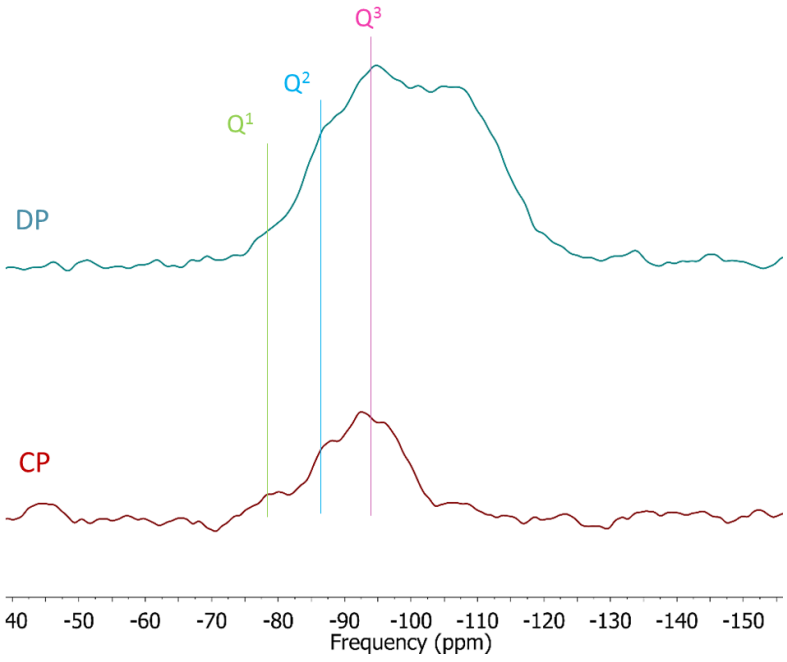

Figure 6.7. Direct (^{29}Si) and cross-polarization ($^{1}H/^{29}Si$) NMR spectra of geopolymer mix dried by solvent at the setting point. DP = direct polarization; CP = cross polarization.

The MAS ^{27}Al NMR results provide some indication that the aluminosilicate gel forms a protective layer near the metakaolin surfaces. In Figure 6.8 (a), aqueous $Al(OH)_4^-$ is observed in MAS ^{27}Al NMR spectrum for hydroxide-activated metakaolin, but not for silicate-activated one. The following mechanism was proposed: in silicate-activated mixes, the high concentration of Si in the liquid would immediately capture Al that is released from metakaolin surfaces to form aluminosilicate gel, before aqueous aluminate diffuses away. In Figure 6.8 (b), more 4-coordinated Al is observed at all tested reaction times, indicating a higher dissolution extent. Deconvolution of a typical NaOH-activated metakaolin is shown in Appendix E. Both the aqueous 4-Al and the solid 4-Al were counted as 4-Al in Figure 6.8 (b). In the silicate-activated mix, the aluminosilicates that formed near the metakaolin surfaces may act as a protective layer and hinder further dissolution. This protective layer mechanism has been proposed by Provis and colleagues (Provis et al. 2005), based on the previously reported nucleation sites around quartz in an aluminate solution. Later, White et al. (2012) postulated the same mechanism in silicate-activated metakaolin based on multiscale simulation, consistent with implications from other nanostructural studies using PDF techniques from the same group (White et al. 2011b). More recently, rheology study by Favier et al. (2013) further supports this mechanism, even though at a macroscale level.

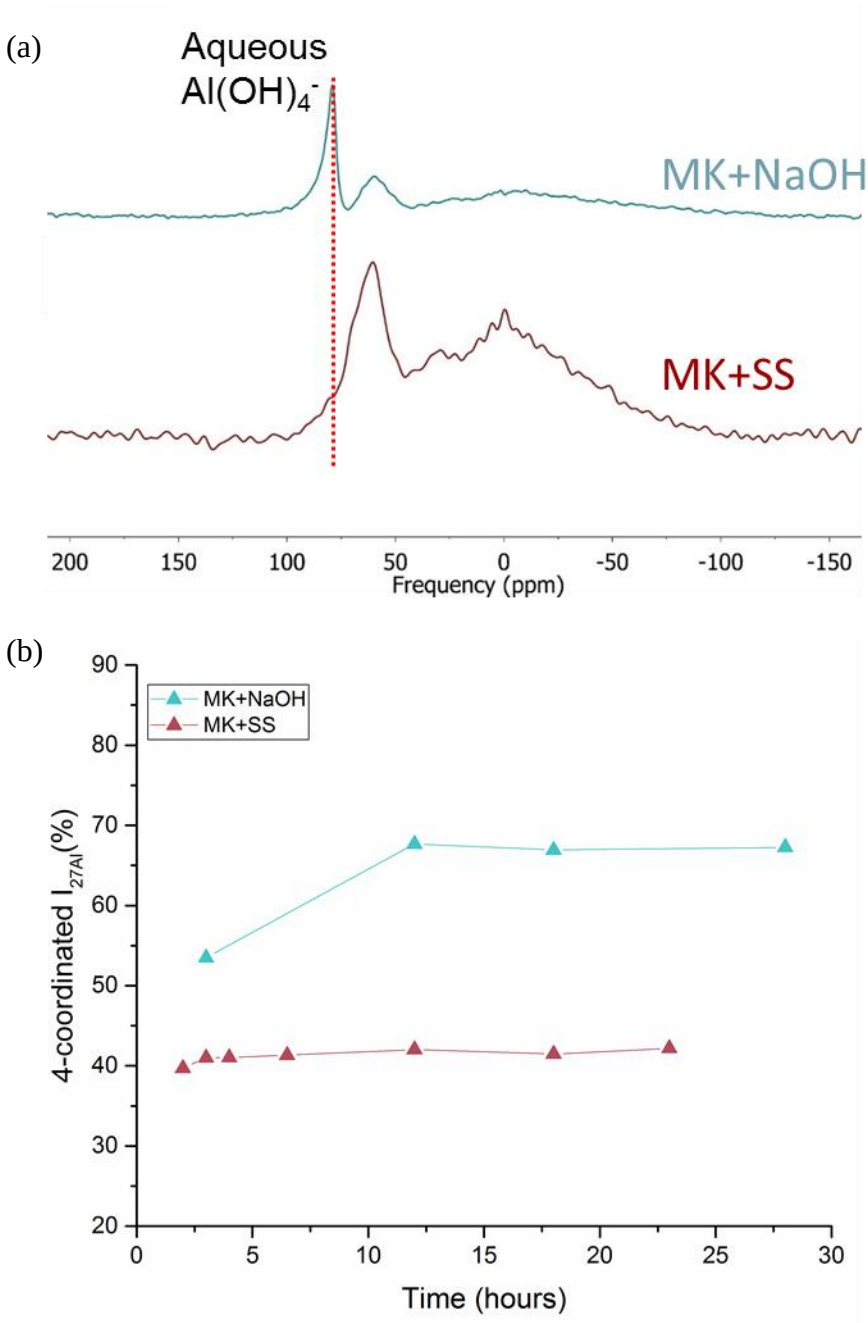

Figure 6.8. Typical MAS ^{27}Al NMR spectra (a) of early age geopolymers "MK+SS", (with composition 1:1:4:11, expressed as Na_2O:Al_2O_3:SiO_2:H_2O). and "MK+NaOH" (with composition 1:1:2:11), and relative percent of 4-Al (b) for both mixes.

6.3.6 Nanostructural evolution model

The nanostructural evolution process indicated by current evidence is depicted in Figure 6.9 (a). This schematic is based on the model of Duxson et al. (2007a) and is consistent with the model of Palomo et al. (2014). It provides greater experimental detail to support previous simulation work (Provis and van Deventer 2007, White et al. 2012) for some reaction stages and explicitly includes set. This schematic is summarized and the mechanism is compared with literature in more detail below.

The first step after mixing metakaolin and sodium silicate solution (up to 10 hours for the current mix) is simultaneous dissolution and condensation. Dissolution is characterized by rapid release of Al, as indicated by the solid-state ^{27}Al NMR results in Figure 6.3. After (or to some extent concurrent with) dissolution, condensation produces a system with silicate ions and aluminosilicate oligomers, mainly in solid phase. This first stage is described as dissolution, equilibration and gelation in the previous model of Duxson et al. (2007a), and as dissolution in the model of Palomo et al. (2014). This current study has advanced the knowledge in this first stage by providing detailed evidence of structural evolution--by systematically monitoring dissolution, it has been shown that condensation occurs rapidly and simultaneously with dissolution.

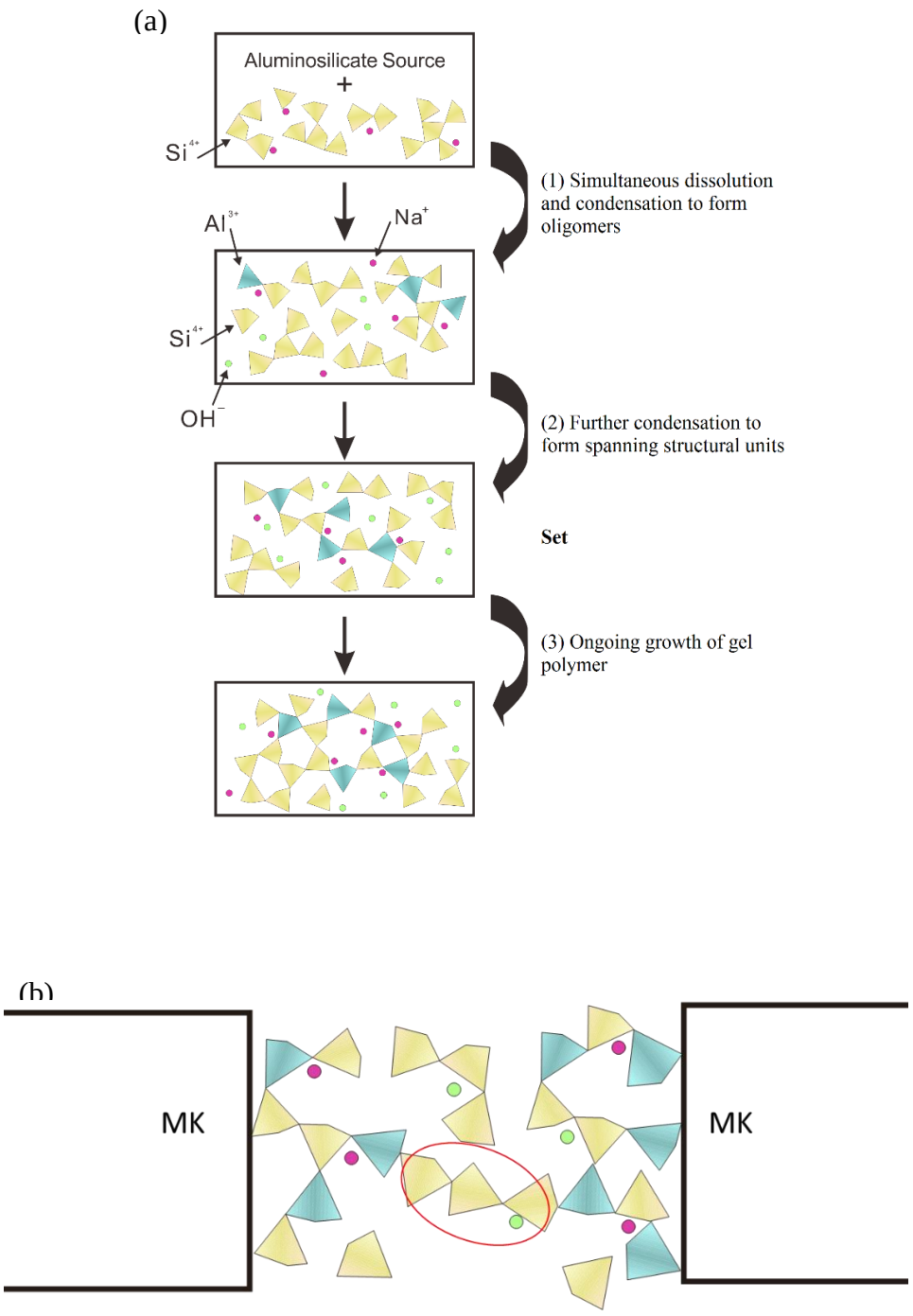

Figure 6.9. Schematic of (a) geopolymerization for the metakaolin geopolymers based on experimental evidence, and (b) nanostructure at set, when silicates in liquid (e.g., as circled) condense with aluminosilicate gel. MK = metakaolin.

The second stage (10-15 hours for the current mix) in Figure 6.9 (a) is further condensation. Dissolution of Al slows, as indicated by the ^{27}Al NMR results, causing formation of additional aluminosilicate oligomers to slow. Condensation takes place mainly between previously-formed aluminosilicate oligomers, as supported by the liquid-state ^{29}Si NMR evidence and studies in the literature, and condensation forms large structural units. This second stage probably corresponds to gelation or reorganization in the previous model of Duxson et al. (2007a) but without clear definition, and to formation of a phase rich in Al in the model by Palomo et al. (2014).

The last stage (15 hours and afterwards) in Figure 6.9 (a) is polymerization. During this stage there is ongoing growth of the network gel structure as small silicate species in the sol attach themselves to the large aluminosilicate structural units to form gel. This process was supported by the observation that low-Q (Q^{2-3}) species observed in liquid-state ^{29}Si NMR spectra decreased in concentration, and that dissolution observed in solid-state ^{27}Al NMR spectra ceased. This last step corresponds to polymerization and hardening in the previous model of Duxson et al. (2007a), or to formation of Si-rich gel in the model by Palomo et al. (2014).

A similar nanostructural-evolution process was described by Scherer and Brinker (1990) for silica gelation. During the initial stage of the process, polymers condense or particles aggregate until clusters form. These clusters then collide and link with each other to form a giant cluster, probably spanning the vessel that contains it. At this time, many clusters are still entangled in a sol. As gelation proceeds, these entangled clusters progressively attach to the spanning cluster, increasing the stiffness. Formation of the aluminosilicate gel described above is thus analogous to the development of silica gel, and at some point (here around 15 hours) the attaching process

contributes to stiffness of the developing aluminosilicate gel similar to the increase in stiffness during silica gelation.

6.3.7 Setting mechanism

At the setting point, it has been confirmed the coexistence of aluminosilicates and low-Q silicates based on NMR tests. Evidence presented here suggests the formation of aluminosilicate gel near the metakaolin particle surface. A schematic diagram was developed, Figure 6.9 (b), to depict the nanostructural evolution. Set occurs when the low-Q silicates in liquid phase condense with aluminosilicate gel to connect metakaolin particles. Such formation of a percolating network is further supported by the rapid increase in penetration strength (Figure 6.1) and is consistent with other evidence in silicate-activated metakaolin based on rheology and SAXS tests (Rouyer and Poulesquen 2015). Study here provides greater detailed nanostructural evidence in terms of speciation connectivity and its reaction at set.

6.4 Conclusions

The objectives of this study were to probe the nanostructural evolution of the aluminosilicates during geopolymerization in the metakaolin based system and to correlate this evolution with setting behavior. By correlating the dissolution with changes in aqueous silicate species during formation of geopolymer gel, it was possible to identify the specific changes associated with set. In the mixture studied, dissolution to release aluminum, characterized by conversion of 5- and 6- to 4-coordinated aluminum, proceeded rapidly at first and then more slowly. With fast release of aluminum, condensation took place to form aluminosilicate oligomers, which appear to occur near metakaolin particle surfaces. These grow by further condensation, as indicated by liquid-state ^{29}Si

results and literature. Then smaller-sized silicate ions attach to these units, as indicated by both ^{27}Al and ^{29}Si NMR spectroscopy, to connect gels and metakaolin particles, a process that is characterized as polymerization and is associated with increased strength and stiffness. Set occurs at the beginning of this attaching process, with the formation of large units that apparently form a percolating structure.

Chapter 7. Effects of calcium on setting of metakaolin geopolymers

7.1 Introduction

In reactive aluminosilicate hydrated in alkaline media, with presence of calcium, the coexistence of geopolymer gel and calcium aluminosilicate hydrate (C-A-S-H) (i.e., Al-substituted calcium silicate hydrate (C-S-H), the latter being the main product when portland cement hydrates) is often observed (Alonso and Palomo 2001b, Alonso and Palomo 2001a, Yip et al. 2005, Yip et al. 2008), as reviewed in more detail in Chapter 2. The geopolymer gel is an aluminosilicate with a three-dimensional network structure (Li et al. 2010). Calcium silicate hydrate (C-S-H), generally the main product from hydrated portland cement, has a calcium oxide layer sandwiched by chains composed of silica tetrahedra (Taylor 1997). When silica tetrahedra are partially substituted by alumina tetrahedra, it becomes C-A-S-H (Andersen et al. 2003), with a similar structure. This hybrid system of both the phases was stated to provide combined advantages of mechanical strength and durability from both phases, and possibly to utilize aluminosilicate wastes with insufficient reactivity when activated alone (Provis and van Deventer 2013).

Early age properties are influenced by calcium. With calcium, setting is much faster for fly-ash and metakaolin geopolymers (Lee and Van Deventer 2002, Suraneni et al. 2014). Early-age strength may increase, depending on curing conditions (Yip and van Deventer 2003, Temuujin et al. 2009). The corresponding mechanisms are not clear, but they could be due to formation of both C-A-S-H and geopolymer gel by interaction of calcium, aluminate and silicate ions (Yip and van Deventer 2003, Yip et al. 2005). In the system Na_2O-CaO-SiO_2-Al_2O_3-H_2O, the co-precipitation of gels has been studied, and the ion exchange of Ca and Na has been found to destabilize the structure of geopolymer gel and favor the formation of C-A-S-H like gels at high pH (> 12) and

high concentration of Ca and Na (Garcia-Lodeiro et al. 2011). This phenomenon however has not been directly correlated to the above changes of geopolymers in early-age (before and around set) properties.

Without calcium, the study of silicate-activated metakaolin in Chapter 6 indicates that setting involves development of gel with an interconnected network structure in the following steps. (1) Al species release rapidly after mixing and immediately condense with silicate species in solution to form larger-sized aluminosilicate oligomers. (2) Oligomers condense to form large structural units, probably spanning across unreacted metakaolin particles. (3) Smaller-sized silicate ions attach to the units to form a gel with a more interconnected network structure. The initial stage of this attaching process is associated with set.

Some hypotheses have been proposed to explain the acceleration of setting with calcium. These hypotheses, together with early-age reaction and structures, are summarized in Figure 7.1. Upon mixing precursor, activating solution and calcium (typically in the form of hydroxide), dissolution begins and aluminate, silicate and calcium ions are released. These ions then condense to form both geopolymer gel and C-A-S-H. One proposed mechanism, with no experimental evidence, is that formation of C-A-S-H consumes H_2O and locally increases pH, thereby enhancing dissolution of the precursor (Temuujin et al. 2009). When slag was added to fly ash geopolymers the enhanced dissolution of fly ash was observed, a phenomenon that was attributed to the pH changes and the need to maintain the Si concentration when it is consumed by forming C-A-S-H (Puligilla and Mondal 2013). Another mechanism is that C-A-S-H formation would itself cause setting, similar to the mechanism for setting in portland cements (Taylor 1997). This mechanism was claimed in the study of fly ash geopolymers (Puligilla and Mondal 2013) and was supported by the presence

of C-A-S-H in their more recent study (Puligilla and Mondal 2015). Additionally, C-A-S-H and calcium hydroxide in the calcium-containing geopolymers could potentially act as nucleation sites for geopolymers (Yip et al. 2008). In some other studies (not direct investigation of the calcium effects), the nucleation effects on the geopolymerization kinetics have been incorporated in a mathematical model by Provis and van Deventer (2007) and have been studied experimentally, for example, by Rees et al. (2008) and Hajimohammadi et al. (2011a).

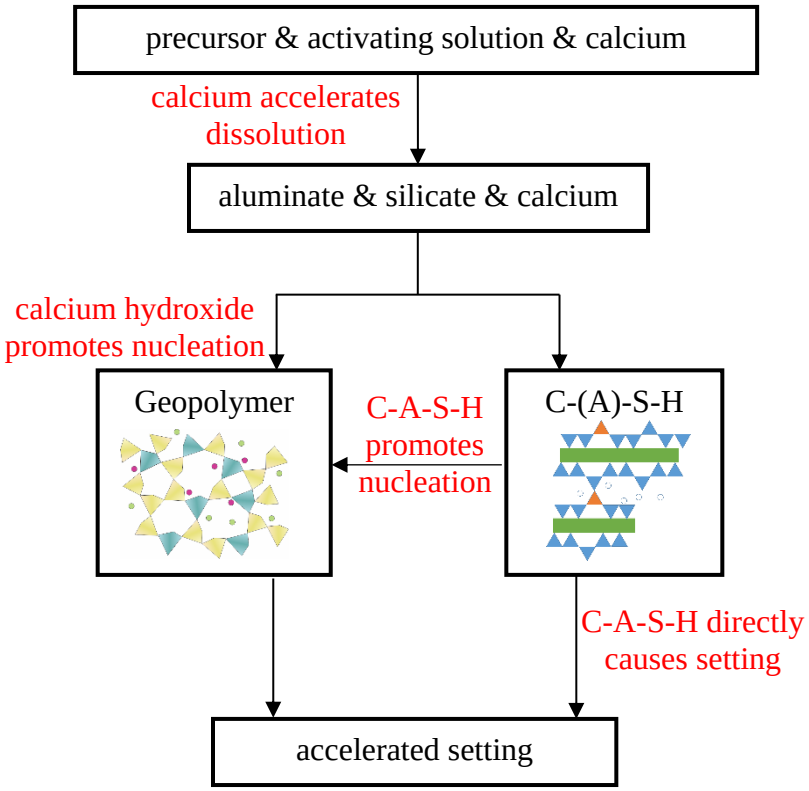

Figure 7.1. Schematic showing changes in early-age reactions and structures with addition of calcium and possible mechanisms of the accelerating effects by calcium (in red, discussed in some detail in the text).

The objective in this chapter was to understand the accelerating effects of calcium. Structures were analyzed, above mechanisms were examined and a more systematic one was proposed based on experiments. Solid-state ^{27}Al NMR tests monitored conversion of 5- and 6-coordinated to 4-coordinated Al (i.e., changes associated with dissolution (Duxson et al. 2005a, Provis and Van Deventer 2009), comparing with a non-calcium mix as studied in depth in Chapter 6. Quantitative solid-state ^{29}Si NMR tests, used in geopolymers (Fernández-Jiménez et al. 2006a, Kim 2012, Bernal et al. 2013), were conducted to quantify phases. Due to long testing time, a two-stage extraction in water and alcohol (i.e., combined extraction developed in Chapter 4) suspended reaction beforehand. For unambiguous structural assignment, extractions in salicylic acid and methanol (SAM) and hydrochloric acid (HCl) dissolved C-A-S-H and geopolymer gel respectively, and residues were also tested.

Study here will benefit research and practice on calcium geopolymers and similar systems. Binders based on a combination of geopolymer gel and C-A-S-H represent an important future trend in construction materials (Provis and van Deventer 2013). Nanostructural experiments provide fundamental understanding of the early-age structural evolution, which has not been well understood. With such understanding, geopolymers with controlled setting can be synthesized using calcium-containing wastes including fly ash and slag.

7.2 Experimental procedure

The molar ratio of the calcium mix (expressed as $CaO:Na_2O:Al_2O_3:SiO_2:H_2O$) was 0.4:1:1:4:12.1, while that of the non-calcium mix was 0:1:1:4:11. Both mixes had the same water/solid ratio. The

raw materials and synthesizing procedure are described in Chapter 3. Setting behaviors were characterized using both penetration resistance and UWR tests.

To estimate the metakaolin dissolution rate and extent, solid-state ^{27}Al NMR tests were conducted every hour. These utilized a Varian Unity Inova spectrometer with magnetic field of 7.04 T. The ^{27}Al pulse width was 0.725 μs, a 30-degree pulse. Recycle delay was 1.0 s and 2048 scans were acquired for each test. These are the same experimental conditions for study in Chapter 6 and are described in more detail in Chapter 3. A few other solid-state ^{27}Al NMR tests were conducted at selected times (1, 6 and 15 hours after mixing) using a Varian NMR spectrometer at 17.6 T (i.e., a higher field). Experimental conditions were similar to the lower field tests, but the MAS spinning rate was 16-kHz and the pulse width was 1.25-μs (15 degree). Relative amounts of 4-, 5- and 6-coordinated Al were thus measured at different times of reaction, and the dissolution extent (i.e., the percent of 5- and 6-coordinated Al converted to 4-coordinated Al) was estimated.

In addition, solid-state ^{29}Si NMR was conducted to quantify phases at the same selected times--1, 6 and 15 hours after mixing. These tests utilized the same Varian Unity Inova spectrometer operating at 7.04 T with a pulse width of 2.5 μs (a 90-degree pulse). Recycle delay was 30 s and number of scans was 2048. Each quantitative ^{29}Si test took around 17 hours. Prior to tests, the combined extraction (COM) was conducted to suspend reaction. For the calcium mix, the COM residue was extracted with SAM, removing any C-(A)-S-H and leaving unreacted metakaolin and geopolymer gel. The SAM residue was further extracted with HCl solution, removing any geopolymer gel and leaving unreacted metakaolin. For the non-calcium mix, HCl extraction was conducted directly on COM residue. The extractions are described in detail in Chapter 3. Spectrum analysis using WSolids and MestReNova was described also in Chapter 3. The peak width and

position for the geopolymer gel phase were based on the deconvolution of the 3-month geopolymer spectrum presented in Chapter 5.

7.3 Results

7.3.1 Setting behavior

Setting was considerably shortened with calcium, as shown in penetration resistance and UWR curves for the calcium and non-calcium mixes Figure 7.2. For the non-calcium mix, the set time was 15-16 hours as shown here and also in Chapter 6. For the calcium mix, it was 50-70 minutes based on the penetration resistance (i.e., time corresponding to 2 MPa, which was assigned to initial set for cement paste (Suraneni et al. 2014)), and 80-100 minutes (corresponding to the same reflection coefficient as the non-calcium mix) based on UWR. UWR was found to be more sensitive to gelation, and penetration resistance to strength development (Suraneni et al. 2014). Here the two tests provided consistent setting times for the non-calcium mix but not for the calcium mix, suggesting the calcium mix involves greater strength development than the non-calcium mix during setting. Both penetration resistance results showed setting around the initiation of the rapid strength development, and therefore, we believe, are more reliable for comparison between the two mixes (set times of roughly 1 versus 15 hours) over the UWR results. The initial drop seen in the UWR curves is attributed to the formation of reaction product for the non-calcium mix as discussed in Chapter 6, and probably also for the calcium mix.

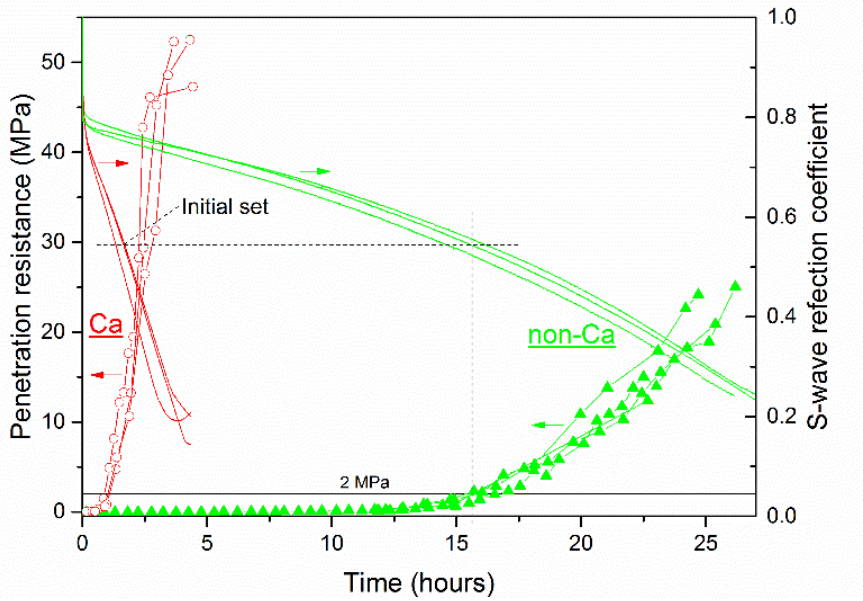

Figure 7.2. Penetration resistance and UWR curves of geopolymers with and without calcium (Ca and non-Ca, respectively). Results for the non-Ca mix are adopted from study in Chapter 6.

7.3.2 Dissolution of metakaolin

To understand why calcium accelerates set in this way, metakaolin dissolution was examined using solid-state ^{27}Al NMR. The results are not quantitative with the lower field probe (7.04 T), but are valid for comparison. In Figure 7.3, each site of 4-, 5- and 6-coordinated Al was estimated and plotted with time. For both specimens, 4-coordinated Al increased while 5- and 6-coordinated Al decreased during dissolution, consistent with other studies (Duxson et al. 2005a, Provis and Van Deventer 2009). For the calcium mix, both dissolution rate and extent were promoted, indicated by the higher slope of the initial part of the 4-coordinated Al curve and the higher intensity at which the 4-coordinated Al curve leveled off, respectively. The initial amount of 4-coordinated Al (at 0.5 hour) was higher in the calcium mix, again indicating faster dissolution with calcium.

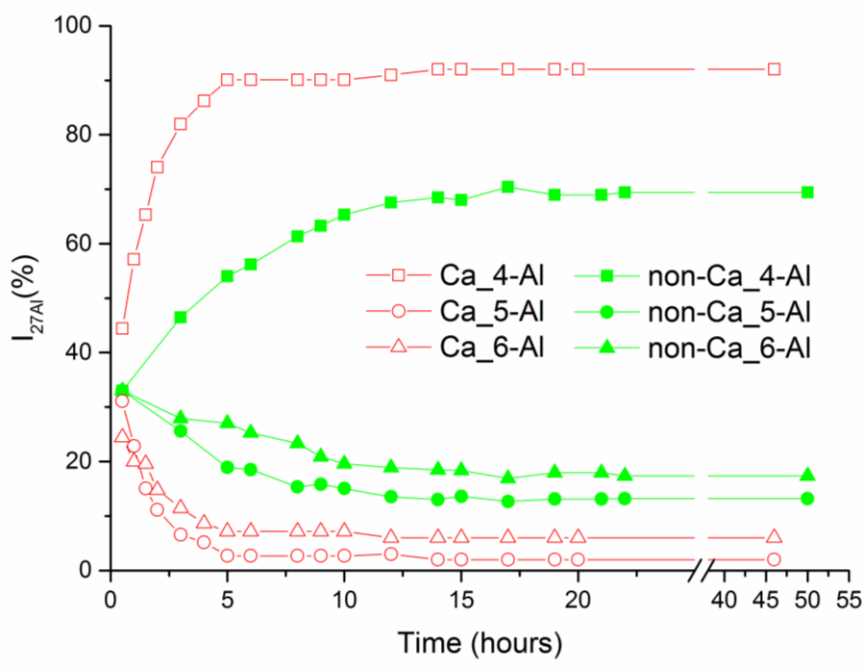

Figure 7.3. Percentage changes of 4-, 5- and 6-coordinated Al with time during dissolution as geopolymerization proceeded for calcium mix (open symbols) and non-calcium mix (filled symbols). Results for the non-calcium mix are adopted from study in Chapter 6.

7.3.3 Formation of C-A-S-H and geopolymer gel

Further tests using solid-state ^{29}Si NMR were conducted to examine how product formation is altered by calcium. These tests were performed at the setting times for both mixes, 1 and 15 hours, and at one intermediate time, 6 hours. Combined extraction leaves unreacted metakaolin, geopolymer gel and, in mixtures containing calcium, C-A-S-H. These phases overlap in ^{29}Si NMR spectra, all in the region -80 to -120 ppm (Duxson et al. 2005c, Puertas et al. 2011, Hunnicutt 2013). SAM and HCl extractions therefore were used to achieve unambiguous peak assignments.

Deconvolution of ^{29}Si NMR spectra was carried out. Figure 7.4 shows the spectra for the calcium mix at 15 hours after mixing, to demonstrate the deconvolution process. Spectrum of the HCl residue (top), expected as unreacted metakaolin, was deconvoluted to two peaks at -92.7 and -107 ppm. They were tentatively assigned as Q^4(0Al) and Q^4(2Al), as metakaolin has been shown by others to contain framework silica (Q^4) and aluminosilica (Q^4(1Al) or Q^4(2Al)) (Rocha and Klinowski 1990). Although tentative, these assignments did not affect our subsequent deconvolution. To deconvolute the SAM spectrum, the two peaks assigned to unreacted-metakaolin were assumed to have the same width, position and relative intensity as observed in the HCl residue. Parameters of other peaks in the SAM residue were adopted from analysis of a mature geopolymer specimen. Similarly, for COM residue (bottom), peak parameters were used from the SAM residue. All additional peaks in the combined extraction residue were assigned to C-A-S-H using parameters obtained from analysis of synthesized C-A-S-H (Hunnicutt 2013). The peak position, width, height and intensity are summarized in Table 7.1.

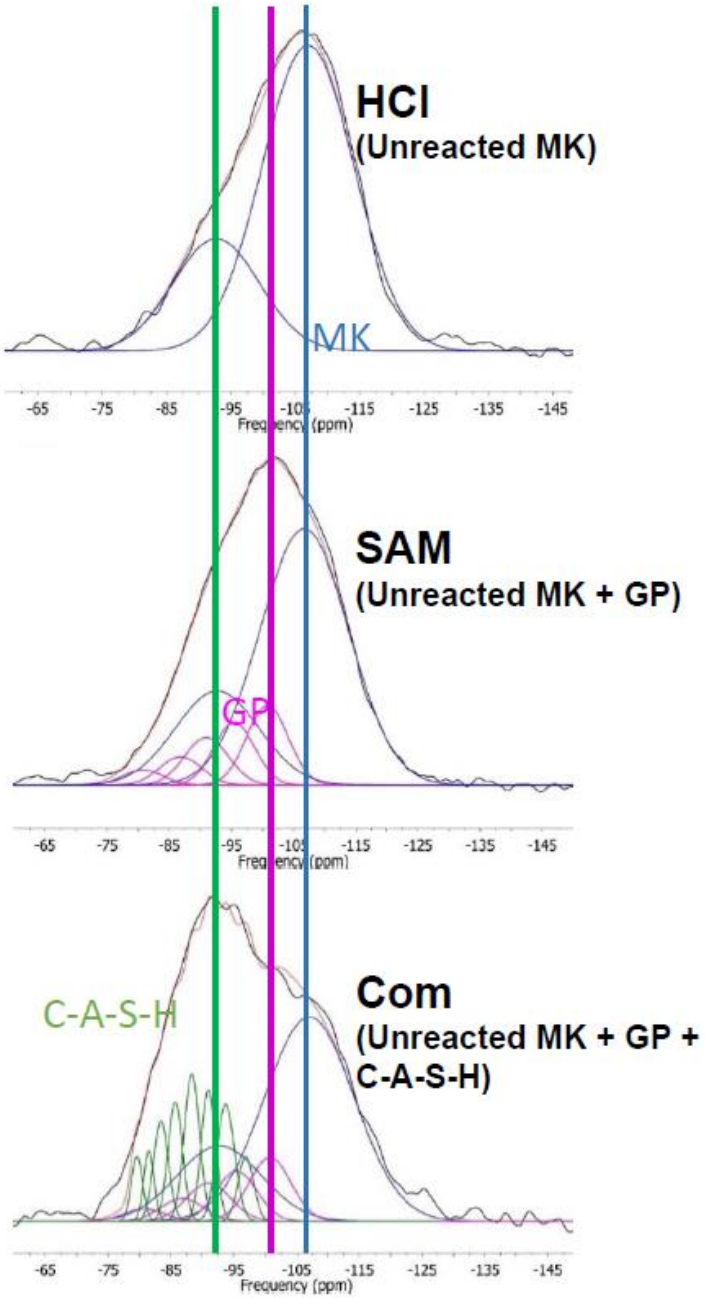

Figure 7.4. Deconvolution of ^{29}Si solid-state spectra of residues from combined (bottom), SAM (middle) and HCl (top) extractions for mix with calcium at 15 hours, showing peaks assigned to metakaolin (MK), C-A-S-H and geopolymer gel (GP).

Table 7.1. Summary of peak position, width, height and intensity for deconvolution in Figure 7.4.

Phases	ppm	Height	Width(Hz)	Area	phases
MK	-92.7	241.0	15.8	39635.2	MK
	-107.1	679.4	16.8	119083.1	MK
GP	-80.8	40.6	7.5	3165.1	Q^4(4Al)
	-86.0	75.6	7.7	6025.5	Q^4(3Al)
	-90.4	150.6	7.0	10978.8	Q^4(2Al)
	-95.5	171.5	7.6	13579.1	Q^4(1Al)
	-100.8	209.0	9.6	20849.4	Q^4(0Al)
C-(A)-S-H	-79.6	215.8	2.1	4741.6	Q^1(0Al)
	-81.5	234.5	1.9	4743.5	Q^2p(1Al)
	-83.4	334.8	2.8	9682.5	Q^2b(0Al)
	-85.7	395.9	2.7	11165.0	Q^2p(0Al)
	-88.3	488.7	2.9	14701.1	Q^3(1Al)
	-91.0	438.3	2.7	12305.4	Q^3(0Al)
	-93.7	388.4	3.3	13479.6	Q^4(2Al)
	-96.9	215.8	2.9	6490.7	Q^4(1Al)

The amount of each phase was estimated from the intensity of each peak. Results were plotted in Figure 7.5. The amount of geopolymer gel at set in molar percent of Si was 7.1% in the non-calcium at set (15 hours) and 10.3% in the calcium mix (1 hour). This 10.3% should not be

contributed by C-A-S-H, because it can be totally dissolved in SAM extraction based on some additional results shown in Appendix F. Comparison here suggests that geopolymer gel by itself could have caused setting in the calcium mix. The amount of geopolymer gel at 1 and 6 hours was almost zero in the non-calcium mix and much higher in the calcium mix, indicating that calcium promoted geopolymer gel formation. Additionally, the amount of unreacted metakaolin decreased more rapidly with the addition of calcium, consistent with the ^{27}Al NMR results and again supporting that calcium promoted its dissolution.

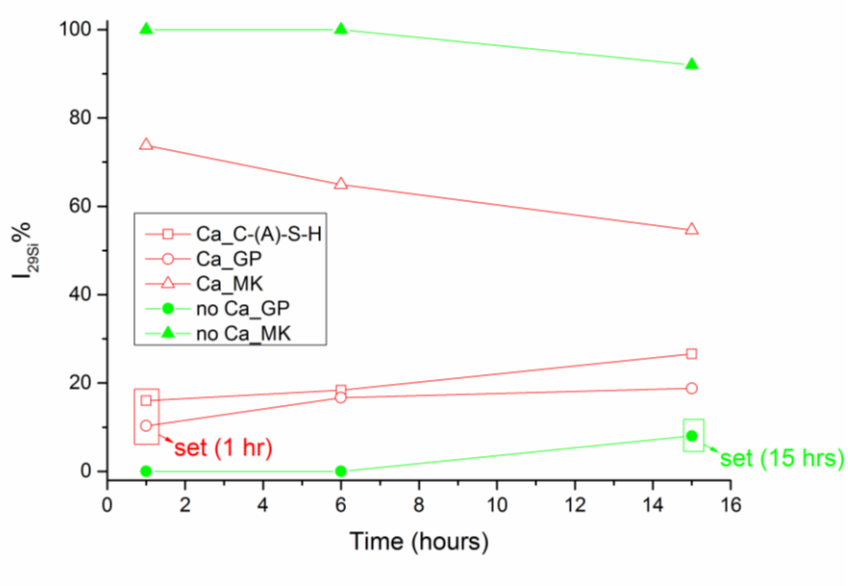

Figure 7.5. Percentage of intensity (molar percentage of Si) associated with each phase in ^{29}Si spectra for specimen with and without calcium as geopolymerization proceeds.

There was one uncertainty regarding the peaks associated with the C-A-S-H phase. Peaks around -95 ppm were removed during SAM extraction and were therefore assigned to the C-A-S-H phase in the deconvolution shown in Figure 7.4. Peaks in this region are usually assigned to Q^3 or to Q^4 with Al substitution (Engelhardt and Michel 1987) and are not seen in conventional C-A-S-H,

which has chain structures of Q^1 and Q^2. The Al in the C-A-S-H can promote a more connected structure with Q^3 or even Q^4 sites (Hunnicutt 2013), especially when carbonated (Sevelsted and Skibsted 2015), but the intensity of these peaks much exceeds our expectation. This uncertainty is discussed in Appendix G and is shown to not affect the later conclusions in the current study. Alternatively, these structures could be associated with a calcium-modified geopolymer gel (i.e., (Ca, Na)-A-S-H), which has been found to coexist with C-A-S-H but whose solubility in SAM is not known. If these peaks with high Q numbers were considered as geopolymer gel, there would be even more geopolymer gel at the investigated age. Regardless of this uncertainty, it is clear from our results geopolymer gel was formed more rapidly with the addition of calcium.

7.3.4 Si/Al of geopolymer gel

The Si/Al in the geopolymer gel was estimated from the intensity of each peak in the ^{29}Si NMR spectra assigned to the gel. These peaks were all assigned to network Si sites with different chemical environments, Q^4(0-4Al). Based on liquid-state ^{29}Si NMR data presented in Chapter 6, Al preferentially condensed with Q^3 and Q^4 silicates to produce mainly Q^4 aluminosilicate gel during early-age reaction. Any remaining low-Q species in liquid phase are removed by the combined extraction prior to the NMR tests. Intensities of the peaks of the gel in the ^{29}Si NMR spectra were then used to estimate the Si/Al of the geopolymer framework based on Equation 2.1. Taking Figure 7.4 as an example, peaks at -80.8, -86.0, -90.4, -95.5, -100.8 ppm were assigned as Q^4(4Al), Q^4(3Al), Q^4(2Al), Q^4(1Al) and Q^4(0Al), respectively. Substituting with intensity values in this equation, Si/Al in the geopolymer gel at this age was estimated to be 3.2. Other ratios for both mixes at selected times are shown in Figure 7.6 (at 1 and 6 hours for the non-calcium mix, the amount of geopolymer gel was not sufficient for accurate estimation).

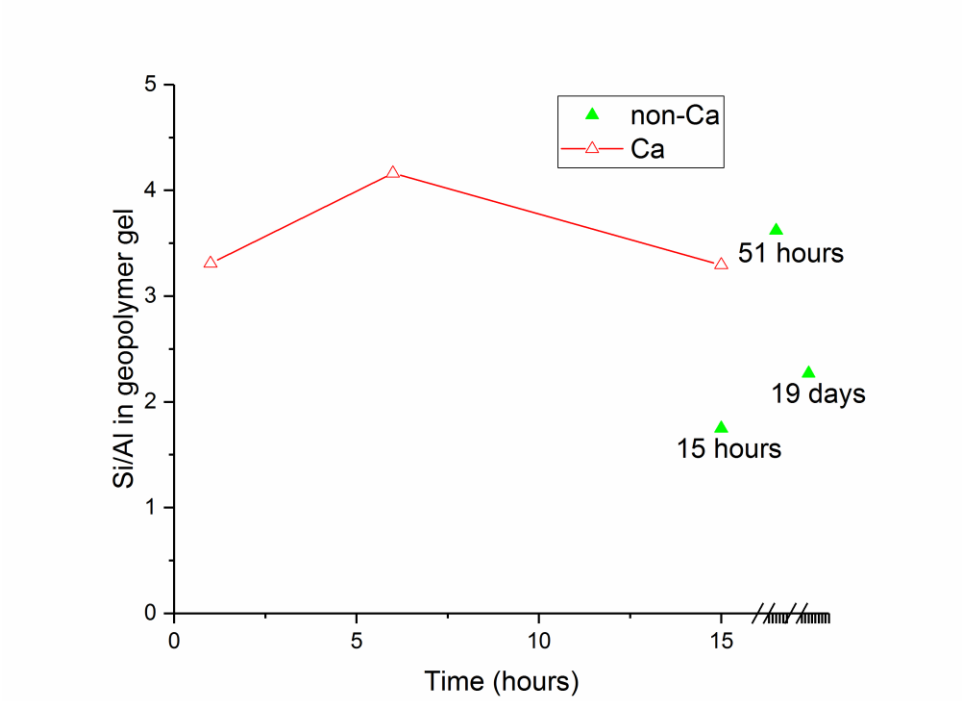

Figure 7.6. Si/Al ratio of geopolymer gel in the calcium and non-calcium mixes at different times.

In the calcium mix, the Si/Al ratio seemed to increase and then decrease over time. Apart from experiment errors, the increase could be associated with the fact that the dissolved Al was able to capture more Si as reaction proceeded, resulting in higher Si/Al at 6 hours than at the beginning of the reaction. Then as reaction proceeded further, the Si/Al decreased to approach the bulk ratio of 2. In the non-calcium mix, Si/Al of the geopolymer gel at 15 hours is somewhat lower. With limited Al, condensation is more likely to occur slowly between silicate species, which if not yet condensed to form a gel could have been dissolved in the combined extraction probably in a similar way as waterglass, leaving residue with low Si/Al ratio. This proposed mechanism explains the lower Si/Al ratio in the geopolymer gel in the non-calcium mix than in the calcium mix. This Al-rich gel in the non-calcium mix became more Si-rich at 51 hours, which is consistent with the

conclusion from the liquid-state NMR results that at 15 hours Si species in solution began to attach to the previously formed aluminosilicates shown in Chapter 6. The Si/Al ratio of this gel then approached the bulk ratio of 2.0 at 19 days.

7.4 Discussion

7.4.1 Setting and gel formation

Setting appears to be associated with the amount of geopolymer gel. A similar amount of geopolymer gel (i.e., 7.1% and 10.3% molar percent of Si in non-calcium and calcium mixes, respectively) was observed at set. In the calcium mix, geopolymer gel by itself seems to be sufficient to cause set. At the same time, the Si/Al of the geopolymer gel in the calcium mix was two times of the non-calcium mix at set, so gel composition does not appear to be a controlling factor.

7.4.2 Si/Al estimation for geopolymerization

In both the calcium and non-calcium mixes studied here, Si was highly concentrated in the activating solutions, and thus the amount of Al available for geopolymerization was a critical kinetics factor. The Si/Al in the geopolymer gel does not seem to correlate with the reaction kinetics. For direct comparison, the Si/Al ratios for geopolymerization in both the mixes were compared at different times to investigate the faster geopolymerization by calcium. These ratios were estimated based on all Si and Al from NMR tests minus that seen in unreacted metakaolin and in any C-A-S-H. Essentially, these ratios are based on Si and Al from solution and geopolymer gel, which are reactive at this intermediate stage. The results are summarized in Table 7.2, detailed

calculation procedures are presented in the following paragraphs and sample calculations for the 6-hour specimens are shown in Appendix H.

The Al available for geopolymer formation was estimated using quantitative solid-state ^{27}Al NMR (measured using the higher-field probe) for the calcium mix. Because this is a rapid test, no substantial change in structure is expected. To estimate the total dissolved Al, the intensity percent of each Al site in non-extracted specimens was estimated and compared with results for the raw metakaolin to estimate the dissolution extent (i.e., the percent of Al that converted from 5- and 6- to 4-Al with respect to the total Al). To estimate the Al in C-A-S-H, the spectrum of each SAM residue was subtracted from the spectrum of the COM residue, and the percent 4-Al in the obtained spectrum with respect to the total Al in the COM residue was estimated. To estimate the Al for geopolymer formation, the Al in C-A-S-H was subtracted from the total dissolved Al. The results are summarized in Table 7.2.

The Al for geopolymer formation was estimated for the non-calcium mix. In quantitative ^{27}Al NMR tests (with the higher-field probe) for the non-calcium mix, intensity changes were seen at error level, indicating little or no Al dissolution and thus high Si/Al available for geopolymerization before set. Therefore, the lower-field results were used for the estimation, during which the dissolution extents (defined above) were estimated for both the calcium and non-calcium mixes and a ratio of the extents was obtained at each selected time. Based on each ratio and the corresponding quantitative dissolution percentage for the calcium mix (from the higher field tests), dissolution extent (as defined before) in the non-calcium mix was calculated and are shown in Table 7.2. In Appendix G, uncertainty in the Si/Al estimation here is discussed and was found to not affect the conclusion regarding the Si/Al ratios for geopolymerization between both

the mixes. For comparison, the Al for geopolymer formation was also estimated by the high-field tests as shown in Appendix H.

Table 7.2. Si and Al for geopolymer formation at the selected times for both the calcium and non-calcium mixes.

Time (hours)	Si for GP formation		Total dissolved Al		Al for GP formation		Si/Al for GP formation	
	Ca	Non-Ca	Ca	Non-Ca	Ca	Non-Ca	Ca	Non-Ca
1	0.78	1.00	0.14	0.03	0.13	0.03	6.2	37.1
6	0.72	1.00	0.29	0.13	0.25	0.13	2.9	7.9
15	0.51	1.00	0.30	0.18	0.22	0.18	2.3	5.4

The relative amounts of Si in each of the unreacted metakaolin, geopolymer gel and/or C-A-S-H are shown in Figure 7.5. In each sample (with and without calcium), 1 mole of Si was from the sodium silicate solution, and another 1 mole of Si was from metakaolin. At the early ages, dissolution of Si from metakaolin is expected to be minimum, i.e., most of the 1 mole Si remains in the unreacted metakaolin. This assumption is regarded as reasonable, as Si is believed to be released more slowly than Al on dissolution of metakaolin (Weng and Sagoe-Crentsil 2007, Provis and Van Deventer 2009), probably because, as shown by thermodynamic calculation, Al-O-Si bonds are more readily broken than Si-O-Si bonds (Hamilton et al. 2001). For the non-calcium mix, Si to form geopolymer gel was 1 mole. For the calcium mix, this amount was 1 mole subtracted by that in C-A-S-H. In the calcium mix at 15 hours, for example, the absolute amount

of Si in C-A-S-H was estimated to be 0.49 mole. Therefore, the Si for geopolymer gel formation is 0.51 mole. This and other such estimates are summarized in Table 7.2.

The Si/Al ratio for geopolymer formation in the non-calcium mix is higher than in the calcium mix at all ages in Table 7.2, with the largest difference at 1 hour when the calcium mix sets. When assuming congruent dissolution (i.e., the same moles of Si releases as Al, contrary to this current assumption), Si/Al for geopolymer formation at 1 hour, for example, were estimated to be 7.3 and 34.3 for the calcium and non-calcium mixes, respectively. Sample calculations when assuming congruent dissolution are shown in Appendix H. This substantial difference is consistent with the current estimation (as shown in Table 7.2). Discussion in this subsection thus indicates the enhanced dissolution of metakaolin by calcium produced a lower Si/Al for geopolymer gel formation.

7.4.3 Si/Al and geopolymerization kinetics

This subsection aims to examine how a lower Si/Al for geopolymer gel formation would affect its kinetics. Literature review indicates a lower Si/Al results in a faster rate. Additional experiments are shown and indicate this effect can be substantial.

Based on literature, lower Si/Al for geopolymer gel formation promotes its rate. Higher amounts of Al were found to shorten the setting time (Silva et al. 2007) and to accelerate reaction kinetics (Fernández-Jiménez et al. 2006b). When more Al is available for reaction, condensation between aluminate and silicate species is more likely; but when more Si is available for reaction, condensation between silicate species is more likely. Based on partial charge modeling, the condensation reaction has been shown to occur more rapidly in the presence of aluminate species

than in the absence, because the positive partial charge of the Al atom is higher than that of the Si atom under the same pH condition (Weng et al. 2005).

Above literature review also explains the different reaction sequence for geopolymer formation between the two mixes. In the non-calcium mix, with higher Si/Al thus involving more Si-O-Si bond formation, geopolymer formation process is slower. A few steps were identified in Chapter 6: aluminosilicate oligomers form; oligomers become larger structural units; and silicates in sol attach to these units. In the calcium mix, with lower Si/Al, more geopolymer gel (stable during combined extraction) formed in the first hour, even more than that at 15 hours in the non-calcium mix (Figure 7.5). Low Si/Al ratio in the calcium mix enhances reaction rate such that the slow step-by-step condensation process is not observed, as also supported by liquid-state ^{29}Si NMR results shown in Appendix I. This difference in reaction sequence might be responsible for the greater strength development at set by calcium shown earlier.

Some additional experiments were conducted aiming to find out if this difference in Si/Al is sufficient to cause such substantially different rate of geopolymer formation. The sol-gel procedure was followed to synthesize geopolymer gel (i.e. N-A-S-H gel) (Garcia-Lodeiro et al. 2010). Three solutions were prepared: 0.2-*M* sodium silicate, 0.1-*M* aluminum nitrate and 10-*M* NaOH. They were mixed to achieve Si/Al at 2, 5, 10 and 30 by keeping Si constant but varying volume of the aluminum nitrate solution, and to keep the pH at around 12.5 by regulating with the NaOH solution. With Si/Al at 2, precipitation was observed in around 2 minutes after mixing, and the precipitate was found to be aluminosilicates by FTIR tests as shown in Appendix J. However, mixtures with Si/Al at 5 or above remained clear for more than 12 hours. Changing Si/Al from 2 to 5 resulted in

significantly delayed precipitation time. There seemed to be a threshold of Si/Al below which precipitation occurs rapidly.

Suggested from these experiments, lower Si/Al for geopolymer formation with calcium is expected to cause such different setting times (1 versus 15 hours). At set for the calcium and non-calcium mixes, Si/Al for geopolymer gel formation was 6.2 and 5.4, respectively. The threshold for precipitation seems to occur at Si/Al around 5 or 6. In the non-calcium mix, the ratio was 37.1 at 1 hour, well above the threshold; more geopolymer gel formed and set occurred only when Si/Al reached this threshold at 15 hours.

7.4.4 Enhanced dissolution by calcium

From above discussion, the enhanced dissolution lowers Si/Al ratio for geopolymer gel formation, and then increases the rate, causing faster setting. It would be interesting to investigate in more detail how the dissolution is enhanced by calcium.

Calcium interacts with the mix by reacting with Si in solution to form C-A-S-H. Varying Si concentration might provide insight into the acceleration effects by calcium. Here mixes without any external Si (i.e., Si only from the metakaolin) were tested using the higher field NMR probe. These mixes (expressed as $CaO:Na_2O:Al_2O_3:SiO_2:H_2O$) were 0:1:1:2:11 and 0.4:1:1:2:12.1, which are named as “non-calcium-NaOH” and “calcium-NaOH”, respectively. A typical spectrum of the NaOH mix without calcium is found in Appendix E and discussed in Chapter 6. To estimate the dissolution extent of both the NaOH mixes, percent for the sum of aqueous and solid 4-coordinated Al peaks is plotted in Figure 7.7. For comparison, the specimens with external Si (i.e., same as

those in Figure 7.3) were tested and the 4-coordinated Al was measured, also using the higher field probe.

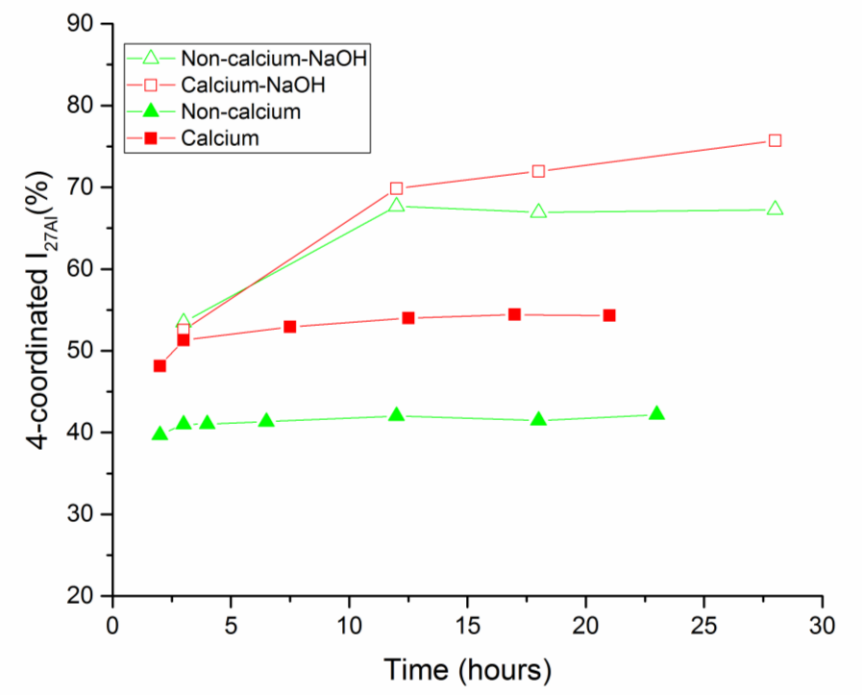

Figure 7.7. Percent of 4-coordinated Al sites in NaOH and external-Si mixes at different times by the quantitative ^{27}Al spectroscopy.

Non-calcium NaOH mix (open triangle) shows much higher 4-coordinated Al percent than the non-calcium mix with external Si (filled triangle), as shown in Figure 7.7. This phenomenon, as discussed in Chapter 6, is attributed to the formation of a protective layer of solid aluminosilicate product on the metakaolin surface (Feng et al. 2004, Provis et al. 2005, White et al. 2011b, White et al. 2012, Favier et al. 2013), which is thought to be more likely in Si-rich mixes than hydroxide-activated ones.

Further examination of Figure 7.7 indicates calcium did not increase the dissolution extent in the two NaOH mixes as substantially as the external-Si mixes (i.e., the two lines with empty symbols are closer to each other, while the two lines with filled symbols show much greater difference). In the two NaOH mixes (open symbols), percent of the 4-coordinated Al is almost the same at 3 and 12 hours and is up to 8% higher with calcium later; in the external-Si mixes (filled symbols), the percent remains different (around 10%) at all tested times and is up to 13% higher with calcium.

This difference could also be explained by the proposed protective-layer mechanism. In the external-Si mixes, calcium reduces Si in solution so a protective layer is less likely to form and thus dissolution is likely to be enhanced. In the NaOH mixes, Si concentration is too low at early ages, and so is its change by calcium. At later ages, more Si is in solution with dissolution and calcium would lower its concentration, and this change explains the increasingly enhanced dissolution by calcium from 12 to 28 hours.

White et al. (2011b) claimed the higher dissolution rate in their hydroxide-activated mix compared to their external-Si mix was due to the higher pH. In the current study, initial pH in the NaOH mixes would also be higher than the external-Si mixes. However, difference in pH does not explain difference in dissolution extent: from 12 to around 25 hours, non-calcium NaOH mix (open triangle) shows consistently 25% higher in 4-coordinated Al than the non-calcium mix (filled triangle) in Figure 7.7. Also pH does not explain the progressively increasing difference between the non-calcium NaOH (open triangle) and calcium NaOH (open square) mixes starting from 12 hours.

7.4.5 Further insight on setting

Analysis suggests C-(A)-S-H is not directly involved in setting. In general, gel that forms on the particle surface more effectively leads to setting than gel that randomly forms in the aqueous phase, because gel on the surface links the particles even when a substantial amount of aqueous phase is present, whereas randomly distributed gel must fill most of the initial non-solid space to establish percolation. In the calcium mix, C-(A)-S-H is expected to form from the aqueous phase upon contact of calcium and silicate ions (both abundant in liquid in the current mix) at such high pH. In cement setting, the hydration extent from calorimetry tests was below 1% at set for mixes with various water/solid ratios (Jiang et al. 1995), suggesting very little gel on the surfaces of cement particles could cause setting. In this study, the C-A-S-H observed at set (16% as molar percent of Si, an observation not straightforward for direct comparison) suggests it is not directly contributing to setting. This reason and the observation above that the amount of geopolymer gel at set is comparable both with and without calcium suggest that geopolymer gel is sufficient to cause setting. Nonetheless, the C-A-S-H would undoubtedly increase strength once a percolation network is established (right after set point), as seen from the higher slope of the penetration curves for the calcium mix compared to the non-calcium mix in Figure 7.2.

7.5 Conclusions

Calcium was confirmed to substantially accelerate setting of metakaolin geopolymers. To the best of our knowledge, this study is the first attempt to systematically investigate the reason behind this effect. NMR tests were carried out to examine the dissolution and product formation for both calcium and non-calcium mixes (with external Si).

The promotion of geopolymer gel formation by calcium appears to be associated with the faster setting. Comparable amount of geopolymer gel was observed at set for both the calcium and non-calcium mixes based on the NMR tests, suggesting the geopolymer gel is sufficient to cause set. Although C-A-S-H was observed in the calcium mix, no evidence indicated that it is directly involved in setting.

Faster geopolymer gel formation was caused by faster dissolution. Faster dissolution yielded more Al and lowered the Si/Al for geopolymer gel formation as confirmed by quantitative analysis using both ^{29}Si and ^{27}Al NMR spectroscopy. This lower Si/Al ratio is considered to be sufficient to cause the significantly different setting behavior, based on validation experiments and literature.

The protective-layer mechanism explains the promoted dissolution by calcium. Calcium consumes Si in the solution, and a protective layer is less likely to form on the metakaolin particles, thus less inhibiting the dissolution. This proposal is consistent with the indirect experimental and simulation results from literature and is supported by additional evidence from NaOH activated metakaolin specimens.

Chapter 8. Reaction extent and strength of geopolymers after set

8.1 Introduction

In silicate-activated metakaolin containing no Ca, for example, all Al is from metakaolin, and a low reaction extent would result in a high Si/Al in solution available for geopolymer formation and thus the high ratio in the geopolymer gel. Both reaction extent and the Si/Al of geopolymer gel influence the mechanical properties and these effects have not been separated in literature. It is interesting to establish relationship between reaction extent and mechanical properties for these non-Ca mixes.

In Chapter 7, Ca was seen to enhance the dissolution kinetics of metakaolin, and the enhanced dissolution was seen to play a critical role to control the reaction kinetics for geopolymer formation and to accelerate setting. It would be interesting to examine how Ca influences the reaction extent at later ages (i.e., after set), and how it influences the mechanical properties.

If not fully reacted, the specimen can be essentially regarded as a matrix of geopolymer gel embedded with some unreacted metakaolin particles. Reaction extent of the geopolymers, in this study defined as the percent (either molar or weight) of unreacted metakaolin in the specimen, determines relative amount and composition of each phase. Quantification of the reaction extent however does not seem to be straightforward. Techniques including acid extraction, calorimetry, FTIR, NMR, AC-impedance spectroscopy, EDS- and XRD-related techniques and computer modelling have been used to examine the dissolution of the precursor and the formation of intermediate and final amorphous geopolymer products, as reviewed in a study by Williams et al. (2011). The solid-state ^{29}Si NMR spectroscopy seems to be a promising technique for

quantification. It has been shown to successfully quantify the composition of the framework in fully (or close to fully) reacted metakaolin geopolymers (Duxson et al. 2005c) rather than SEM-EDS in which the bulk composition is obtained (Rowles and O'Connor 2009). It should be noted that quantitative deconvolution of ^{29}Si NMR spectroscopy is not as straightforward when the specimen is not fully reacted, as discussed in Chapter 5.

The correlation between reaction extent and compressive strength has not been established experimentally. The unreacted phases have been proposed to serve as defect sites, while Si/Al ratio in geopolymer gel has been found to greatly influence Young's modulus and compressive strength (Duxson et al. 2005b). However, their contribution to strength has not been separated. In the study by Williams et al. (2011), the relative amount of unreacted metakaolin was inversely correlated with the mechanical strength, however the authors attributed this difference in strength mainly to the changes in the Si/Al ratio of the geopolymer gel. In their low-strength mixes, substantial amount of Si was added as sodium silicate solution, and a very high Si/Al ratio in solution for geopolymer formation was expected when little metakaolin participated in reaction (i.e., low reaction extent). Therefore, it is not straightforward to distinguish the effects of reaction extent and the Si/Al ratio of the gel on the strength.

The geopolymer reaction extent can be controlled by the ratio of charge-balancing cations and Al ions, for example by the Na/Al ratio in the case of Na-based geopolymers. During the structural formation process, the alkaline cations participate in the reaction to balance the charges induced by the incorporation of Al (Duxson et al. 2005a). Insufficient amount of Na would result in incomplete incorporation of Al into the geopolymer framework. By varying Na/Al ratio, the

reaction extent could be controlled and be correlated with the strength independent of the Si/Al ratios.

With the addition of Ca, the structures of the specimens are altered. In these mixes, C-(A)-S-H phase is present in addition to the geopolymer phase and the unreacted metakaolin (Yip and van Deventer 2003). Unlike the two-dimensional chain-like C-S-H or somewhat more polymerized C-A-S-H, the structure of geopolymers is a three-dimensional network (Li et al. 2010).

The structure of geopolymers with Ca has not been well correlated with the mechanical properties. In one study, the higher strength with addition of Ca was tentatively attributed to filling of voids and gaps within geopolymer binder by the C-A-S-H gel (Yip et al. 2005). In another study, insufficient development of three-dimensional geopolymeric network was proposed to explain the decreased strength in Ca-geopolymers when cured at elevated temperature (Temuujin et al. 2009). In the same study, strength has been found to increase with addition of Ca at room temperature, attributed to the precipitation of C-A-S-H and enhanced dissolution of the precursor (Temuujin et al. 2009), but no experimental validation was presented. In the presence of limestone, the dissolution of Si and Al from metakaolin by alkaline leaching was reduced at early age (during first few hours) but enhanced later (after 20 hours), behavior that was believed to be controlled by equilibrium solubility of the Si, Al and Ca species (Cwirzen et al. 2014). In the presence of calcium hydroxide, dissolution of the metakaolin precursor in terms of rate and extent has been found to be enhanced around setting, supported by the solid-state ^{27}Al NMR results presented in Chapter 7. It would be interesting to study how the addition of calcium influences the reaction extent at a relatively later age and thus the mechanical strength.

The objectives of the study here were to confirm if the Na/Al ratio controls the reaction extent, and to correlate the reaction extent with the mechanical properties in non-Ca mixes; and to examine the effects of Ca on the reaction extent and to correlate with the mechanical properties. By establishing the composition-structure-property relationships, mixes with better structures and mechanical performance could be designed. Effects of Ca on the reaction extent provide insight into structures of geopolymers with addition of Ca, as well as similar systems such as hybrid cement, both of which represent the future of sustainable construction materials (Shi et al. 2011, Provis et al. 2015).

In this chapter, the NMR and compressive strength data were collected by Kim (2012). But this NMR data were analyzed and validated differently and yielded different amount and composition of phases in the specimens, and these quantitative results were correlated with the compressive strength data.

8.2 Experimental methods

To synthesize geopolymers, a commercial sodium silicate solution, metakaolin and water were used as raw materials as described in Chapter 3. Different from those in previous chapters, mixes with different Na/Al ratio and with varying calcium content were designed as summarized in Table 8.1. Mixes 1-5 do not contain any Ca. By varying the Na/Al ratios, specimens with different reaction extent, being independent of Si/Al of the mix, were expected. Si/Al ratio of these mixes varied within a range of 1.1 to 1.5, much narrower as compared with mixes studied by Williams et al. (2011), aiming to examine if small changes in Si/Al would still predominantly affect the mechanical properties over the reaction extent. In Mixes 6-8, different amount of Ca was added,

with Ca/Si up to 0.15. The amount of each raw material for a batch of each mix is summarized in Appendix K. The synthesizing procedure is described in Chapter 3.

Table 8.1. Composition of mixtures presented in this chapter.

Mix number	Na/Al	Si/Al	H_2O/Na_2O	Ca/Si
1	0.54	1.10	20	0
2	0.59	1.20	20	0
3	0.64	1.30	20	0
4	0.55	1.35	20	0
5	0.74	1.50	20	0
6	0.74	1.50	20	0.05
7	0.74	1.50	20	0.10
8	0.74	1.50	20	0.15

Right after mixing, each specimens were placed in the 50 x 50 x50 mm plastic cube molds in two layers. Once filled in molds, all specimens were vibrated for around 30 seconds to achieve good consolidation. Specimens were stored in the curing room with 25^{o}C temperature and 100% humidity for around 3 hours and then were placed into an oven at 60^{o}C at ambient humidity and pressure for 2 hours. After the heat treatment, they were put back to the curing room and demolded at around 24 hours after mixing. The compressive tests were conducted at 7 days after mixing.

To understand the composition-structure-strength relationship for geopolymers with and without Ca, NMR and compressive tests were carried out at 7 days after mixing. Compressive tests were conducted in accordance with ASTM C109: Standard Test Method for Compressive Strength of

Hydraulic Cement Mortars. Solid-state ^{29}Si NMR tests were conducted using a Varian Unity Inova spectrometer with magnetic field of 7.04 T at a resonance frequency of 59.6 MHz. A 4-mm probe was used. Recycle delay and number of scans were 30 seconds and 2048, respectively. Prior to the ^{29}Si NMR testing, grounded samples were solvent extracted to stop hydration, as developed in Chapter 4. For non-Ca mixes, HCl extractions (Granizo et al. 2002, Palomo et al. 2004) were conducted to remove any geopolymer gel. For Ca-mixes, methanol-salicylic acid (SAM) extractions were carried out to remove any C-A-S-H phase prior to the HCl extractions. Procedure for both extractions were described in detail in Chapter 3. Residues from these extractions were also tested using the ^{29}Si NMR tests for unambiguous peak assignment of each phase. The amount and Si/Al ratio of the geopolymer gel were calculated based on intensity of the deconvoluted peaks.

8.3 Results and discussion

8.3.1 Non-Ca mixes

8.3.1.1 Structural quantification by NMR tests

Reaction extent was estimated by deconvolution of the ^{29}Si NMR spectra. The solid-state ^{29}Si NMR spectrum in Figure 8.1 is typical for the non-Ca mixes. The spectrum was deconvoluted to peaks in blue and magenta colors, attributed to unreacted metakaolin and geopolymer gel phases, respectively. During deconvolution, peaks for unreacted metakaolin were determined prior to those for geopolymer gel. Intensity at -110 to -120 pm is contributed only by unreacted metakaolin, as little intensity in this region was seen in fully (or nearly fully) reacted metakaolin geopolymers (Duxson et al. 2005c). The same widths and relative intensities of peaks were applied to deconvolute the unreacted metakaolin. The remaining part of the spectrum was attributed to geopolymer phase and was deconvoluted by adding additional peaks (magenta). The widths and

positions of these peaks were kept close to those from deconvolution of the mature geopolymer (in Figure 5.3 in Chapter 5), with fine adjustments to ensure good fitting.

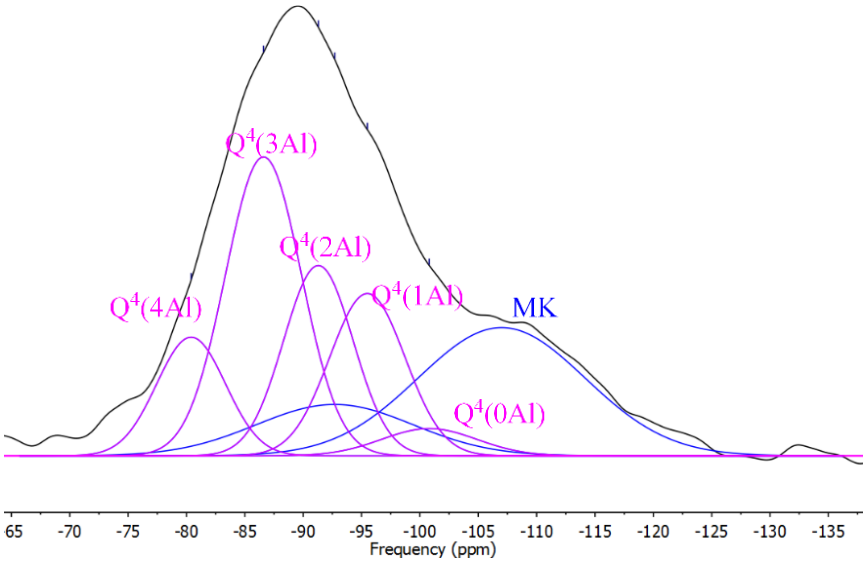

Figure 8.1. Deconvolution of the ^{29}Si NMR spectrum of the Mix 5 with Si/Al of 1.5. Black curve is the experimental spectrum, and deconvoluted peaks in magenta and blue colors are assigned to geopolymer and unreacted metakaolin phases, respectively.

Based on known ranges for sites with different Al substitution, these peaks for geopolymer gel at -80, -87, -91, -95 and -101 were assigned to Q^4(4Al), Q^4(3Al), Q^4(2Al), Q^4(1Al) and Q^4(0Al), respectively. With the intensity value for each peak, the Si/Al ratio of the geopolymer gel was estimated using Equation 2.1. Similar analysis was conducted for all the other non-Ca mixes. The Si/Al ratio in the geopolymer gel and the percentage of Si in the unreacted metakaolin for each mix are summarized in Table 8.2.

Table 8.2. Percentages of Si in each phase and Si/Al of geopolymer gel from the deconvolution of the ^{29}Si NMR spectra.

Mix No.	Mix design		Results from NMR deconvolution			Si/Al in unreacted MK	Estimated MK (wt %)
	Na/Al	Si/Al	Si/Al in GP gel	Unreacted MK (Si, mol%)	GP gel (Si, mol%)		
1	0.54	1.10	1.40	57.7%	42.3%	0.95	56.7%
2	0.59	1.20	1.64	50.1%	49.9%	0.95	51.0%
3	0.64	1.30	1.77	45.3%	54.7%	0.98	46.5%
4	0.55	1.35	1.64	50.1%	49.9%	1.15	48.8%
5	0.74	1.50	1.69	33.3%	66.7%	1.22	31.9%

The Si/Al of the unreacted metakaolin was calculated and shown in Table 8.2, by considering the consistent overall Si/Al before and after geopolymer reaction. Additionally, the weight percent of each phase was calculated by following the following procedures. By assuming the total amount of Si in each mix is 1.0 mole, the amount of Si in metakaolin and geopolymer gel were calculated. To estimate weights for the phases, formulas were assumed to be $(SiO_2)_{2m}\cdot(Al_2O_3)$ for the HCl residue with *m* being the Si/Al ratio of the unreacted metakaolin and assumed to be $(SiO_2)_{2n}\cdot(Al_2O_3)\cdot(Na_2O)$ for the geopolymer gel with *n* being the Si/Al ratio of gel. The weight percent of unreacted metakaolin with respect to the sum of unreacted metakaolin and geopolymer gel was calculated for each mix, as shown in Table 8.2.

8.3.1.2 Validation of structural quantification

To validate the reaction extent from the NMR analysis, HCl extraction and theoretical estimation based on Na/Al ratio were conducted. The weight percent of unreacted metakaolin with respect to the whole specimen was calculated from HCl extraction. In the theoretical estimation, the amount of reacted Al was estimated when all Na participates in geopolymer formation, as each Na ion balances the framework charge produced by each Al. By assuming the same moles of Si and Al were released in dissolution, the weight percentage of the unreacted metakaolin was calculated. This assumption may not allow an accurate estimation of the percent but would provide a reliable trend by comparing the different mixes. A sample calculation is presented in Appendix K.

Weight percentages of unreacted metakaolin from the three independent tests were plotted versus Na/Al in Figure 8.2. Trend lines were added for each set of data, and all show a decreasing linear relationship with Na/Al, suggesting NMR deconvolution yielded reasonable trend of reaction extent as Na/Al ratio changed. The lowest amounts of unreacted metakaolin from the theoretical estimation among all the three independent tests is expected, because this estimation assumes maximum reaction extent (i.e., all Na participated in geopolymer formation). The lower values from HCl extraction than those from the NMR analysis are also expected. In estimation from the NMR analysis, no water in the geopolymer gel is assumed when calculating its weight whereas a significant amount of water should be present in these non-extracted specimens (similar analysis in Chapter 5 was for extracted specimens). This assumption results in a lower weight percent of geopolymer gel and thus a higher percent of unreacted metakaolin.

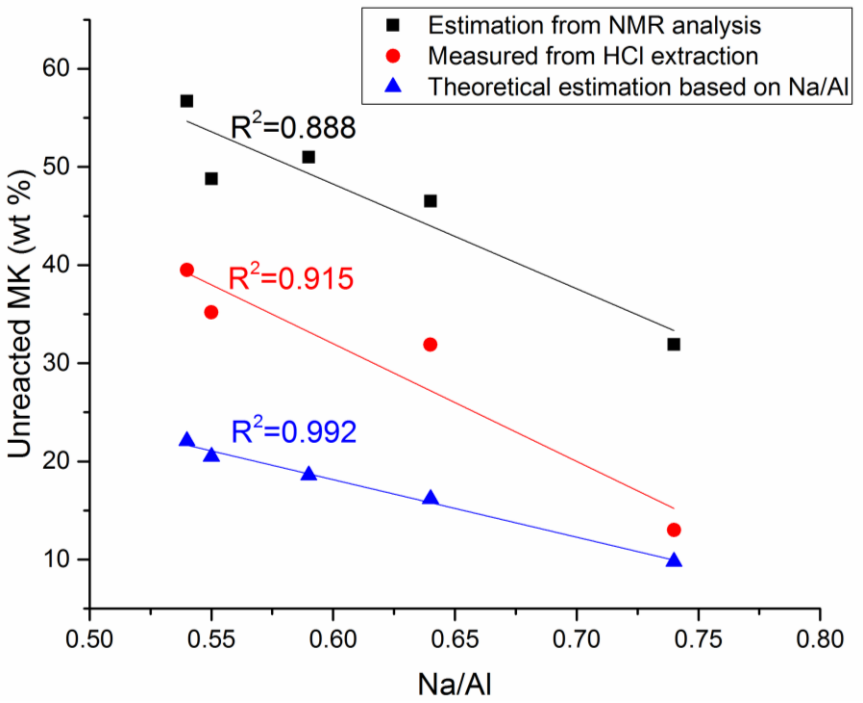

Figure 8.2. Weight percentages of unreacted metakaolin from NMR analysis, HCl extraction and Na/Al based theoretical estimation at different Na/Al ratios.

8.3.1.3 Structures and compressive strength

The compressive strength was plotted versus the Si/Al of the geopolymer gel and the Si (mol%) in unreacted metakaolin and best fit lines were added as shown in Figure 8.3. The Mix 1 was excluded, as it showed extremely low workability and its strength is considered unreliable. By comparing the coefficients of determination (R^2), the compressive strength was seen to correlate with the amount of Si in the unreacted metakaolin (Figure 8.3b) rather than with the Si/Al in the geopolymer gel (Figure 8.3a).

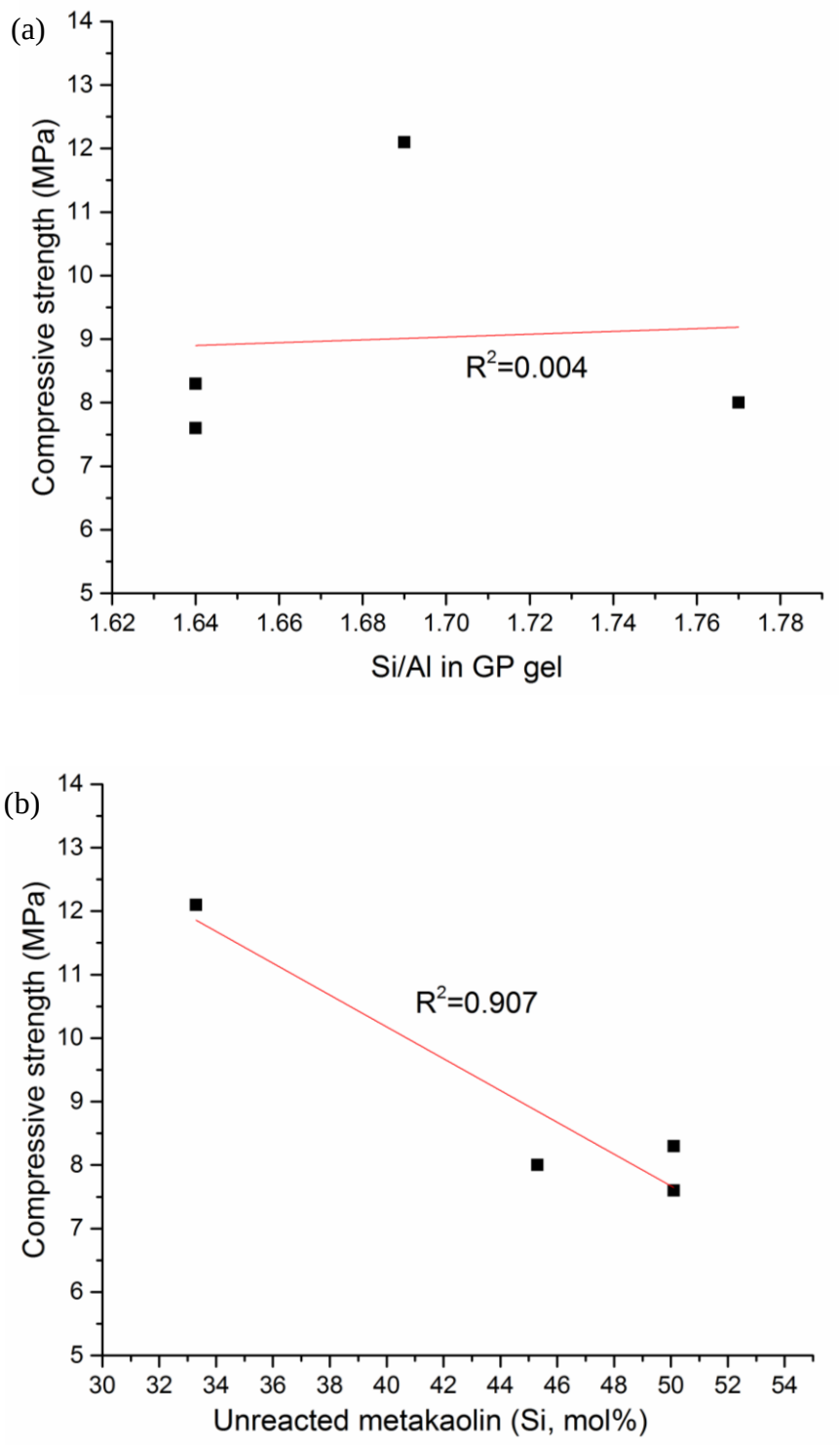

Figure 8.3. Compressive versus Si/Al of geopolymer gel (a) and versus molar percentage of Si in unreacted metakaolin (b).

Study here extended substantially the investigation by Kim (2012). In his work, the compressive strengths were plotted with the bulk Si/Al ratios of the mixes. In this study, the strengths were analyzed at fundamental level by correlating with the essential structural parameters including the reaction extent and the geopolymer gel compositions.

The reaction extent and Si/Al of the geopolymer gel are generally linked with each other in geopolymer mixes with silicate-containing activating solution, as discussed in the Introduction. Effects of both factors on strength have not been separated. In the study by Williams et al. (2011), for example, the mix with compressive strength of 3.1 MPa showed a Si/Al ratio of 21 in the geopolymer gel. In this mix, very little Al was released to the highly Si-concentrated activating solution. Both the extremely high Si/Al of the gel and the low reaction are expected to decrease the strength of the mix. The authors attributed the low strength only to the high Si/Al ratio (Williams et al. 2011), probably because of the Si/Al was extremely high as compared to the ratio (around 2.0) for optimum strength (Duxson et al. 2005b).

This study was able to separate the effects of the reaction extent and the Si/Al ratio of the geopolymer gel. The reaction extent was controlled independent of the Si/Al ratio by varying the Na/Al ratio. Additionally, the bulk Si/Al ratio was not higher than 1.5, and thus the Si/Al ratio in solution during reaction was not extremely high even at a low reaction extent. Results in Figure 8.3 indicate the reaction extent controlled the compressive strength when the Si/Al ratios of the geopolymer gel vary between 1.6 and 1.8, a relative narrow range.

8.3.2 Ca mixes

8.3.2.1 Ca content and reaction extent

The ^{29}Si NMR tests were conducted for mixes with varying amount of Ca. As an example, the spectra for mix with Ca/Si of 0.15 are shown in Figure 8.4. The geopolymer specimen was extracted using SAM extraction to remove the C-A-S-H phase, and the residue was further extracted using HCl extraction to remove the geopolymer gel phase. The Figures 8.4 (a-c) show spectra of the HCl residue, SAM residue and the specimen before extraction. The spectrum of the HCl residue was deconvoluted to two peaks, both assigned to unreacted metakaolin. Peaks with the same width, position and the relative intensity as these two were used to represent the unreacted metakaolin in the SAM residue. Peaks with similar widths and positions to those for non-Ca specimens were used to represent the geopolymer gel phase, with fine adjustment to enable good fitting. Additional peaks were introduced to represent the C-A-S-H phase, according to deconvolution of synthesized C-A-S-H (Hunnicutt 2013).

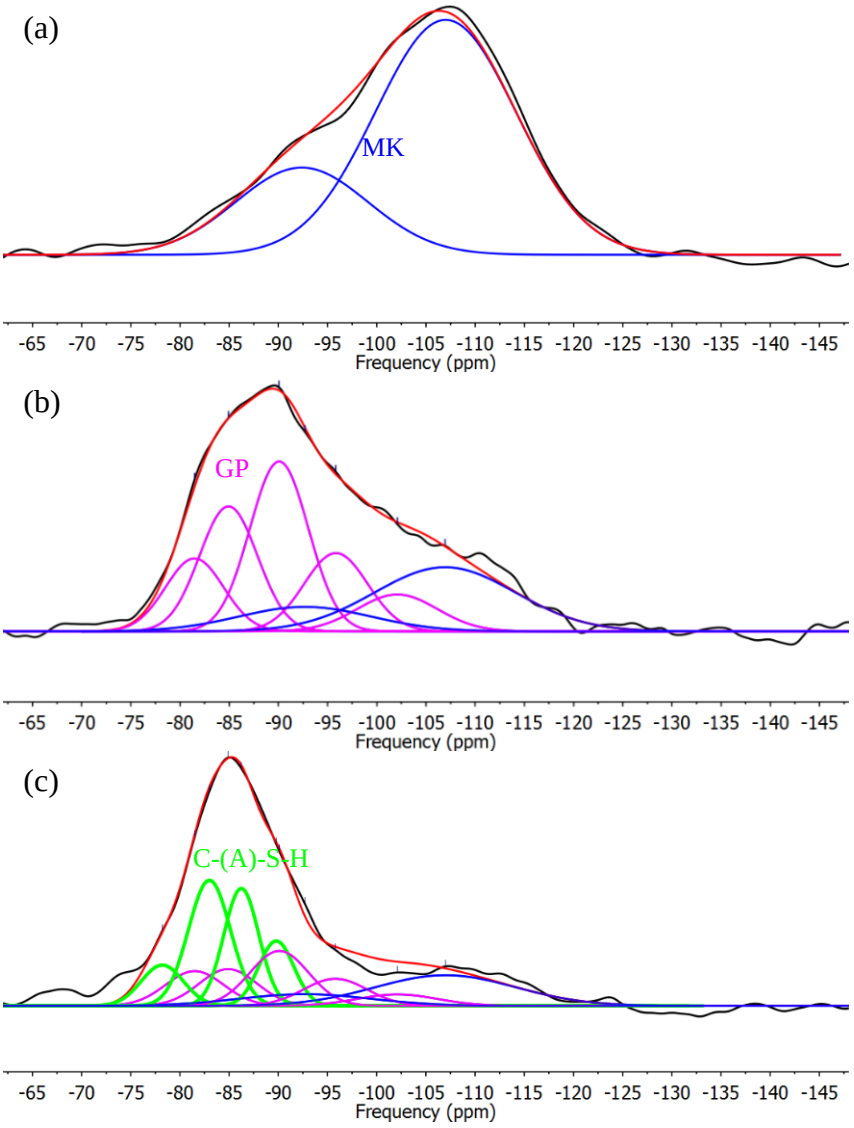

Figure 8.4. Deconvolution of ^{29}Si NMR spectra of HCl (a) and SAM (b) residues and the specimen extracted by solvent (c) for the Ca-mix with Ca/Si of 0.15 and Si/Al of 1.5. Black curve is the experimental spectrum, and deconvoluted peaks in magenta, green and blue colors are assigned to geopolymer, C-A-S-H and unreacted metakaolin phases, respectively.

Based on the deconvolution, the molar percentages of C-A-S-H, geopolymer gel and metakaolin were estimated to be 45.8%, 34.2% and 20.0%, respectively. The five peaks for geopolymers at -

81.5, -84.9, -90.1, -95.8 and -102.1 ppm were assigned to Q^4(4Al), Q^4(3Al), Q^4(2Al), Q^4(1Al) and Q^4(0Al), respectively. The Si/Al of the geopolymer gel was calculated to be 1.85, higher than the 1.61 estimated for the non-Ca mix. In the current study, the Si/Al in the C-A-S-H was estimated to be 1.5, by assuming constant bulk Si/Al ratio before and after reaction. This Si/Al ratio is lower than 5, the lower boundary of Si/Al believed for conventional C-A-S-H gel with chain structures (Myers et al. 2015). However, it is in the range between 1.2 to 10.0, the range for a calcium modified geopolymer gel, i.e., (Ca, Na)-A-S-H, with three-dimensional structures (Garcia-Lodeiro et al. 2011). Though the SAM solubility of this phase is unknown, it might be removed by the SAM extraction together with some conventional C-A-S-H with chain structures. Then the geopolymer gel (N-A-S-H) was removed by further HCl extraction.

In addition to the change in Si/Al ratio, the presence of Ca also affected the reaction extent of the specimens. Figure 8.5 shows the superimposed NMR spectra of the geopolymer specimens with addition of different amounts of Ca. The region from -110 to -120 ppm (as circled) only belongs to the metakaolin. In this figure, the relative intensity in this region is lower in mixes with Ca/Si of 0.10 and 0.15 than mixes with lower Ca contents. This difference indicates the reaction extent was increased with addition of Ca.

To be more quantitative, the percent of unreacted metakaolin in terms of molar percentage of Si was estimated by deconvolution of each spectrum and was plotted and best fit line was added in Figure 8.6. The enhanced reaction extent with Ca is consistent with the results in Chapter 7 at earlier ages during geopolymerization and also studies by others. Chapter 7 confirmed the dissolution of metakaolin was faster and its extent was higher with addition of Ca before and around setting. It was proposed that addition of calcium consumes Si in solution and further

enhances dissolution kinetics. In systems with low amount of Si in solution or those activated by hydroxide solution, the hydrolysis of the strained Al could lead to some degree of exfoliation of the structure and thus expose more layers for further dissolution, as proposed by White and colleagues (White et al. 2011b). Additionally, in a study by Temuujin et al. (2009), a faster dissolution by the addition of Ca was proposed, because the pH is believed to be locally increased with the consumption of H_2O by the formation of C-A-S-H (Temuujin et al. 2009).

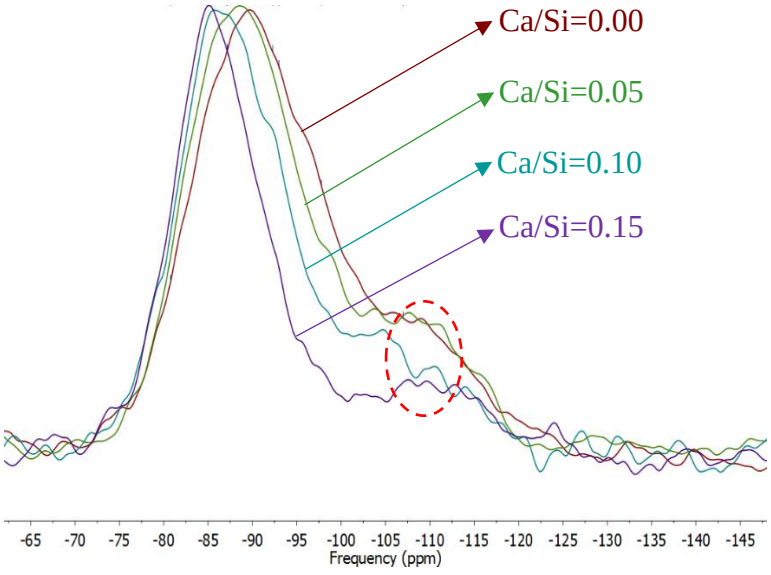

Figure 8.5. NMR spectra of geopolymers at 7 days with different amounts of Ca.

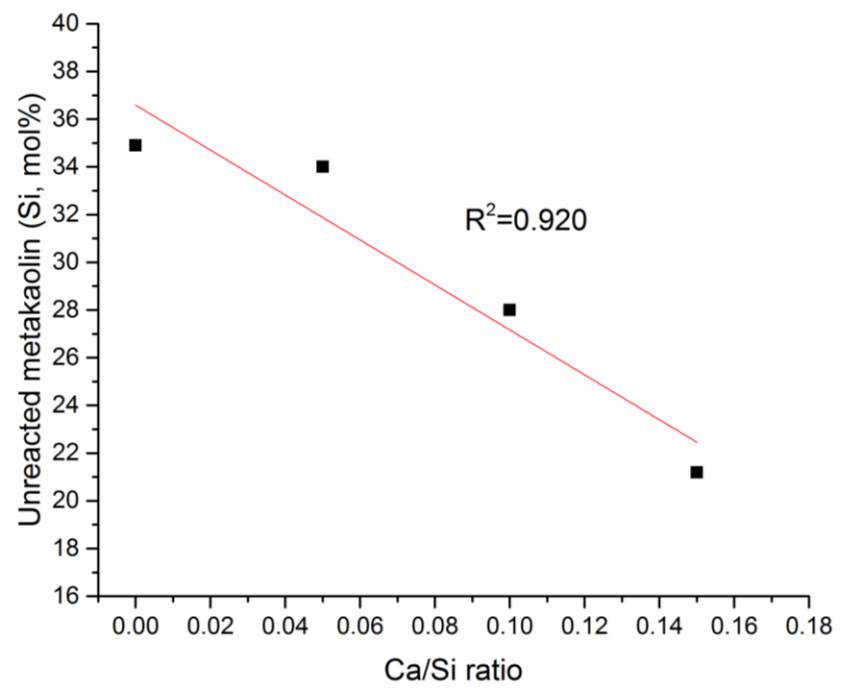

Figure 8.6. Reaction extent in term of mol% of Si in unreacted metakaolin for geopolymers with different Ca/Si ratios at 7 days.

8.3.2.2 Reaction extent and compressive strength

Compressive strength was plotted versus the reaction extent for mixes with different amount of Ca in Figure 8.7. As shown in this figure, mixes with Ca/Si below or equal to 0.10 show a strong linear relationship between compressive strength versus the molar percentage of Si in the unreacted metakaolin. The coefficient of determination (R^2) of the best fit line is larger than 0.99. It should be noted that the mix with Ca/Si of 0.15 showed a low workability, which is believed to cause such an extremely low compressive strength and was not included in the regression analysis.

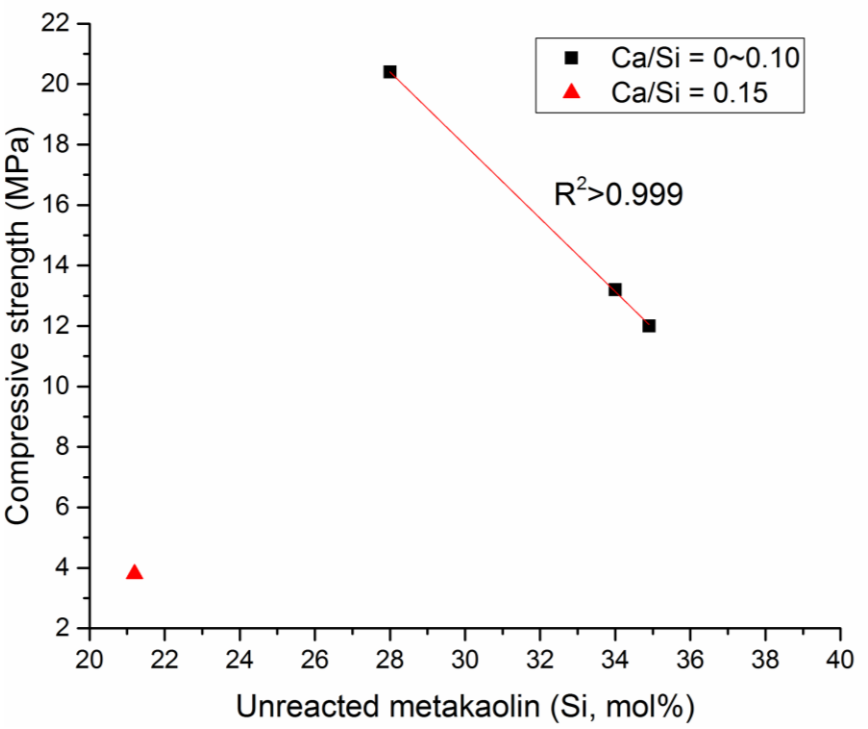

Figure 8.7. Compressive strength of Ca-mixes at 7 days versus unreacted metakaolin.

8.4 Conclusions

This study aimed to establish the composition-structure-strength relationship for metakaolin geopolymers with and without Ca. Reaction extent was quantified using solid-state ^{29}Si NMR. This quantification was found to be consistent with HCl extraction and theoretical estimation based on Na/Al ratio in the mix, and it was validated by the bulk Si/Al ratio in the mix. The Na/Al ratio greatly influenced the reaction extent. Ca increased the reaction extent. For both non-Ca and Ca mixes, reaction extent was linearly correlated with compressive strength. In addition to establishing the composition-structure-strength relationship, this study presented a method to quantify geopolymer structures.

Chapter 9. Conclusions

To use geopolymers in construction, the setting behavior needs to be well understood and controlled. Calcium has been seen to strongly speed up setting. The objectives of this study were to understand setting at nanostructural level for both non-calcium and calcium mixes. To begin with, it was necessary to stop the geopolymer formation prior to NMR characterization. Then the nanostructural evolution was examined and correlated with setting for both the mixes. Finally, the effects of calcium on properties and structures at a later age were investigated.

Extraction methods were developed to stop geopolymer formation.

1. In a preliminary extraction using methanol/acetone solvent, dissolution was stopped but condensation continued as indicated by the MAS NMR tests. This observation suggests extraction used in many papers to stop geopolymerization is ineffective if the solvent amount not well controlled.
2. A controlled protocol for solvent extraction using methanol and acetone was developed and shown to suspend reaction up to 53 hours. For early-age specimens, soluble species precipitated during this treatment, confounding the NMR interpretation of geopolymer gel structure. Therefore, this protocol is suitable only for more mature geopolymers.
3. To avoid confounding effects noted above, a combination of water and the solvent extraction removed the soluble silicates that would otherwise precipitate upon solvent extraction and thereby stopped reaction.
4. This combined extraction either before or a few hours after set was found to stop geopolymer reaction for at least one week for specimens both with and without calcium.

Protocol was developed to quantify structures of geopolymers.

1. The Si/Al ratio of a natural zeolite based on relative intensities of deconvoluted peaks of the ^{29}Si MAS NMR spectrum, when peaks are appropriately assigned, was consistent with the bulk Si/Al ratio.
2. The Si/Al ratio of a mature geopolymer specimen based on relative intensities of deconvoluted peaks of the ^{29}Si MAS NMR spectrum was consistent with its bulk ratio.
3. For earlier-age specimens (51 hours and 19 days), combined extraction (as noted above) and HCl extraction were used to stop the geopolymer reaction and to separate phases, respectively. By analyzing the ^{29}Si MAS NMR spectra of these residues, the Si/Al ratio and the amount (molar percent of Si) of geopolymer gel were estimated. The amount of the geopolymer gel was higher and its Si/Al ratio was lower in the 19-day specimen than in the 51 hour-specimen.
4. The Si/Al ratios from NMR deconvolution were consistent with those from intensity analysis of NMR tests, during which the moles of Si and Al were estimated by comparing spectrum intensity with control specimens of known composition.
5. Weight percent of each phase was estimated from the NMR results by assigning a corresponding reasonable compositional formula, and was consistent with the recorded weights of extraction residues.

For geopolymer without calcium, setting was shown to be a percolation process.

1. Both UWR and penetration resistance tests showed setting time around 15 hours for the geopolymer mix $1Na_2O{\cdot}1Al_2O_3{\cdot}4SiO_2{\cdot}11H_2O$.

2. The Al dissolution, characterized by conversion of 5- and 6- to 4-coordinated aluminum, proceeded fast upon mixing until 10 hours, then slowed down and became immeasurable from 15 hours.
3. Based on liquid-state ^{29}Si NMR tests, the Q^4 silicate peak was broader than others, suggesting the Q^4 molecules were larger and less mobile than the lower-Q species; the ratio of Q^4/Q^3 increased progressively with time, indicating species kept growing.
4. Based on both ^{27}Al and ^{29}Si NMR results, Al upon dissolution appeared to be immediately incorporated into solid aluminosilicate oligomers which tend to enlarge over time.
5. Further NMR tests support that these aluminosilicate products form on the surface of metakaolin particles, consistent with the proposed mechanism in literature.
6. Starting from around 15 hours, the amount of aqueous Q^2 and Q^3 silicates decreased due to their attaching to the aluminosilicate products on metakaolin surface.
7. The initiation of this attaching process coincides with the setting time. As the low-Q silicates attach to aluminosilicates on the surface of the metakaolin particles, the gel bridges the gaps between metakaolin particles and a network structure starts to form, as supported by the rapid increase of strength and stiffness right after set.

For geopolymer with calcium, the enhanced metakaolin dissolution and gel formation caused more rapid setting.

1. In the presence of calcium, setting time was substantially reduced, from 15 hours for the control mix (without calcium) to 1 hour for the investigated calcium mix.

2. In the presence of calcium, Al dissolution in terms of both rate and extent was substantially enhanced.
3. In the presence of calcium, C-A-S-H formed, and substantially more geopolymer gel formed than in the non-calcium mix.
4. The accelerated setting was attributed to the enhanced formation of geopolymer gel. The Si (mol%) of geopolymer gel at set was somewhat higher in the calcium (1 hour) mix than in the non-calcium (15 hours) mix.
5. The effects on setting of C-A-S-H formation (expected randomly in pore solution) do not seem to be as important as the geopolymer formation (on metakaolin surface).
6. The Si/Al for geopolymer formation was estimated. This ratio is much lower in the calcium mix than in the non-calcium mix at early ages, an observation that explains the enhanced geopolymer formation in the calcium mix.
7. The different Si/Al ratios above are mainly due to the fast Al dissolution in the calcium mix. Calcium consumes Si in the solution, and a protective layer is less likely to form on the metakaolin particles, thus less inhibiting the dissolution.

Calcium and Na/Al ratio affected reaction extent and compressive strength after set.

1. The quantification methodology of reaction extent based on relative intensities of deconvoluted NMR peaks was again found to be effective, as supported by HCl extraction and theoretical estimation from the Na/Al ratio of each mix.
2. The reaction extent was controlled by Na/Al ratio in the non-calcium mixes.
3. The reaction extent increased linearly with the amount of calcium.

4. In either calcium or non-calcium mixes, the compressive strength increased linearly with the reaction extent.
5. In the non-calcium mixes, the reaction extent was controlled without affecting the Si/Al ratio of geopolymer gel by altering Na/Al ratio. Since both amount and composition of the geopolymer gel affect the compressive strength, this strategy provided a way to separate the effects of the Si/Al and Na/Al ratios, a mix design strategy that has not previously been reported.
6. In the non-calcium mixes, the Si/Al ratios in the geopolymer gel, when varied in a narrow range, do not seem to correlate with compressive strength.

This study provides basis for further investigations and helps promote applications of geopolymers in construction. The combined extraction developed to stop geopolymer formation at early ages can be used in further kinetics studies for geopolymers and probably also for similar aluminosilicates such as zeolites. By monitoring evolution of structural coordination and connectivity during dissolution and condensation, the setting of the non-calcium mix has been understood at a much more advanced level. The quantification of phases at early age provides direct evidence to understand the accelerated setting by calcium. This understanding paves the way to use geopolymers in construction where calcium is contained in many common precursors. Nanostructural characterization techniques used here could be applied to study other factors that may also affect kinetics of geopolymerization for metakaolin as well as other precursor systems, including fly ashes, other industrial wastes and synthetic aluminosilicate precursors. Additionally, methodology here also helps understand properties of geopolymers after set.

References

Akporiaye, D. E., I. M. Dahl, H. B. Mostad and R. Wendelbo (1996). "Aluminum Distribution in Chabazite: An Experimental and Computational Study." The Journal of Physical Chemistry **100**(10): 4148-4153.

Alonso, S. and A. Palomo (2001a). "Alkaline Activation of Metakaolin and Calcium Hydroxide Mixtures: Influence of Temperature, Activator Concentration and Solids Ratio." Materials Letters **47**(1-2): 55-62.

Alonso, S. and A. Palomo (2001b). "Calorimetric Study of Alkaline Activation of Calcium Hydroxide–Metakaolin Solid Mixtures." Cement and Concrete Research **31**(1): 25-30.

Andersen, M. D., H. J. Jakobsen and J. Skibsted (2003). "Incorporation of Aluminum in the Calcium Silicate Hydrate (C−S−H) of Hydrated Portland Cements: A High-Field ^{27}Al and ^{29}Si MAS NMR Investigation." Inorganic Chemistry **42**(7): 2280-2287.

Anseau, M. R., J. P. Leung, N. Sahai and T. W. Swaddle (2005). "Interactions of Silicate Ions with Zinc(II) and Aluminum(III) in Alkaline Aqueous Solution." Inorganic Chemistry **44**(22): 8023-8032.

Ashenhurst, J., G. Wu and S. Wang (2000). "Syntheses, Structures, Solution, and Solid-State ^{27}Al NMR Studies of Blue Luminescent Mononuclear Aluminum Complexes: Al(7-azain)$_2$(7-azain-H)(CH_3), Al(7-azain)$_3$(7-azain-H), and Al(7-azain)(7-azain-H)(OCH(CF_3)$_2$)$_2$(7-azain-H=7-azaindole)." Journal of the American Chemical Society **122**(11): 2541-2547.

ASTM Standard C403. (2008). ASTM Test Method for Time of Setting of Concrete Mixtures by Penetration Resistance, ASTM International, West Conshohocken, PA.

ASTM Standard C191. (2008). ASTM Test Method for Time of Setting of Hydraulic Cement by Vicat Needle, ASTM International, West Conshohocken, PA.

Bakharev, T. (2005). "Resistance of Geopolymer Materials to Acid Attack." Cement and Concrete Research **35**(4): 658-670.

Barbosa, V. F., K. J. MacKenzie and C. Thaumaturgo (2000). "Synthesis and Characterisation of Materials Based on Inorganic Polymers of Alumina and Silica: Sodium Polysialate Polymers." International Journal of Inorganic Materials **2**(4): 309-317.

Bass, J. L. and G. L. Turner (1997). "Anion Distributions in Sodium Silicate Solutions. Characterization by ^{29}Si NMR and Infrared Spectroscopies, and Vapor Phase Osmometry." The Journal of Physical Chemistry B **101**(50): 10638-10644.

Bentz, D. P. and E. J. Garboczi (1991). "Percolation of Phases in a Three-Dimensional Cement Paste Microstructural Model." Cement and Concrete Research **21**(2): 325-344.

Bernal, S. A., J. L. Provis, B. Walkley, R. San Nicolas, J. D. Gehman, D. G. Brice, A. R. Kilcullen, P. Duxson and J. S. J. van Deventer (2013). "Gel Nanostructure in Alkali-Activated Binders Based on Slag and Fly Ash, and Effects of Accelerated Carbonation." Cement and Concrete Research **53**(0): 127-144.

Bish, D. L. and D. W. Ming (2001). Natural Zeolites: Occurrence, Properties, Applications, Volume 45, Reviews in Mineralogy & Geochemistry, Mineralogical Society of America and the Geochemical Society, Washington, D.C.

Brinker, C. J. and G. W. Scherer (1990). Sol-Gel Science: the Physics and Chemistry of Sol-Gel Processing, Academic Press, San Diego, CA.

Brus, J., L. Kobera, M. Urbanová, D. Koloušek and J. Kotek (2012). "Insights into the Structural Transformations of Aluminosilicate Inorganic Polymers: A Comprehensive Solid-State NMR Study." The Journal of Physical Chemistry C **116**(27): 14627-14637.

Chen, B. and Y. Huang (2006). "^{17}O Solid-State NMR Spectroscopic Studies of the Involvement of Water Vapor in Molecular Sieve Formation by Dry-Gel Conversion." Journal of the American Chemical Society **128**(19): 6437-6446.

Chen, C., W. Gong, W. Lutze, I. L. Pegg and J. Zhai (2011). "Kinetics of Fly Ash Leaching in Strongly Alkaline Solutions." Journal of Materials Science **46**(3): 590-597.

Cheng, T. W. and J. P. Chiu (2003). "Fire-resistant Geopolymer Produced by Granulated Blast Furnace Slag." Minerals Engineering **16**(3): 205-210.

Chindaprasirt, P., P. Silva, K. Sagoe-Crentsil and S. Hanjitsuwan (2012). "Effect of SiO_2 and Al_2O_3 on the Setting and Hardening of High Calcium Fly Ash-Based Geopolymer Systems." Journal of Materials Science **47**(12): 4876-4883.

Chung, C.-W. (2010). Ultrasonic Wave Reflection Measurements on Stiffening and Setting of Cement Paste, Ph.D. Thesis, University of Illinois at Urbana-Champaign.

Chung, C.-W., I.-Y. Park, L. J. Struble and M. Mroczek (2010). "On the Evaluation of Setting Time of Cement Paste Based on ASTM C403 Penetration Resistance Test." Journal of Testing and Evaluation **38**(5): 1-7.

Chung, C.-W., P. Suraneni, J. S. Popovics and L. J. Struble (2012). "Setting Time Measurement Using Ultrasonic Wave Reflection." ACI Materials Journal **109**(1): 109-117.

Criado, M., A. Fernández-Jiménez, A. Palomo, I. Sobrados and J. Sanz (2008). "Effect of the SiO_2/Na_2O Ratio on the Alkali Activation of Fly Ash. Part II: ^{29}Si MAS-NMR Survey." Microporous and Mesoporous Materials **109**(1–3): 525-534.

Cwirzen, A., J. L. Provis, V. Penttala and K. Habermehl-Cwirzen (2014). "The Effect of Limestone on Sodium Hydroxide-Activated Metakaolin-Based Geopolymers." Construction and Building Materials **66**: 53-62.

Davidovits, J. (1982). "The Need to Create a New Technical Language for the Transfer of Basic Scientific Information." Transfer and Exploitation of Scientific and Technical Information, EUR **7716**: 316-320.

Davidovits, J. (1991). "Geopolymers, Inorganic Polymeric New Materials." Journal of Thermal Analysis **37**(8): 1633-1656.

Duxson, P., A. Fernández-Jiménez, J. L. Provis, G. C. Lukey, A. Palomo and J. S. J. van Deventer (2007a). "Geopolymer Technology: the Current State of the Art." Journal of Materials Science **42**(9): 2917-2933.

Duxson, P., G. Lukey, F. Separovic and J. Van Deventer (2005a). "Effect of Alkali Cations on Aluminum Incorporation in Geopolymeric Gels." Industrial & Engineering Chemistry Research **44**(4): 832-839.

Duxson, P., S. W. Mallicoat, G. C. Lukey, W. M. Kriven and J. S. J. van Deventer (2007b). "The Effect of Alkali and Si/Al Ratio on the Development of Mechanical Properties of Metakaolin-Based Geopolymers." Colloids and Surfaces A: Physicochemical and Engineering Aspects **292**(1): 8-20.

Duxson, P., J. L. Provis, G. C. Lukey, S. W. Mallicoat, W. M. Kriven and J. S. J. van Deventer (2005b). "Understanding the Relationship between Geopolymer Composition, Microstructure and Mechanical Properties." Colloids and Surfaces A: Physicochemical and Engineering Aspects **269**(1–3): 47-58.

Duxson, P., J. L. Provis, G. C. Lukey, F. Separovic and J. S. J. van Deventer (2005c). "^{29}Si NMR Study of Structural Ordering in Aluminosilicate Geopolymer Gels." Langmuir **21**(7): 3028-3036.

Duxson, P., J. L. Provis, G. C. Lukey and J. S. J. van Deventer (2007c). "The Role of Inorganic Polymer Technology in the Development of 'Green Concrete'." Cement and Concrete Research **37**(12): 1590-1597.

Eichele, K. (2015, August 3rd, 2015). "WSolids1, a Program to Simulate Solid State NMR Spectra." Retrieved November 6th, 2015, from ttp://anorganik.uni-tuebingen.de/klaus/soft/.

Engelhardt, G. and D. Michel (1987). High-Resolution Solid-State NMR of Silicates and Zeolites, John Wiley & Sons, New York.

Favier, A., G. Habert, J. B. d'Espinose de Lacaillerie and N. Roussel (2013). "Mechanical Properties and Compositional Heterogeneities of Fresh Geopolymer Pastes." Cement and Concrete Research **48**: 9-16.

Favier, A., G. Habert, N. Roussel and J.-B. d'Espinose de Lacaillerie (2015). "A Multinuclear Static NMR Study of Geopolymerisation." Cement and Concrete Research **75**: 104-109.

Feng, D., H. Tan and J. Van Deventer (2004). "Ultrasound Enhanced Geopolymerisation." Journal of Materials Science **39**(2): 571-580.

Fernández-Jiménez, A., A. G. de la Torre, A. Palomo, G. López-Olmo, M. M. Alonso and M. A. G. Aranda (2006a). "Quantitative Determination of Phases in the Alkaline Activation of Fly Ash. Part II: Degree of Reaction." Fuel **85**(14–15): 1960-1969.

Fernández-Jiménez, A. and A. Palomo (2005). "Mid-Infrared Spectroscopic Studies of Alkali-Activated Fly Ash Structure." Microporous and Mesoporous Materials **86**(1–3): 207-214.

Fernández-Jiménez, A., A. Palomo, I. Sobrados and J. Sanz (2006b). "The Role Played by the Reactive Alumina Content in the Alkaline Activation of Fly Ashes." Microporous and Mesoporous Materials **91**(1–3): 111-119.

Fyfe, C. A., J. Bretherton and L. Lam (2000). "Detection of the 'Invisible Aluminium' and Characterisation of the Multiple Aluminium Environments in Zeolite USY by High-Field Solid-State NMR." Chemical Communication (17): 1575-1576.

Garcia-Lodeiro, I., A. Fernández-Jiménez, M. T. Blanco and A. Palomo (2007). "FTIR Study of the Sol–Gel Synthesis of Cementitious Gels: C–S–H and N–A–S–H." Journal of Sol-Gel Science and Technology **45**(1): 63-72.

Garcia-Lodeiro, I., A. Fernández-Jiménez, A. Palomo and D. E. Macphee (2010). "Effect of Calcium Additions on N–A–S–H Cementitious Gels." Journal of the American Ceramic Society **93**(7): 1934-1940.

Garcia-Lodeiro, I., A. Palomo, A. Fernández-Jiménez and D. E. Macphee (2011). "Compatibility Studies between N-A-S-H and C-A-S-H Gels. Study in the Ternary Diagram Na_2O–CaO–Al_2O_3–SiO_2–H_2O." Cement and Concrete Research **41**(9): 923-931.

Ginter, D. M., G. T. Went, A. T. Bell and C. J. Radke (1992). "A Physicochemical Study of the Aging of Colloidal Silica Gels Used in Zeolite Y Synthesis." Zeolites **12**(6): 733-741.

Granizo, M. L., S. Alonso, M. T. Blanco-Varela and A. Palomo (2002). "Alkaline Activation of Metakaolin: Effect of Calcium Hydroxide in the Products of Reaction." Journal of the American Ceramic Society **85**(1): 225-231.

Granizo, M. L. and M. T. Blanco (1998). "Alkaline Activation of Metakaolin An Isothermal Conduction Calorimetry Study." Journal of Thermal Analysis and Calorimetry **52**(3): 957-965.

Granizo, N., A. Palomo and A. Fernandez-Jiménez (2014). "Effect of Temperature and Alkaline Concentration on Metakaolin Leaching Kinetics." Ceramics International **40**(7, Part A): 8975-8985.

Hajimohammadi, A., J. L. Provis and J. S. J. van Deventer (2010). "Effect of Alumina Release Rate on the Mechanism of Geopolymer Gel Formation." Chemistry of Materials **22**(18): 5199-5208.

Hajimohammadi, A., J. L. Provis and J. S. J. van Deventer (2011a). "Time-Resolved and Spatially-Resolved Infrared Spectroscopic Observation of Seeded Nucleation Controlling Geopolymer Gel Formation." Journal of Colloid and Interface Science **357**(2): 384-392.

Hajimohammadi, A., J. L. Provis and J. S. J. van Deventer (2011b). "The Effect of Silica Availability on the Mechanism of Geopolymerisation." Cement and Concrete Research **41**(3): 210-216.

Hamilton, J. P., S. L. Brantley, C. G. Pantano, L. J. Criscenti and J. D. Kubicki (2001). "Dissolution of Nepheline, Jadeite and Albite Glasses: toward Better Models for Aluminosilicate Dissolution." Geochimica et Cosmochimica Acta **65**(21): 3683-3702.

Hass, E. C., P. G. Mezey and P. J. Plath (1981). "A Non-Empirical Molecular Orbital Study on Loewenstein's Rule and Zeolite Composition." Journal of Molecular Structure: Themchem **76**(4): 389-399.

Hunnicutt, W. A. (2013). Characterization of Calcium-Silicate-Hydrate and Calcium-Alumino-Silicate-Hydrate, M.S. Thesis, University of Illinois at Urbana-Champaign.

Hunnicutt, W. A. (2016). Schematics of C-S-H and C-A-S-H from personal communication.

Iler, R. K. (1979). The Chemistry of Silica: Solubility, Polymerization, Colloid and Surface Properties, and Biochemistry, Wiley, New York.

Ismail, I., S. Bernal, J. Provis, S. Hamdan and J. J. Deventer (2013). "Drying-Induced Changes in the Structure of Alkali-Activated Pastes." Journal of Materials Science **48**(9): 3566-3577.

Jiang, S. P., J. C. Mutin and A. Nonat (1995). "Studies on Mechanism and Physico-Chemical Parameters at the Origin of the Cement Setting. I. The Fundamental Processes Involved During the Cement Setting." Cement and Concrete Research **25**(4): 779-789.

Davidovits, J. (2011). Geopolymer Chemistry & Applications, 4th Edition, Institut Geopolymere, Saint-Quentin, France.

Keeler, J. (2011). Understanding NMR spectroscopy, Wiley, Hoboken, NJ.

Khater, H., B. El-Sabbagh, M. Fanny, M. Ezzat and M. Lottfy (2012). "Effect of Nano-Silica on Alkali Activated Water-Cooled Slag Geopolymer." ARPN Journal of Science and Technolog **2**(3): 170-176

Khater, H. M. (2013) "Effect of Cement Kiln Dust on Geopolymer Composition and its Resistance to Sulfate Attack." Green Materials **1**, 36-46.

Kim, E. H. (2012). Understanding Effects of Silicon/Aluminum Ratio and Calcium Hydroxide on Chemical Composition, Nanostructure and Compressive Strength for Metakaolin Geopolymers. M.S. Thesis, University of Illinois at Urbana and Champaign.

Kim, Y. and R. J. Kirkpatrick (1998). "High-Temperature Multi-Nuclear NMR Investigation of Analcime." American Mineralogist **83**(3-4): 339-347.

Kinrade, S. D. and T. W. Swaddle (1989). "Direct Detection of Aluminosilicate Species in Aqueous Solution by Silicon-29 and Aluminum-27 NMR Spectroscopy." Inorganic Chemistry **28**(10): 1952-1954.

Kocaba, V., E. Gallucci and K. L. Scrivener (2012). "Methods for Determination of Degree of Reaction of Slag in Blended Cement Pastes." Cement and Concrete Research **42**(3): 511-525.

Kriven, W. M., J. L. Bell and M. Gordon (2003). Microstructure and Microchemistry of Fully-Reacted Geopolymers and Geopolymer Matrix Composites. Advances in Ceramic Matrix Composites IX, John Wiley & Sons, Inc.**:** 227-250.

Lee, S. K. and J. F. Stebbins (2000). "Al–O–Al and Si–O–Si Sites in Framework Aluminosilicate Glasses with Si/Al=1: Quantification of Framework Disorder." Journal of Non-Crystalline Solids **270**(1–3): 260-264.

Lee, S. K., J. F. Stebbins, C. A. Weiss and R. J. Kirkpatrick (2003). "^{17}O and ^{27}Al MAS and 3QMAS NMR Study of Synthetic and Natural Layer Silicates." Chemistry of Materials **15**(13): 2605-2613.

Lee, W. and J. Van Deventer (2002). "The Effect of Ionic Contaminants on the Early-Age Properties of Alkali-Activated Fly Ash-Based Cements." Cement and Concrete Research **32**(4): 577-584.

Li, C., H. Sun and L. Li (2010). "A Review: The Comparison between Alkali-Activated Slag (Si + Ca) and Metakaolin (Si + Al) Cements." Cement and Concrete Research **40**(9): 1341-1349.

Lippmaa, E., M. Maegi, A. Samoson, M. Tarmak and G. Engelhardt (1981). "Investigation of the Structure of Zeolites by Solid-State High-Resolution Silicon-29 NMR Spectroscopy." Journal of the American Chemical Society **103**(17): 4992-4996.

Lloyd, R. R., J. L. Provis and J. S. J. van Deventer (2009). "Microscopy and Microanalysis of Inorganic Polymer Cements. 2: the Gel Binder." Journal of Materials Science **44**(2): 620-631.

Loewenstein, W. (1954). "The Distribution of Aluminum in the Tetrahedra of Silicates and Aluminates." American Mineralogist **39**(1-2): 92-96.

Luke, K. and F. P. Glasser (1987). "Selective Dissolution of Hydrated Blast Furnace Slag Cements." Cement and Concrete Research **17**(2): 273-282.

MacKenzie, K. J. D., I. W. M. Brown, R. H. Meinhold and M. E. Bowden (1985). "Outstanding Problems in the Kaolinite-Mullite Reaction Sequence Investigated by ^{29}Si and ^{27}Al Solid-state Nuclear Magnetic Resonance: I, Metakaolinite." Journal of the American Ceramic Society **68**(6): 293-297.

Macphee, D. E. and I. Garcia-Lodeiro. Activation of Aluminosilicates-Some Chemical Considerations. Proceedings of the Second International Slag Valorisation Symposium, the Transition to Sustainable Materials Management, April 2011, Luven, Gelgium.

Man, P. P. and J. Klinowski (1988). "Quantitative Determination of Aluminium in Zeolites by Solid-State ^{27}Al NMR Spectroscopy." Journal of the Chemical Society, Chemical Communications(19): 1291-1294.

Massiot, D., C. Bessada, J. Coutures and F. Taulelle (1990a). "A Quantitative Study of ^{27}Al MAS NMR in crystalline YAG." Journal of Magnetic Resonance (1969) **90**(2): 231-242.

Massiot, D., C. Bessada, J. P. Coutures and F. Taulelle (1990b). "A Quantitative Study of ^{27}Al MAS NMR in crystalline YAG." Journal of Magnetic Resonance (1969) **90**(2): 231-242.

Massiot, D., F. Fayon, M. Capron, I. King, S. Le Calvé, B. Alonso, J.-O. Durand, B. Bujoli, Z. Gan and G. Hoatson (2002). "Modelling One- and Two-Dimensional Solid-State NMR Spectra." Magnetic Resonance in Chemistry **40**(1): 70-76.

McCormick, A., A. Bell and C. Radke (1989). "Multinuclear NMR Investigation of the Formation of Aluminosilicate Anions." The Journal of Physical Chemistry **93**(5): 1741-1744.

McCormick, A. v. and A. Bell (1989). "The Solution Chemistry of Zeolite Precursors." Catalysis Reviews—Science and Engineering **31**(1-2): 97-127.

McLellan, B. C., R. P. Williams, J. Lay, A. van Riessen and G. D. Corder (2011). "Costs and Carbon Emissions for Geopolymer Pastes in Comparison to Ordinary Portland Cement." Journal of Cleaner Production **19**(9–10): 1080-1090.

Merzbacher, C. I., B. L. Sherriff, J. S. Hartman and W. B. White (1990). "A High-Resolution ^{29}Si and ^{27}Al NMR Study of Alkaline Earth Aluminosilicate Glasses." Journal of Non-Crystalline Solids **124**(2–3): 194-206.

Mindess, S., J. F. Young and D. Darwin (2003). Concrete, 2nd Edition. Prentice Hall, Upper Saddle River, NJ.

Myers, R. J., E. L'Hôpital, J. L. Provis and B. Lothenbach (2015). "Effect of Temperature and Aluminium on Calcium (Alumino)Silicate Hydrate Chemistry under Equilibrium Conditions." Cement and Concrete Research **68**: 83-93.

Navrotsky, A., K. L. Geisinger, P. McMillan and G. V. Gibbs (1985). "The Tetrahedral Framework in Glasses and Melts — Inferences from Molecular Orbital Calculations and Implications for Structure, Thermodynamics, and Physical Properties." Physics and Chemistry of Minerals **11**(6): 284-298.

North, M. R. and T. W. Swaddle (2000). "Kinetics of Silicate Exchange in Alkaline Aluminosilicate Solutions." Inorganic Chemistry **39**(12): 2661-2665.

Oh, J. E., P. J. M. Monteiro, S. S. Jun, S. Choi and S. M. Clark (2010). "The Evolution of Strength and Crystalline Phases for Alkali-Activated Ground Blast Furnace Slag and Fly Ash-Based Geopolymers." Cement and Concrete Research **40**(2): 189-196.

Palomo, A., S. Alonso, A. Fernandez- Jiménez, I. Sobrados and J. Sanz (2004). "Alkaline Activation of Fly Ashes: NMR Study of the Reaction Products." Journal of the American Ceramic Society **87**(6): 1141-1145.

Palomo, A., M. Grutzeck and M. Blanco (1999). "Alkali-Activated Fly Ashes: A Cement for the Future." Cement and Concrete Research **29**(8): 1323-1329.

Palomo, A., P. Krivenko, I. Garcia-Lodeiro, E. Kavalerova, O. Maltseva and A. Fernández-Jiménez (2014). "A Review on Alkaline Activation: New Analytical Perspectives." Materiales de Construcción; Vol 64, No 315 (2014).

Pelmenschikov, A. G., E. A. Paukshtis, M. O. Edisherashvili and G. M. Zhidomirov (1992). "On the Loewenstein Rule and Mechanism of Zeolite Dealumination." The Journal of Physical Chemistry **96**(17): 7051-7055.

Provis, J. and J. van Deventer (2013). Alkali Activated Materials: State-of-the-Art Report, RILEM TC 224-AAM, Springer Science & Business Media, New York.

Provis, J. L. and S. A. Bernal (2014). "Geopolymers and Related Alkali-Activated Materials." Annual Review of Materials Research **44**(1): 299-327.

Provis, J. L., G. C. Lukey and J. S. J. van Deventer (2005). "Do Geopolymers Actually Contain Nanocrystalline Zeolites? A Reexamination of Existing Results." Chemistry of Materials **17**(12): 3075-3085.

Provis, J. L., A. Palomo and C. Shi (2015). "Advances in Understanding Alkali-Activated Materials." Cement and Concrete Research **78, Part A**: 110-125.

Provis, J. L. and J. S. J. van Deventer (2007). "Geopolymerisation Kinetics. 2. Reaction Kinetic Modelling." Chemical Engineering Science **62**(9): 2318-2329.

Provis, J. L. and J. S. J. Van Deventer (2009). Geopolymers: Structures, Processing, Properties and Industrial Applications, CRC Press, Boca Raton.

Puertas, F., M. Palacios, H. Manzano, J. S. Dolado, A. Rico and J. Rodríguez (2011). "A Model for the C-A-S-H Gel Formed in Alkali-Activated Slag Cements." Journal of the European Ceramic Society **31**(12): 2043-2056.

Puligilla, S. and P. Mondal (2013). "Role of Slag in Microstructural Development and Hardening of Fly Ash-Slag Geopolymer." Cement and Concrete Research **43**: 70-80.

Puligilla, S. and P. Mondal (2015). "Co-existence of Aluminosilicate and Calcium Silicate Gel Characterized through Selective Dissolution and FTIR Spectral Subtraction." Cement and Concrete Research **70**: 39-49.

Purdon, A. (1940). "The Action of Alkalis on Blast-Furnace Slag." Journal of the Society of Chemical Industry **59**(9): 191-202.

Rahier, H., J. Wastiels, M. Biesemans, R. Willlem, G. Assche and B. Mele (2007). "Reaction Mechanism, Kinetics and High Temperature Transformations of Geopolymers." Journal of materials science **42**(9): 2982-2996.

Rees, C. A., J. L. Provis, G. C. Lukey and J. S. J. van Deventer (2007a). "Attenuated Total Reflectance Fourier Transform Infrared Analysis of Fly Ash Geopolymer Gel Aging." Langmuir **23**(15): 8170-8179.

Rees, C. A., J. L. Provis, G. C. Lukey and J. S. J. Van Deventer (2007b). "In Situ ATR-FTIR Study of the Early Stages of Fly Ash Geopolymer Gel Formation." Langmuir **23**(17): 9076-9082.

Rees, C. A., J. L. Provis, G. C. Lukey and J. S. J. van Deventer (2008). "The Mechanism of Geopolymer Gel Formation Investigated through Seeded Nucleation." Colloids and Surfaces A: Physicochemical and Engineering Aspects **318**(1–3): 97-105.

Rivera, A., T. Farias, A. R. Ruiz-Salvador and L. C. de Ménorval (2003). "Preliminary Characterization of Drug Support Systems Based on Natural Clinoptilolite." Microporous and Mesoporous Materials **61**(1–3): 249-259.

Rocha, J. (1999). "Single- and Triple-Quantum ^{27}Al MAS NMR Study of the Thermal Transformation of Kaolinite." The Journal of Physical Chemistry B **103**(44): 9801-9804.

Rocha, J. and J. Klinowski (1990). "Solid- State NMR Studies of the Structure and Reactivity of Metakaolinite." Angewandte Chemie International Edition in English **29**(5): 553-554.

Rouyer, J. and A. Poulesquen (2015). "Evidence of a Fractal Percolating Network During Geopolymerization." Journal of the American Ceramic Society **98**(5): 1580-1587.

Rovnaník, P. (2010). "Effect of Curing Temperature on the Development of Hard Structure of Metakaolin-Based Geopolymer." Construction and Building Materials **24**(7): 1176-1183.

Rowles, M. and B. O'Connor (2003). "Chemical Optimisation of the Compressive Strength of Aluminosilicate Geopolymers Synthesised by Sodium Silicate Activation of Metakaolinite." Journal of Materials Chemistry **13**(5): 1161-1165.

Rowles, M. R. and B. H. O'Connor (2009). "Chemical and Structural Microanalysis of Aluminosilicate Geopolymers Synthesized by Sodium Silicate Activation of Metakaolinite." Journal of the American Ceramic Society **92**(10): 2354-2361.

Roy, D. M. (1999). "Alkali-Activated Cements Opportunities and Challenges." Cement and Concrete Research **29**(2): 249-254.

Sartbaeva, A., N. H. Rees, P. P. Edwards, A. J. Ramirez-Cuesta and E. Barney (2013). "Local Probes show that Framework Modification in Zeolites Occurs on Ammonium Exchange without Calcination." Journal of Materials Chemistry A **1**(25): 7415-7421.

Schmücker, M. and K. J. D. MacKenzie (2005). "Microstructure of Sodium Polysialate Siloxo Geopolymer." Ceramics International **31**(3): 433-437.

Sevelsted, T. F. and J. Skibsted (2015). "Carbonation of C–S–H and C–A–S–H Samples Studied by ^{13}C, ^{27}Al and ^{29}Si MAS NMR Spectroscopy." Cement and Concrete Research **71**: 56-65.

Shi, C., A. F. Jiménez and A. Palomo (2011). "New Cements for the 21st Century: The Pursuit of an Alternative to Portland Cement." Cement and Concrete Research **41**(7): 750-763.

Shi, C., D. Roy and P. Krivenko (2006). Alkali-Activated Cements and Concretes, CRC Press, Boca Raton.

Silva, P. D., K. Sagoe-Crenstil and V. Sirivivatnanon (2007). "Kinetics of Geopolymerization: Role of Al_2O_3 and SiO_2." Cement and Concrete Research **37**(4): 512-518.

Singh, P. S., M. Trigg, I. Burgar and T. Bastow (2005). "Geopolymer Formation Processes at Room Temperature Studied by ^{29}Si and ^{27}Al MAS-NMR." Materials Science and Engineering: A **396**(1–2): 392-402.

Smith, B. C. (2011). Fundamentals of Fourier transform infrared spectroscopy, CRC Press, Boca Raton.

Steins, P., A. Poulesquen, O. Diat and F. Frizon (2012). "Structural Evolution during Geopolymerization from an Early Age to Consolidated Material." Langmuir **28**(22): 8502-8510.

St. Cloud Natural Company (2007). Product Information Sheet: St. Cloud Natural Zeolite (clinoptilolite), New Mexico, USA.

Struble, L. (1985). "The Effect of Water on Maleic Acid and Salicylic Acid Extractions." Cement and Concrete Research **15**(4): 631-636.

Struble, L. J. (2013). Effects of Calcium on the Geopolymer Reaction. Presented in 4th Advances in Cement-Based Materials: Characterization, Processing, Modeling and Sensing meeting, the American Ceramic Society Cement Division, Urbana, IL.

Stutzman, P. E. (1996). Guide for X-ray Powder Diffraction Analysis of Portland Cement and Clinker, US Department of Commerce, Technology Administration, National Institute of Standards and Technology, Office of Applied Economics, Building and Fire Research Laboratory.

Suraneni, P., S. Puligilla, E. Kim, X. Chen, L. Struble, P. Mondal, E. H. Kim and L. J. Struble (2014). “Monitoring Setting of Geopolymers.” Advances in Civil Engineering Materials, ASTM International. **3:** 177-192.

Sutrisno, A., L. Liu, J. Dong and Y. Huang (2012). "Solid-State ^{91}Zr NMR Characterization of Layered and Three-Dimensional Framework Zirconium Phosphates." The Journal of Physical Chemistry C **116**(32): 17070-17081.

Swaddle, T. W. (2001). "Silicate Complexes of Aluminum(III) in Aqueous Systems." Coordination Chemistry Reviews **219–221**: 665-686.

Talling, B. and J. Brandstetr (1989). "Present State and Future of Alkali-Activated Slag Concretes." Special Publication, International Concrete Abstracts Portal **114**: 1519-1546.

Taylor, H. F. W. (1997). Cement chemistry, Thomas Telford Services Ltd, London

Temuujin, J., A. Van Riessen and R. Williams (2009). "Influence of Calcium Compounds on the Mechanical Properties of Fly Ash Geopolymer Pastes." Journal of Hazardous Materials **167**(1): 82-88.

Tossell, J. (1993). "A Theoretical Study of the Molecular Basis of the Al Avoidance Rule and of the Spectral Characteristics of Al-O-Al Linkages." American Mineralogist **78**: 911-920.

Van Jaarsveld, J. G. S., J. S. J. Van Deventer and L. Lorenzen (1997). "The Potential use of Geopolymeric Materials to Immobilise Toxic Metals: Part I. Theory and Applications." Minerals Engineering **10**(7): 659-669.

Walkley, B., R. San Nicolas, M.-A. Sani, G. J. Rees, J. V. Hanna, J. S. J. van Deventer and J. L. Provis (2016). "Phase Evolution of C-(N)-A-S-H/N-A-S-H Gel Blends Investigated via Alkali-Activation of Synthetic Calcium Aluminosilicate Precursors." Cement and Concrete Research **89**: 120-135.

Wang, S.-D., X.-C. Pu, K. Scrivener and P. Pratt (1995). "Alkali-Activated Slag Cement and Concrete: A Review of Properties and Problems." Advances in Cement Research **7**(27): 93-102.

Wastiels, J., X. Wu, S. Faignet and G. Patfoort (1994). "Mineral Polymer Based on Fly Ash." Journal of Engineering and Technology Management **22**(3): 135-141.

Weng, L. and K. Sagoe-Crentsil (2007). "Dissolution Processes, Hydrolysis and Condensation Reactions during Geopolymer Synthesis: Part I—Low Si/Al Ratio Systems." Journal of Materials Science **42**(9): 2997-3006.

Weng, L., K. Sagoe-Crentsil, T. Brown and S. Song (2005). "Effects of Aluminates on the Formation of Geopolymers." Materials Science and Engineering: B **117**(2): 163-168.

White, C. E., J. L. Provis, B. Bloomer, N. J. Henson and K. Page (2013). "In Situ X-ray Pair Distribution Function Analysis of Geopolymer Gel Nanostructure Formation Kinetics." Physical Chemistry Chemical Physics **15**(22): 8573-8582.

White, C. E., J. L. Provis, G. J. Kearley, D. P. Riley and J. S. van Deventer (2011a). "Density Functional Modelling of Silicate and Aluminosilicate Dimerisation Solution Chemistry." Dalton Transactions **40**(6): 1348-1355.

White, C. E., J. L. Provis, A. Llobet, T. Proffen and J. S. van Deventer (2011b). "Evolution of local structure in geopolymer gels: an in situ neutron pair distribution function analysis." Journal of the American Ceramic Society **94**(10): 3532-3539.

White, C. E., J. L. Provis, T. Proffen and J. S. J. van Deventer (2012). "Molecular Mechanisms Responsible for the Structural Changes Occurring during Geopolymerization: Multiscale Simulation." AIChE Journal **58**(7): 2241-2253.

Williams, R. P., R. D. Hart and A. Van Riessen (2011). "Quantification of the Extent of Reaction of Metakaolin- Based Geopolymers Using X- Ray Diffraction, Scanning Electron Microscopy, and Energy- Dispersive Spectroscopy." Journal of the American Ceramic Society **94**(8): 2663-2670.

Yao, X., Z. Zhang, H. Zhu and Y. Chen (2009). "Geopolymerization Process of Alkali–Metakaolinite Characterized by Isothermal Calorimetry." Thermochimica Acta **493**(1–2): 49-54.

Yip, C., G. Lukey and J. Van Deventer (2005). "The Coexistence of Geopolymeric Gel and Calcium Silicate Hydrate at the Early Stage of Alkaline Activation." Cement and Concrete Research **35**(9): 1688-1697.

Yip, C. K., G. C. Lukey, J. L. Provis and J. S. J. van Deventer (2008). "Effect of Clcium Silicate Sources on Geopolymerisation." Cement and Concrete Research **38**(4): 554-564.

Yip, C. K. and J. S. J. van Deventer (2003). "Microanalysis of Calcium Silicate Hydrate Gel Formed within a Geopolymeric Binder." Journal of Materials Science **38**(18): 3851-3860.

Zhang, J. and G. W. Scherer (2011). "Comparison of Methods for Arresting Hydration of Cement." Cement and Concrete Research **41**(10): 1024-1036.

Appendix A. Estimation of low-Q species in early age geopolymers

Figure A-A-1 shows the direct-polarization MAS ^{29}Si NMR spectrum of the crystalline sodium silicate ($Na_2SiO_3.9H_2O$). In this section, a crystalline sodium silicate was used as a reference material to roughly estimate the amount of low-Q silicates in early age geopolymer gel. In total 1024 scans were collected, and recycle delay of 30 seconds was used. The absolute integrated intensity of this spectrum was 78.5 (arbitrary unit).

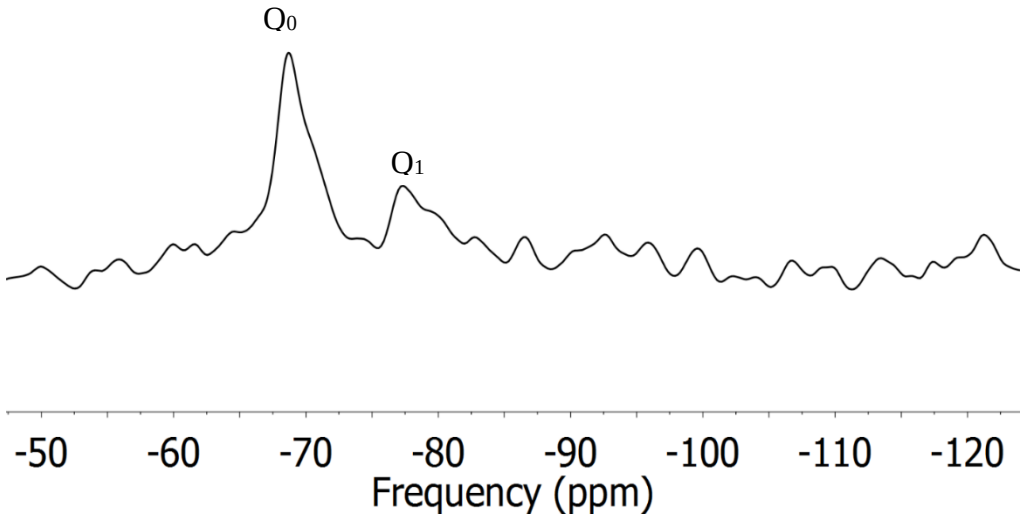

Figure A-A-1. Direct-polarization MAS ^{29}Si NMR spectrum of crystalline sodium silicates.

Figure A-A-2 presents spectrum of cross-polarization MAS ^{29}Si NMR spectra of crystalline sodium silicate. The contact time was optimized to show the maximum intensity. The relaxation time was 10.0 seconds, and the number of scans was 1024. The intensity was estimated to be 237.8 (arbitrary unit)

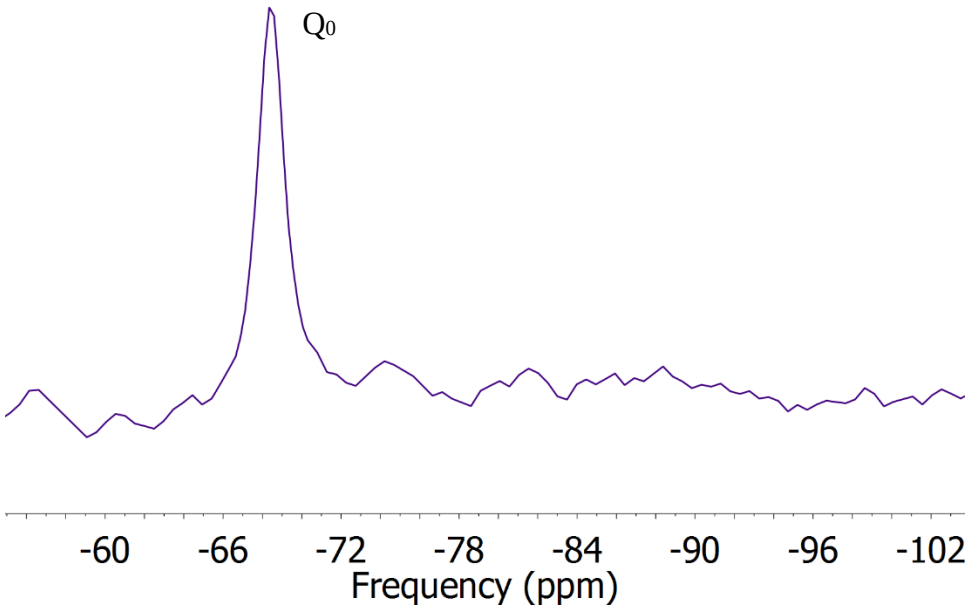

Figure A-A-2. Cross-polarization MAS ^{29}Si NMR spectrum of crystalline sodium silicates.

For comparison, intensity of the direct and cross polarization spectra for geopolymer gel at 51 hours was estimated and summarized in Table A-A-1 below. The intensity of direct and cross-polarization spectra for both materials was summarized. The mol% of the low-Q sites was estimated to be 8.2% (i.e., 0.25/3.03*100%).

Table A-A-1. Comparison of intensity of cross- and direct-polarization spectra for both crystalline sodium silicates and the geopolymer gel phase at 51 hours.

Materials	I_{DP} (arbitrary unit)	I_{CP} (arbitrary unit)	I_{CP}/ I_{DP}	Low Q-sites (mol%)
Crystalline SS	78.5	237.8	3.03	100% (known)
51-hour geopolymer	3448.2	857.7	**0.25**	**8.2% (calculated)**

Appendix B. ^{27}Al MAS NMR spectra at 15 hours and 3 months

Figure A-B-1 shows the ^{27}Al MAS NMR spectra of the mix 1:1:4:11 (Na2O:Al2O3:SiO2:H2O) at 15 hours (red) and at 3 months (green) using a 7.06-T probe. It can be clearly seen that the intensity at the 5- and 6-Al region in the spectrum is much higher at 15 hours than at 3 months. This difference indicates additional dissolution in this period.

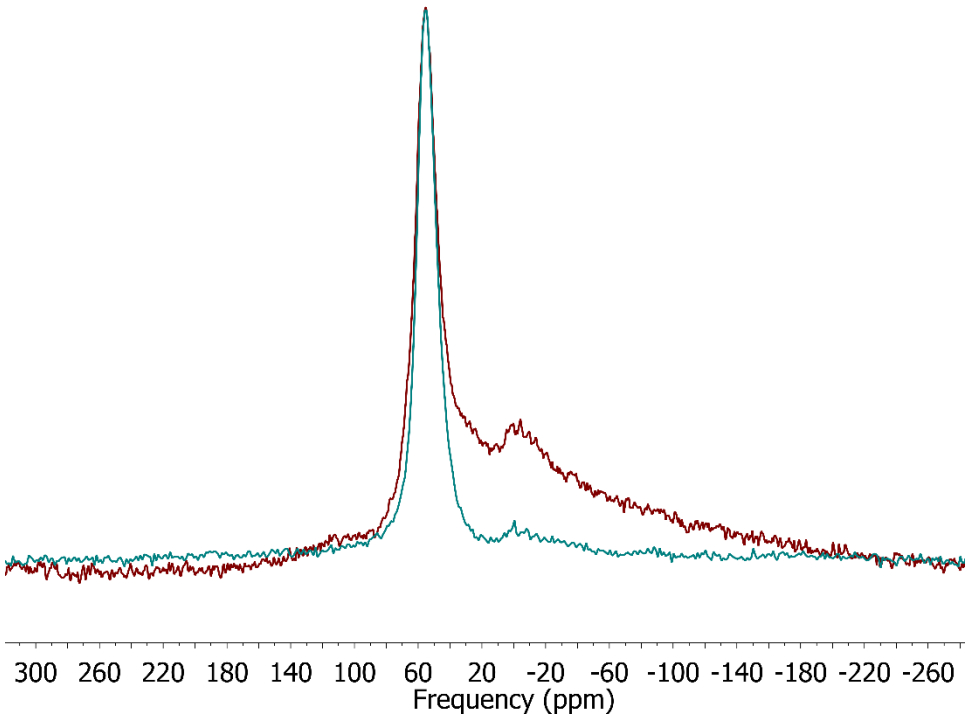

Figure A-B-1. ^{27}Al MAS NMR spectra of the mix 1:1:4:11 (Na_2O:Al_2O3:SiO_2:H_2O) at 15 hours (red) and at 3 months (green) using a 7.06-T probe.

Appendix C. Static ^{27}Al NMR tests of early age geopolymer

Static ^{27}Al NMR tests were conducted on early age geopolymer specimens. Since solid phase shows broad peak under static NMR tests, any Al intensity detected here is regarded to be from liquid phase. The specimen with the same mix composition (1:1:4:11) in Chapter 6 was examined at different times. As control, a $NaAlO_2$ solution with known amount was tested and the intensity of the ^{27}Al spectrum was recorded.

The spectra of the geopolymer specimen at 1, 11 and 20 hours after mixing are shown in Figure A-C-1 below. The intensity is shown to increase over time, probably because more Al is dissolved over time.

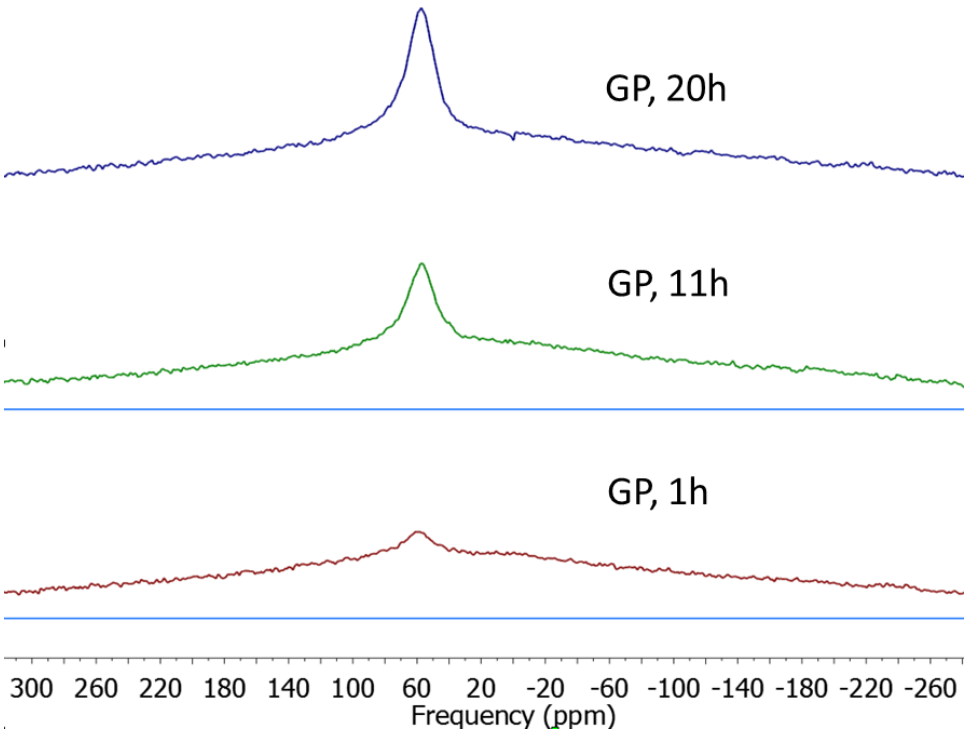

Figure A-C-1. Static ^{27}Al NMR spectra of geopolymer (1:1:4:11) at different times after mixing.

For comparison, the three spectra in Figure A-C-1 are stacked with that of the $NaAlO_2$ solution shown in Figure A-C-2. All the spectra were normalized so that the total Al in each specimen is the same. The intensity of the geopolymer spectra however is very low, indicating the amount of the Al in liquid phase is low. By comparing with the intensity of the reference solution, the moles of detected Al in liquid were calculated. With total Al calculated based on the weight and mix composition of the geopolymer specimen, the percent of liquid-phase Al in the geopolymer with respect to the total Al was estimated. All results are summarized in Table A-C-1.

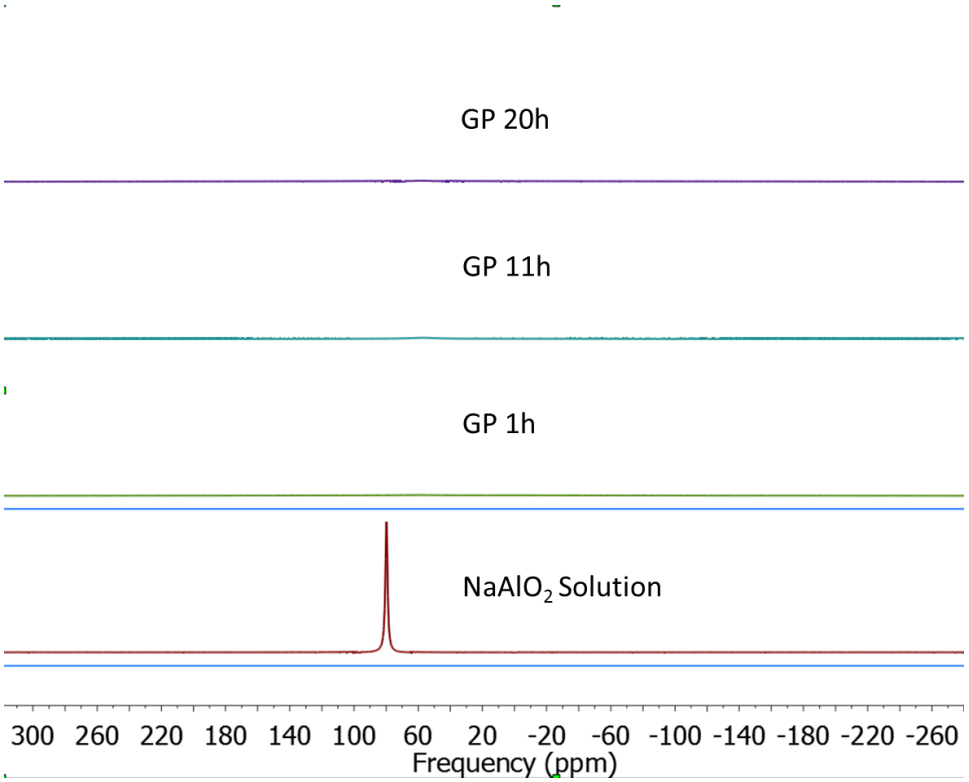

Figure A-C-2. Static ^{27}Al NMR spectra of geopolymer (1:1:4:11) at different times and the $NaAlO_2$ solution after mixing.

Table A-C-1. Amount of detected Al by Static ^{27}Al NMR at 1, 11 and 20 hours.

Time (hours)	Spectrum intensity (arbitrary unit)	Liquid Al (mole)	Total Al (mole)	Percent of liquid Al (%)
2	128626	2.10E-06	6.76E-04	0.31%
11	150207	2.46E-06		0.36%
20	163036	2.67E-06		0.39%

Appendix D. Solid-state ^{29}Si examination of solvent-extracted specimens

The specimens (composition expressed as 1:1.4:4.2:15, with Si/Al = 1.5) were synthesized by following the same procedure as described in Chapter 3. They were treated by solvent extraction at different early ages, and the residues were tested by solid-state ^{29}Si NMR spectroscopy. The setting curves (UWR and penetration resistance tests) is shown in Figure A-D-1. Spectra at different times shown in Figure A-D-2 were deconvoluted and peaks were assigned as geopolymer gel and unreacted metakaolin, which are magenta and navy colors, respectively.

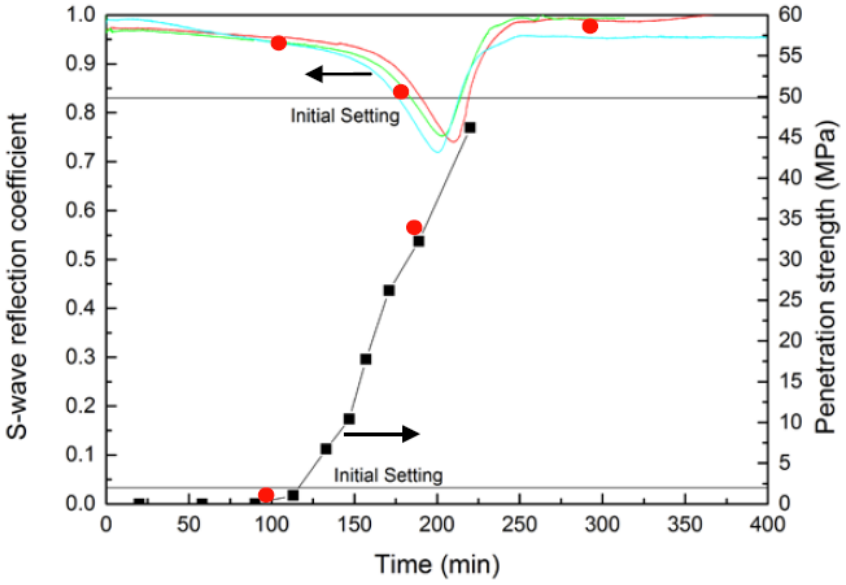

Figure A-D-1. Penetration resistance and UWR curves of geopolymer with composition $1Na_2O{\cdot}1.4Al_2O_3{\cdot}4.2SiO_2{\cdot}15H_2O$.

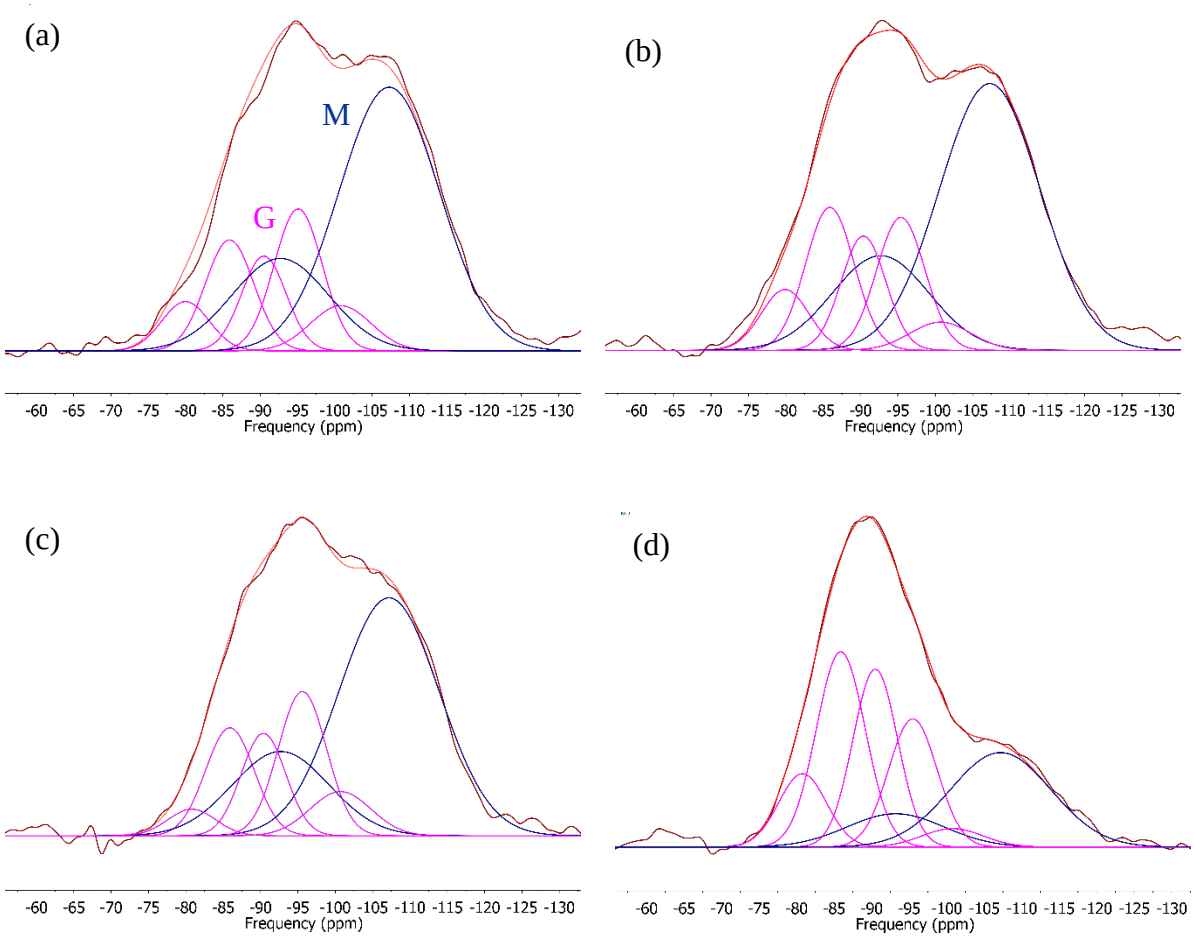

Figure A-D-2. Deconvolution of NMR spectra of geopolymers treated using solvent extraction at different times: (a) 100 minutes, (b) 180 minutes, (c) 300 minutes and (d) 7 days, with magenta and navy peaks assigned as geopolymer and unreacted metakaolin peaks, respectively.

Table A-D-1 summarizes the deconvolution results for the four spectra in Figure A-D-2. The relative molar percent of metakaolin and geopolymer was calculated based on the intensity associated with each phase. The Si/Al of geopolymer gel was calculated using Equation 2.1.

The Si/Al ratio for unreacted metakaolin was assumed to be 1.03, the same as the raw metakaolin. Then the overall Si/Al ratios (i.e., for both the phases) were estimated based on the Si/Al and amount of both phases. All values are presented in Table A-D-1.

Table A-D-1. Amount of metakaolin (MK) and geopolymer (GP) phases, and Si/Al ratios.

Times	100 minutes	180 minutes	300 minutes	7 days
MK* (mol%)	62.1%	60.8%	60.7%	31.0%
GP# (mol%)	37.9%	39.2%	39.3%	69.0%
Si/Al_GP	2.1	1.89	2.25	1.75
Si/Al_MK	1.03	1.03	1.03	1.03
Si/Al_Overall	**1.25**	**1.25**	**1.31**	**1.44**

* MK = metakaolin phase; # GP = geopolymer phase

Values shown in Table A-D-1 suggest the presence of lower-Q species around set. The overall Si/Al ratios were 1.25, 1.25, 1.31 at 100, 180 and 300 minutes, respectively, all lower than 1.5, the actual bulk ratio. This discrepancy could be due to the presence of lower Si species. The lower-Q species overlap with Q^4 Si with Al substitution. When estimating Si/Al, all species are considered as Q^4 Si substituted by Al, and thus the estimated Si/Al is lower than the actual value. At 7 days, the ratio 1.44 is closer to 1.5 than other ages, probably because less lower-Q Si species are present.

Appendix E. Solid-state ^{27}Al NMR spectrum of NaOH activated metakaolin

Figure A-E-1 shows the spectrum of the non-calcium-NaOH mix at 3 hours, typical for those obtained in these tests. Peaks at around 78.2, 65.1, 30.8 and 4.3 ppm were assigned to aqueous 4-coordinated Al, and solid 4-, 5- and 6-coordinated Al. Aqueous Al (around 80 ppm) has been observed in NaOH activated metakaolin (Duxson et al. 2005a). As reaction proceeded, the aqueous Al peak were reduced to zero progressively.

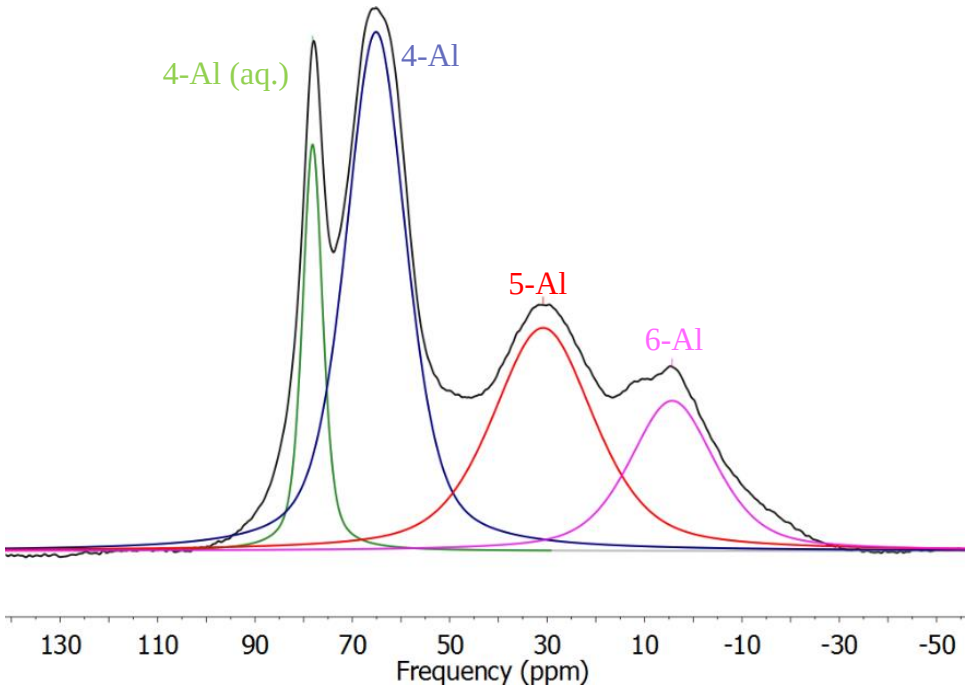

Figure A-E-1. Deconvolution of solid-state ^{27}Al NMR spectrum of the non-calcium NaOH mix at 3 hours after mixing (experimental spectrum and deconvoluted peaks).

Appendix F. SAM extraction of synthesized C-S-H and C-A-S-H

SAM extraction was conducted on both synthesized C-S-H and C-A-S-H, which have been synthesized by Hunnicutt (2013). The compositions are summarized in Table A-F-1. Each sample was treated by SAM solution with amount suggested in literature, i.e., 1.0-g specimen with 4.0-g salicylic acid and 60-ml methanol, named as “CSH-N” and “CASH-N”, respectively. Meanwhile, both specimens were also treated by SAM solution with five-times the suggested amount, named as “CSH-H” and “CASH-H”, respectively. In Table A-F-1, the percent of mass loss for each extraction is also summarized. It should be noted a 100% mass loss was seen in the CASH-H specimen.

In the early-age geopolymer specimens investigated in this thesis research, the amount of C-A-S-H phase was not higher than 20% (Si molar ratio) with respect to the specimen. When the normal amount of SAM solution is used for a specimen, its amount is equivalent to or higher than 5 times of the normal amount of solution with respect to a pure C-A-S-H specimen.

Table A-F-1. Summary of composition and SAM extraction for both C-S-H and C-A-S-H.

Specimens	C(A)SH Composition		Naming	SAM		Extraction Results		
	Ca/Si	Al/Si		Salicylic acid (g)	Methanol (ml)	Before (g)	After (g)	Mass Loss (wt%)
CSH	1	0	CSH-N	4	60	0.995	0.624	37
			CSH-H	20.02	300	0.997	0.262	74
CASH	1	0.2	CASH-N	4.03	60	1.034	0.184	82
			CASH-H	20.04	300	1.058	0.003	100

XRD patterns of both specimens are shown in Figure A-F-1. Both C-S-H and C-A-S-H do not show carbonation before the SAM extraction. Five-times of the suggested amount of SAM solution is shown to remove the featured peaks associated with C-S-H. Both the SAM residues of C-A-S-H were too little to conduct XRD tests.

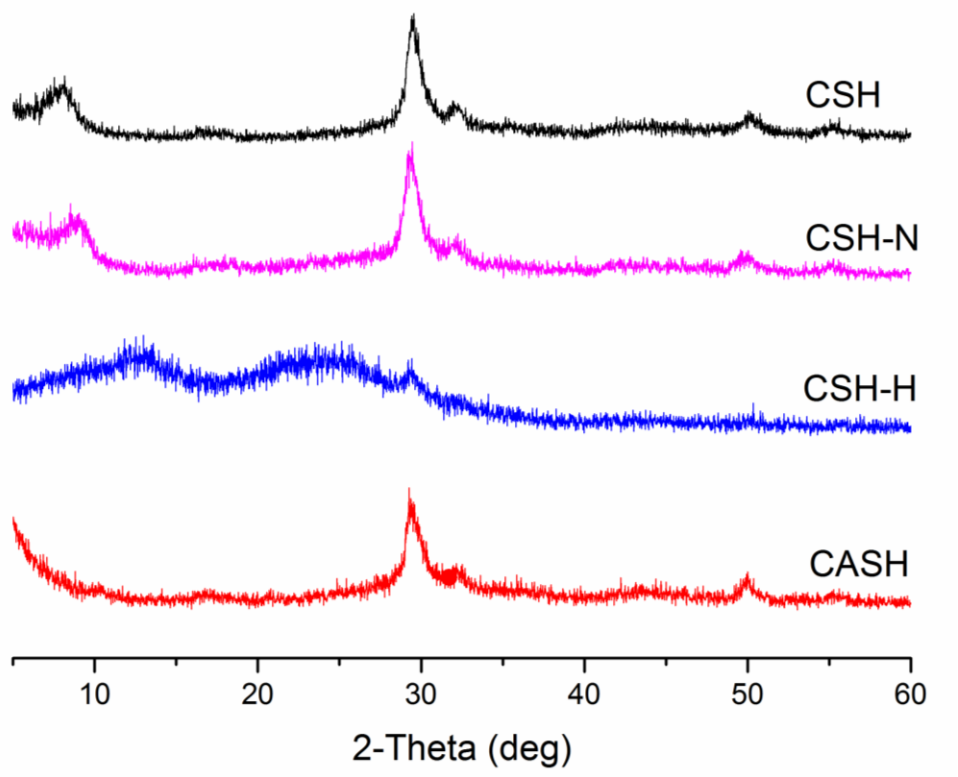

Figure A-F-1. XRD patterns of C-S-H and C-A-S-H, and SAM residues of C-S-H ("N" and "H" represent normal and higher amount of solution, respectively).

FTIR results (Figure A-F-2) were consistent with the XRD investigation. In the CSH-H spectrum, the peak in the region between 1000-1200 cm^{-1} is attributed to formation of silica gel. In the spectrum of the residue CASH-N, the main peak position of C-A-S-H shifted from 960 cm^{-1} to 1060 cm^{-1}. Some other peaks in the CASH-N spectrum are similar to those in the salicylic acid spectrum shown in Figure A-F-3.

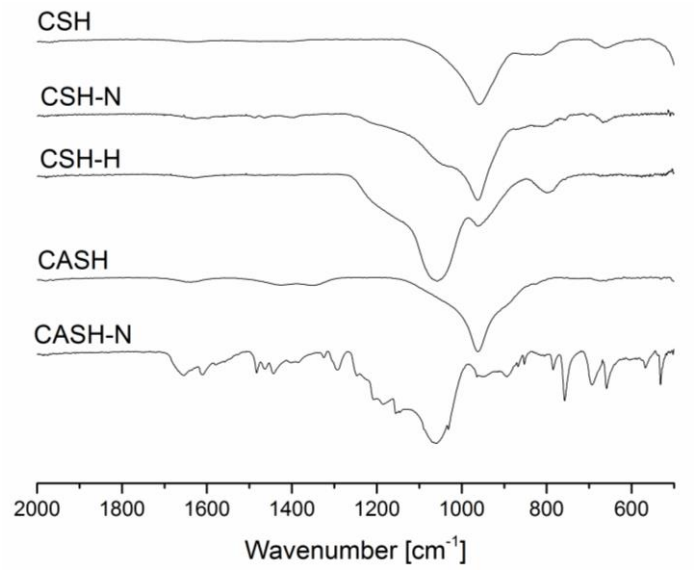

Figure A-F-2. FTIR spectra of CSH and CASH before and after SAM extraction.

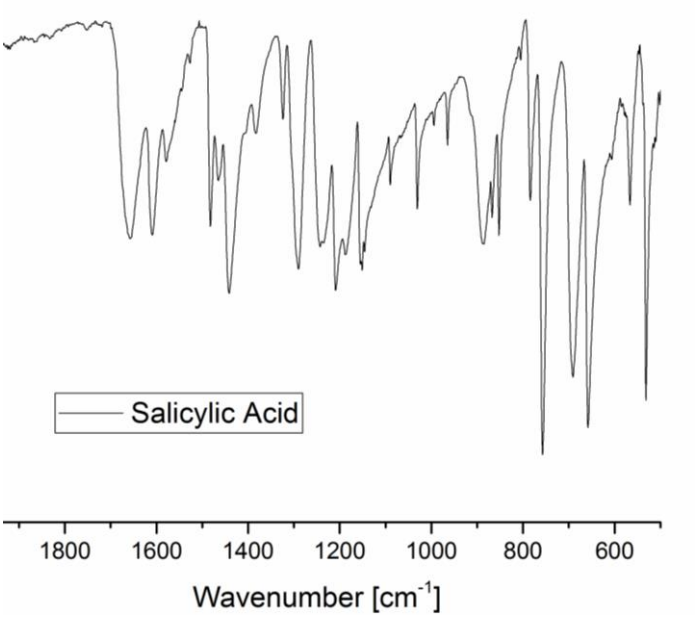

Figure A-F-3. FTIR spectrum of the salicylic acid.

Appendix G. Uncertainties in estimating of Si/Al ratios for geopolymer formation

There is some uncertainty regarding the assignment of high-Q peaks to C-A-S-H. As discussed in the text, these peaks may alternatively be assigned as the calcium modified geopolymer gel. Generally, the Si/Al in conventional chain-like C-A-S-H is higher than 10, while that for calcium modified geopolymer gel is in the range of 1.2 to 10 (Garcia-Lodeiro et al. 2011). If these high-Q peaks had been considered as the geopolymer gel, the obtained Si/Al ratio for geopolymer gel formation would have been even lower than our current estimation in the calcium.

There is also some uncertainty in estimation of Si/Al for geopolymer gel formation is discussed. The dissolution extent percent for the non-calcium mix would be overestimated under the lower field NMR, as larger portion of 4-Al with respect to actual total 4-Al is detected in the lower-field ^{27}Al NMR test and smaller portion for 5- and 6-coordinated Al. This overestimation of dissolution extent is true for both the calcium and non-calcium mixes, however more severe in the non-calcium mix for the following reason. In the non-calcium mix, relatively more 5- and 6-coordinated and less 4-coordinated Al are present compared to the calcium mix due to lack of enhanced dissolution by calcium, and therefore lower portion of total Al can be detected. With a smaller amount of total Al as denominator, percent of 4-coordinated Al is more overestimated in the non-calcium mix than the calcium mix, and therefore the Si/Al ratio for geopolymer gel formation would be less overestimated in the non-calcium mix.

The first uncertainty might result in an overestimated Si/Al for geopolymerization in the calcium mix, and the second uncertainty results in less overestimated Si/Al ratio in the non-calcium mix

than the calcium mix. Despite both uncertainties, the conclusion does not change: this ratio is lower in the calcium mix.

Appendix H. Estimation of Si/Al ratios for geopolymerization

Calculations to estimate Si/Al ratio for geopolymerization are presented here by taking both the calcium and non-calcium mixes at 6 hour for examples. In these calculations, the total amount of Al is 1 mole, and total amount of Si is 2 moles with half (i.e., 1 mole) from activating solution and half (i.e., 1 mole) from metakaolin in each specimen.

In the calcium-specimen at 6 hour, the totally dissolved Al was estimated at first. The relative intensities of 4-, 5- and 6-Al were 54.0%, 30.2% and 15.8% respectively in the in-situ calcium mix at 6 hour and were 35.6%, 43.3% and 21.1% respectively in the raw metakaolin specimen. These values are considered quantitative and were based on spectra collected in NMR tests at the higher field (17.6 T). The sum of 5- and 6-Al intensities were therefore 46.4% in this 6-hour specimen and 64.4% in the raw metakaolin. The dissolution extent, defined as percent of 5- and 6-Al converted to 4-Al, was calculated as

$$\frac{64.4\%-46.0\%}{64.4\%} = 28.6\% \qquad \text{(A8-1)}$$

In the specimen with 1 mole of total Al, the total dissolved Al is 0.29 mole (i.e., 1 mole multiplied by 28.6%).

Then Al in the C-A-S-H phase was estimated in this specimen. Using the same calculation method right above, the sum of relative intensity percent of 5- and 6-Al was 18.4% higher in the combined extraction residue than that in the raw metakaolin and was 14.1% higher in the SAM extraction residue than in the raw metakaolin. The difference between the two values, 4.3%, was corresponding to the amount of Al in the C-A-S-H phase with respect to the total Al. Therefore,

the amount of Al in the C-A-S-H phase in this calcium mix at 6 hours was 0.04 mole (i.e., 1 mole multiplied by 4.3%). The amount of Al for geopolymer formation (in geopolymer gel and in aqueous phase) is calculated to be 0.25 mole (i.e., 0.29 mole minus 0.04 mole).

The amount of Si in the C-A-S-H was then estimated. Based on the ^{29}Si MAS NMR tests (results of which are shown in Figure 7.5), the amounts of Si in C-A-S-H, geopolymer gel and unreacted metakaolin the combined extraction residue are 18.4%, 16.7% and 64.9%. When assuming zero dissolution of Si from the metakaolin at this age, the amount of Si in the unreacted metakaolin remains 1 mole. Then the amount of Si in the C-A-S-H can be calculated as

$$1 mole * \frac{18.4\%}{64.9\%} = 0.28\, mole \quad \text{(A8-2)}$$

The amount of Si in the geopolymer gel and in aqueous phase (i.e., that available for reaction) is calculated to be 0.72 mole (i.e., 1 mole minus 0.28 mole).

The Si/Al ratio for geopolymerization for the calcium mix at 6 hours is calculated as

$$\frac{0.72\, mole}{0.25\, mole} = \mathbf{2.9} \quad \text{(A8-3)}$$

For the non-calcium mix, the dissolved Al was also estimated based on the lower field results (probed at 7.04 T, shown in Figure 7.3) as discussed in the text in Chapter 7. Based on these lower-field results, the dissolution extents (as defined above) at 6 hours for both calcium and non-calcium mixes were 86.0% and 36.9%, respectively. Their ratio is 2.33 (i.e., 86.0% divided by 36.9%). Considering the dissolved Al in the calcium mix at 6 hours based on the quantitative NMR results

(i.e., probed at 17.6 T) was 0.29 mole. The amount of dissolved Al in the non-calcium mix was estimated as

$$\frac{0.29\ mole}{2.33} = 0.13\ mole \quad \text{(A8-4)}$$

The amount of Al estimated here would be overestimated because the results were from the lower field probe. This overestimation and its influence on the comparison of estimated Si/Al ratio for geopolymerization between the calcium and the non-calcium are discussed in Appendix G and are shown to not affect the final conclusions.

The total Si for geopolymerization is 1 mole by assuming zero Si from dissolution of metakaolin. The Si/Al ratio for geopolymerization for the non-calcium mix at 6 hours is calculated as

$$\frac{1\ mole}{0.13\ mole} = \mathbf{7.9} \quad \text{(A8-5)}$$

In the above calculations in this appendix, Si dissolution was assumed to be zero. When assuming congruent dissolution, considering the dissolved Al was 0.29 mole in the calcium at 6 hours, the dissolved Si was also 0.29 mole. The amount of Si in the unreacted metakaolin was 0.71 mole (i.e., 1 mole minus 0.29 mole).

Then the amount of Si in the C-A-S-H can be calculated as

$$0.71 mole * \frac{18.4\%}{64.9\%} = 0.20\ mole \quad \text{(A8-6)}$$

The amount of Si in geopolymer gel and in aqueous phase is calculated as

$$1mole + 0.29mole - 0.20\ mole = 1.09\ mole \quad \text{(A8-7)}$$

The Si/Al ratio for geopolymerization for the calcium mix at 6 hours by assuming congruent dissolution is calculated as below.

$$\frac{1.09\ mole}{0.25\ mole} = \mathbf{4.4} \quad \text{(A8-8)}$$

In the non-calcium mix, the amount of dissolved Al was 0.13 mole, and thus the amount of dissolved Si was also 0.13 mole. The total Si for geopolymerization was therefore 1.13 mole. The Si/Al ratio for geopolymerization for the non-calcium mix at 6 hours by assuming congruent dissolution is calculated as below.

$$\frac{1.13\ mole}{0.13\ mole} = \mathbf{8.7} \quad \text{(A8-9)}$$

Calculations were conducted at the other times by also assuming congruent dissolution. The Si/Al available for geopolymers were obtained for both the mixes are shown in Table A-H-1. For comparison, the Si/Al ratios in Table 7.2 (those by assuming zero dissolution of Si) are also shown in Table A-H-1 here. It is clear that the Si/Al for geopolymerization is lower in the calcium mix than in the non-calcium mix, regardless of the assumption of congruent or incongruent dissolution.

Table A-H-1. Si/Al for geopolymerization in both mixes at different time by assuming either zero Si dissolution or congruent dissolution.

Ages (hour)	Assumptions	Zero Si dissolution			Equal Si and Al dissolution		
	Mixes	Ca	Non-Ca		Ca	Non-Calcium	
			Lower field	Higher field		Lower field	Higher field
1	Si/Al ratio for geopolymerization	6.2	37.1	20.5	7.3	34.3	21.0
6		2.9	7.9	12.5	4.4	8.7	13.5
15		2.3	5.4	11.1	4.3	6.6	12.1

In the above analysis, the amount of Al in the non-calcium mix was based on lower field (7.04 T) results. For comparison, the amount of Al in the non-calcium mix was again estimated, but directly based on the higher field probe (17.6 T). The corresponding results were calculated as below by taking 6 hour specimen as an example and were summarized in Table A-H-1. At 6 hours, the 4-, 5- and 6-coordinated Al were estimated to be 40.9%, 36.3% and 22.8%, respectively. The sum of 5- and 6-Al was therefore 59.1%. The dissolution extent was calculated as

$$\frac{64.4\%-59.1\%}{64.4\%} = 8.3\% \quad \text{(A8-10)}$$

In the specimen with 1 mole of total Al, the total dissolved Al is 0.08 mole (i.e., 1 mole multiplied by 8.3%).

The total Si for geopolymerization is 1 mole by assuming zero Si from dissolution of metakaolin. The Si/Al ratio for geopolymerization for the non-calcium mix at 6 hours is calculated as

$$\frac{1\ mole}{0.08\ mole} = \mathbf{12.5} \quad \text{(A8-11)}$$

The total Si for geopolymerization is 1.08 mole (i.e., 1 + 0.08 mole) by assuming congruent dissolution of metakaolin. The Si/Al ratio for geopolymerization for the non-calcium mix at 6 hours is calculated as

$$\frac{1.08\ mole}{0.08\ mole} = \mathbf{13.5} \quad \text{(A8-12)}$$

Appendix I. Summary of ^{29}Si liquid-state NMR results for the calcium mix

Figure A-I-1 shows the normalized amounts of $Q^{(0-4)}$ sites from liquid-state ^{29}Si NMR as geopolymerization proceeded for the calcium mix ($0.4CaO:1Na_2O:1Al_2O_3:4SiO_2:12.1H_2O$). The slow step-by-step condensation process as observed in the non-calcium mix was not seen here. In the first 5 hours shown in this figure, rapid drop of Q^1, Q^2 and Q^3 were observed, as accompanied by rapid Al dissolution. This observation supports rapid formation of C-A-S-H and geopolymer gel, as confirmed by Figure 7.5 in Chapter 7. This early stage involves rapid product formation (without slow step-by-step condensation seen in the non-calcium mix) and is associated with setting. Afterwards, Q^1 and Q^2 continued to decrease and Q^3 started to increase, an observation that indicates formation of more C-A-S-H but little geopolymer gel, as again confirmed by changes in amount of products from 6 to 15 hours in the Figure 7.5.

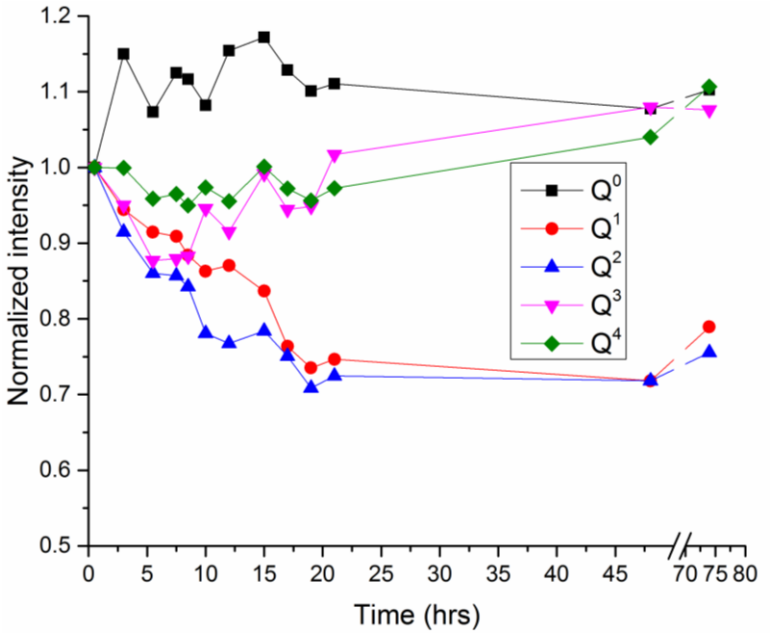

Figure A-I-1. Normalized amounts of $Q^{(0-4)}$ sites from liquid-state ^{29}Si NMR as geopolymerization proceeded for the calcium mix ($0.4CaO:1Na_2O:1Al_2O_3:4SiO_2:12.1H_2O$).

Appendix J. FTIR spectrum of precipitate in aluminosilicate solution

The spectrum of the precipitate collected from the mixture of sodium silicate, aluminum nitrate and sodium hydroxide solutions (with Si/Al 2.0) is shown in Figure A-J-1. Peaks at 864, 1406 and 1434 cm^{-1} are attributed to carbonates. The peak at around 980 cm^{-1} is associated with Si-O-T bonding, a little lower than reported value for N-A-S-H gel probably due to the presence of some liquid in the current specimen.

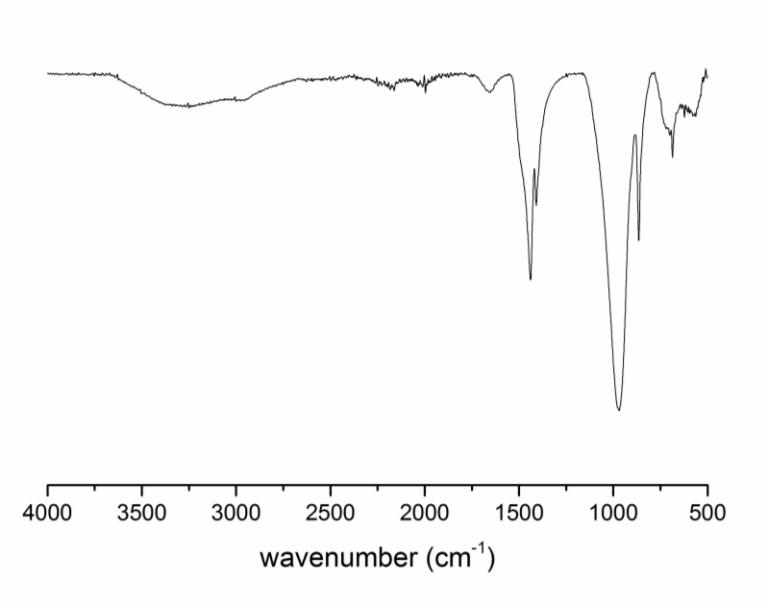

Figure A-J-1. FTIR spectrum of precipitate from the mix of precipitate by mixing sodium silicate, aluminum nitrate and sodium hydroxide solutions with Si/Al of 2.0.

Appendix K. Estimation of unreacted metakaolin based on Na/Al ratio

A more detailed mix design is shown in Table A-K-1, which presents amount of each raw material in a batch for the same mixes in Table 8.1. As mentioned in Chapter 3, the weight percentages of SiO_2, Na_2O and H_2O in the commercial solution were 29.02%, 9.00% and 61.98%, respectively.

Table A-K-1. Amount of raw materials in a batch for the mixes in Table 8.1 in Chapter 8.

Mix number	Weight (g) in a batch				
	Metakaolin	NaOH	Sodium silicate solution	H2O	Calcium hydroxide
1	310	53	41	239	0
2	307	51	95	227	0
3	316	52	154	175	0
4	377	48	200	201	0
5	448	70	377	286	0
6	448	70	377	286	22
7	448	70	377	286	45
8	448	70	377	286	67

A lower bound for unreacted metakaolin can be estimated mainly based on the Na/Al ratio. In Mix Number 1, for example, the weight percent of metakaolin with respect to the total weight of the mix is calculated as below:

$$\frac{Weight\ of\ metakaolin}{Total\ weight\ of\ the\ mix} = \frac{310}{310 + 53 + 41 + 239} = 48.2\ wt\%$$

At the maximum reaction extent, all Na ions have participated in the geopolymer reaction, the percent of reacted Al with respect to total Al is equal to the Na/Al ratio, which in this mix was 0.54. By assuming congruent dissolution of metakaolin, the amount of reacted metakaolin would be 54%. Therefore, the percent of unreacted metakaolin with respect to the total weight is calculated below:

$$48.2\ wt\% * (1 - 54\%) = \mathbf{22.1\ wt}\%$$